ANALYSIS OF THE PHYSIOLOGICAL ROLE OF HISTONE DEACETYLASE 3 (HDAC3) AND ITS REGULATION BY INOSITOL PHOSPHATES

Thesis submitted for the degree of
Doctor of Philosophy
at the University of Leicester

by
Lyndsey Claire Wright BSc (University of Leicester)
Department of Molecular and Cell Biology
University of Leicester

June 2017

Lyndsey Wright

Analysis of the physiological role of histone deacetylase 3 (HDAC3) and its regulation by inositol phosphates.

Histone deacetylase 3 (HDAC3) acts as the catalytic core of the SMRT/NCoR co-repressor complex which regulates chromatin structure and gene expression. It was recently shown that HDAC3 binds, and is regulated *in vitro*, by the binding of inositol phosphates (IP). We used transcriptional reporter assays to interrogate whether HDAC3-mediated repression *in vivo* is dependent of IP. Manipulation of intracellular IP levels through chemical inhibition of enzymes involved in IP metabolism or RNAi-mediated protein knockdown were inconclusive. However, mutation of key IP binding residues in both SMRT and HDAC3 directly impacts the repressive ability of the co-repressor complex, presumably through an impaired ability to bind IP and failure to fully activate the enzyme. Germline deletion of HDAC3 in the mouse results in early embryonic lethality (around e9.5) suggesting it plays an essential role in embryogenesis. To further investigate the role of HDAC3 in embryonic development, I have generated a conditional knockout embryonic stem cell line in which HDAC3 can be specifically inactivated. Loss of the protein occurs within 3 days suggesting a half-life of approximately 24 hours and correlates with concomitant decrease in co-repressor complex components, indicating HDAC3 contributes to co-repressor integrity. Unlike deletion of HDAC1 and -2, loss of HDAC3 does not cause a significant reduction in total deacetylase activity with only minor changes in the acetylation levels of histones. However, the proliferative capacity of knockout cells is inhibited with a delay in cell doubling time. Upon differentiation, we find that embryoid bodies (EBs) lacking HDAC3 are significantly smaller and morphologically different compared to controls. Microarray analysis over a 7-day time course of EB differentiation reveals that endodermal cell markers are over-expressed at both early and late stages of development, suggesting that HDAC3 plays an important role in regulating gene expression during embryonic development.

Acknowledgements

I would firstly like to thank my supervisor, Dr. Shaun Cowley, for his support, encouragement, guidance and endless patience throughout my PhD studies. I would also like to thank my committee members, Prof. John Schwabe and Dr. Peter Watson, for their helpful comments and discussion. My thanks also go to Dr. Richard Kelly for not judging my inane questions and for all his invaluable help and support and to Dr. Emma Kelsall as my lab wife for a shoulder to cry on during the dark days of gene targeting and for being there, anytime day or night. Thanks also go to lab colleagues for their friendship, encouragement and help throughout my time in the lab. Finally, to my fiancé Benjamin: you may not understand chromatin or histones as I do not understand engineering but I couldn't have got through this process without you.

List of contents

Table of Contents

List of figures

Abbreviations

4-OHT	4-hydroxtamoxifen
aa	amino acid
ac	acetyl
AP	alkaline phosphatase
ATA	aurintricarboxylic acid
ATP	adenosine triphosphate
BMP4	bone morphogenic protein 4
BocK	Boc-acetyl lysine
bp	base pair
BP-GO	biological process gene ontology
Brachyury	T box transcription factor
CaMK	calcium/calmodulin-dependent protein kinase
CDK	cyclin dependent kinase inhibitors
cDNA	complimentary deoxyribonucleic acid
CHA	chlorogenic acid
CHD	chromodomain helicase DNA
ChIP	chromatin immunoprecipitation
cKO	conditional knockout
CNS	central nervous system
CoREST	co-repressor to REST
CreER	Cre recombinase, estrogen receptor
Ct	cross threshold

DAD	deacetylase activation domain
DAVID	Database for Annotation, Visualisation and Integrated Discovery
DMEM	Dulbecco's modified eagle medium
DMSO	dimethyl-sulpoxide
DNA	deoxyribonucleic acid
DNMT	DNA methyltransferases
dNTP	deoxyribonucleotide triphosphate
EBs	embryoid bodies
ELM2	egl-27 and MTA1 homology 2 domain
ERK	extracellular signal regulated kinase
ES cell	embryonic stem cell
Essrb	estrogen related receptor beta
FACS	fluorescence activated cell sorting
FBS	foetal bovine serum
Fc	fold change
Fgf5	fibroblast growth factor 5
Fgfr1	FGF receptor 1
FlpO	optimised Flipase recombination enzyme
FoxA2	forkhead box A2
FRT	Flp recombination target site
Gal4	Gal4-DNA binding domain
Gapdh	glyceraldehyde 3-phosphate dehydrogenase

Gata4	Gata binding protein 4
Gata6	Gata binding protein 6
gDNA	genomic deoxyribonucleic acid
Gps2	G protein suppressor 2
H2	histone 2
H3	histone 3
H4	histone 3
HAT	histone acetyltransferases
HDAC	histone deacetylase
Hhex	hematopoietically expressed homeobox
HID	HDAC interaction domain
HNF	hepatic nuclear factor
Hyg	hygromycin B
Id	inhibitor of differentiation
IL-4	interleukin-4
IPMK	inositol phosphate multikinase
IPPK	inositol phosphate protein kinase
Klf4	Kruppel-like factor 4
LB	Luria-Bertani
LBD	Ligand binding domain
LIF	leukemia inhibitory factor

LoxP	locus of X over P1
LSD1	lysine demethylase-1
Lys	lysine
MadN35	N-terminal 35 amino acids of Mad1
MAPK	mitogen activated protein kinase
MBD	methyl-CpG binding domain
ME	mesendoderm
MEF	mouse embryonic fibroblast
MEF2	myocyte enhancer factor
Mef2c	myocyte enhancer factor 2C
Mi2β	chromodomain helicase DNA binding protein 3
MiDAC	mitotic deacetylase complex
mRNA	messenger ribonucleic acid
MTA1-3	metastasis associated protein 1-3
Myf	myogenic regulatory factor
MyoD	myogenic differentiation 1
MyoG	myogenin
NAD	nicotinaminde adenine dinucleotide
Nanog	nanog homeobox
NCoR	nuclear receptor co-repressor
Neo	neomycin

NODE	Nanog- and Oct4-associated deacetylase complex
NuRD	nucleosome remodelling and histone deacetylase complex
Oct4	POU domain, class 5, transcription factor 1
p21	cyclin dependent kinase inhibitor 1
p300	histone acetyltransferase p300
PAH	paired amphipathic helix
Pax6	paired box protein 6
PBS	phosphate buffered saline
PCA	principal component analysis
PCR	polymerase chain reaction
PI	propidium iodide
PLB	protein loading buffer
Pou3f2	POU class 3 homeobox 2
PTM	post-translational modification
qRT-PCR	quantitative real-time polymerase chain reaction
RbAp46/48	Retinoblastoma associated protein
REST	repressor element-1 silencing transcription factor
Rex1	Zinc finger protein 42 (Zfp42)
RIN	RNA integrity number
RNAi	RNA interference
RT	room temperature

SAM	S-adenosylmethionine
SDS	sodium dodecyl sulphate
SDS-PAGE	sodium dodecyl sulphate polyacrylamide gel electrophoresis
SDS3	suppressor of defective silencing 3
SEM	standard error of the mean
shRNA	short hairpin RNA
Sin3A	SWI-independent 3
SIRT	sirtuin
SMRT	silencing mediator of retinoid and thyroid receptor
Sox2	SRY box 2
STAT3	signal transducer and activator transcription 3
SUMO	small ubiquitin-related modifier
SWI/SNF	SWI/sucrose non fermentable
TBL1	transducin β-like 1
Tk Luc	thymidine kinase luciferase
TSA	trichostatin A
Tyr	tyrosine
UAS	upstream activation sequence
UPL	universal probe library
WCE	whole cell extract
Wnt	wingless intergration 1

WT	wildtype
XtDAD	extended deacetylase activation domain

Chapter One: Introduction

1.1 Chromatin structure and function

The eukaryotic genome is subject to multiple levels of organisation that facilitates compaction of DNA into chromatin, a highly organised and dynamic DNA-protein structure, the conformation of which dictates gene transcription (Kornberg & Lorch, 1999). Chromatin can be classified into two distinct conformations during interphase dependent on its level of compaction: highly condensed heterochromatin which is transcriptionally silent, or uncondensed euchromatin containing gene-rich and transcriptionally active genomic loci.

The basic unit of chromatin is the nucleosome (FIGURE 1.1), which comprises 146 base pairs of DNA wrapped 1.7 times around an octamer of core histone proteins, an H3-H4 tetramer and two H2A-H2B histone dimers (Luger *et al.*, 1997). Each histone protein contains a globular head domain in addition to an unstructured N-terminal tail, which protrudes from the core nucleosome structure (Luger & Richmond, 1998). It is this N-terminal tail which is the target for a variety of post-translational modifications that serve to alter chromatin condensation and the accessibility of DNA to transcriptional machinery thereby altering gene expression.

The first stage of chromatin compaction is the formation of polynucleosome arrays; here, adjacent nucleosomes separated by between 20-70 base pairs of linker DNA associate with non-histone proteins and an additional histone protein, histone H1, which stabilises the nucleosome, to form a 10nm fibre known as “beads on a string” (Zhou *et al.*, 1998; Thoma *et al.*, 1979). Subsequent compaction results in the formation of the 30nm fibre in which 6 nucleosomes per turn are present in a helical structure. Finally, during metaphase, chromatin is further compacted in combination with fibrous proteins to form highly condensed chromatin.

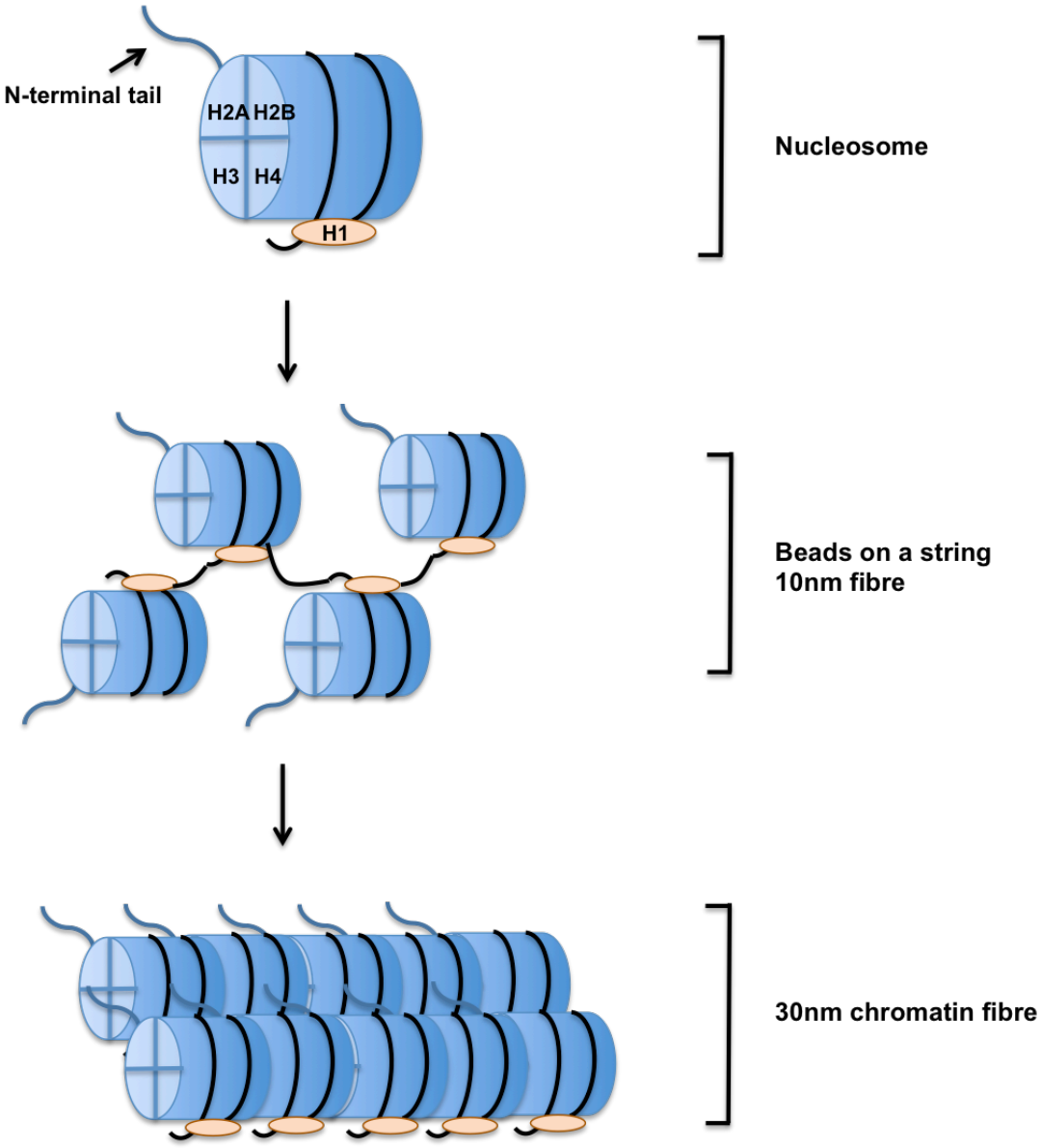

Figure 1.1 Compaction of chromatin. DNA is wrapped 1.7 times around a core octamer of histone proteins, H2A, H2B, H3 and H4, which then associate with linker histone H1 and other non-histone proteins to form polynucleosome arrays. Further compaction results in the formation of the 30nm chromatin fibre during metaphase.

Chromatin architecture directly impacts on the ability of transcriptional machinery to access DNA, thus gene expression is not only controlled at the sequence level, through the functional sequence elements present in the DNA, but also through manipulation of the structural organisation of chromatin. Chromatin state can be altered in a number of ways including DNA methylation, ATP-dependent chromatin remodelling and post-translational modification of histone proteins.

DNA methylation is a common epigenetic modification associated with gene silencing. It occurs on the 5-position (C5) of cytosine nucleotides that are found adjacent to guanine nucleotides (CpG dinucleotides) to form 5-methyl cytosine in a reaction catalysed by DNA methyltransferases. Such CpG dinucleotides are often found close to gene promoters of genes in so-called CpG islands. Methylated CpGs are recognised by methyl-CpG binding proteins (MBDs), which are often found as part of larger multi-protein complexes, often with histone-modifying activities to induce chromatin compaction and gene silencing. For example, MBD2 is associated with the NuRD co-repressor complex, which contains deacetylase activity due to the presence of HDAC1 and 2; similarly, Mi2α and -β proteins are also found within the complex and are known to have ATP dependent chromatin-remodelling activity (Xue *et al.*, 1998; Zhang *et al.*, 1999; Hendrich *et al.*, 2001). Accordingly, repression of gene expression is reinforced at the histone level through the deacetylation of histone tails following targeting of the complex to methylated regions via MBD2.

Direct chromatin remodelling is facilitated through the action of ATP-dependent chromatin remodelling complexes which use the energy from ATP hydrolysis to disrupt histone-DNA interaction and reposition nucleosomes. Classified into two main groups, the SWI/SNF and imitation SWI (ISWI) families, who are responsible for gene activation and repression respectively, all members contain an ATPase subunit that belongs to the SNF2 family of proteins (Eisen *et al.*, 1995).

Chromatin structure can also be modified through the covalent modification of histone proteins. This occurs principally on the unstructured N-terminal tail of histone proteins and functions to either directly alters the electrostatic potential between DNA and histone proteins or facilitate the recruitment of other non-histone proteins with chromatin or histone modifying activities to alter chromatin structure and bring about changes in gene transcription. The work in this thesis will focus on lysine acetylation of histone proteins (discussed in more detail below), which is regulated by two families of enzymes, histone acetyltransferases (HATs) and histone deacetylases (HDACs).

1.2 Histone modifications

Post translational modification of histone proteins were first identified in the 1960s by Allfrey *et al.*, who noted that histone proteins could be acetylated and subsequently showed that histone acetylation was associated with transcriptional activity (Allfrey *et al.*, 1964) Following the characterisation of the crystal structure of the nucleosome (Luger *et al.*, 1997), which identified that the N-terminal tail of histone proteins are able to make contact with adjacent nucleosomes, it was suggested that modifications serves to directly alter inter-nucleosomal interactions. Indeed, not only do post-translational modification of histone proteins directly alter chromatin architecture (through altering histone-DNA, histone-histone and histone-non histone interactions), they can also be recognised by non-histone protein complexes. This “histone code hypothesis” proposes that the number, location and pattern of modifications act as a code, which can be “read” by protein complexes and can directly modulate gene expression through their chromatin-remodelling and histone-modifying properties (Strahl & Allis, 2000).

More than 60 different histone residues have been identified which are the targets for covalent modification including acetylation, methylation, phosphorylation, ubiquitylation, sumoylation, arginine deamination, ADP-ribosylation and proline isomerisation (summarised in Table 1.1)

Modification	Histone	Residue	Effect on transcription	Common location
DNA methylation		CpG dinucleotides	Repression	Heterochromatin
Acetylation	H2A	K5	Activation	
	H2B	K5, K12, K15, K20	Activation	
	H3	K4, K9, K14, K18, K36, K56	Activation	Euchromatin
	H4	K5, K8, K12, K16	Activation	Euchromatin
Methylation	H3	K4, K36, K79	Activation	Euchromatin
		K9, K27	Repression	Heterochromatin
		R2, R17	Activation	
	H4	K20	Repression	
		R3	Activation	
Phosphorylation	H2A	S1, T120	Mitosis	
	H3	T3, T11, S10	Mitosis	
		S28	Activation	
	H4	S1	Activation	
		S10	Mitosis	
Ubiquitylation	H2A	K119	Repression	
	H2B	K120	Activation	
Sumoylation	H2A	K126	Repression	
	H2B	K6, K7	Repression	
	H4		Repression	

Table 1.1 Post-translational modification of histone tails and their functional outcomes. H: histone, K: lysine, R: arginine, S: serine, T: threonine. Adapted from Kouzarides, 2007.

(Kouzarides, (2007). Chromatin state (actively transcribed euchromatin or inactive heterochromatin) is associated with distinct set of histone modifications. Typically, histone hyperacetylation and tri-methylated H3K4, H3K36 and H3K79 are associated with euchromatic regions whereas heterochromatin is typically associated with histone hypoacetylation and elevated H3K9, H3K27 and H4K20 methylation.

1.2.1 Acetylation

Histone acetylation occurs on ε amino groups of evolutionarily conserved lysine residues in the N-terminal tail of histone proteins: lysine 4, 9, 14, 18, 23, 27 and 36 on histone H3 and lysine 5, 8, 12 and 16 of histone H4. Steady state levels are controlled through the action of two opposing families of enzymes: histone acetylatransferases (HATs) and histone deacetylases (HDACs) (FIGURE 1.2).

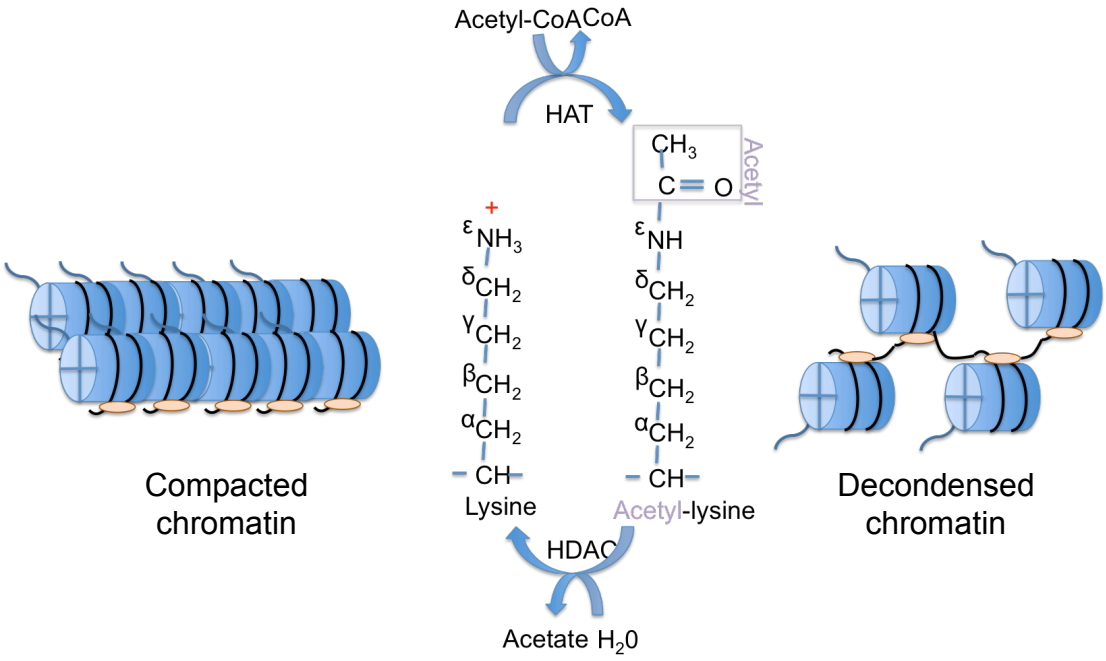

Figure 1.2 Steady state acetylation of lysine residues. The reaction is maintained by histone acetyltransferases (HATs), which catalyse the addition of an acetyl group to lysine residues, and histone deacetylases (HDACs), which remove the moiety.

HATs catalyse the addition of an acetyl group to lysine residues, which causes neutralisation of the positive charge on histone tails. Consequently, the electrostatic interaction between negatively charged DNA and positively charged histone proteins is weakened thus compacted chromatin becomes loosened, facilitating access to transcriptional activators. HATs can be classified into three families: general control non-derepressible 5 (Gcn5)-related N-acetyltransferases (GNATs), p300/CBP

and MYST proteins (Sterner & Berger, 2000). Broadly speaking, HATs can be also classified into two categories: type A proteins which are located in the nucleus and catalyse the acetylation of nucleosomal histone proteins or type B enzymes which acetylate newly synthesised free histones in the cytoplasm for transport into the nucleus (Garcea & Alberts, 1980; Ruiz-Carrillo *et al.*, 1975). Conversely, HDACs (discussed in more detail later) deacetylate histone proteins, restoring the positive charge on the protein, inducing chromatin compaction and gene silencing.

1.2.2 Phosphorylation

Phosphorylation of serine, threonine and tyrosine residues is also associated with transcription activation. The reaction is catalysed by protein kinases which cause the addition of a phosphate group to residues, creating a negative charge on histone tails and thereby loosening the DNA-histone interaction and promoting gene transcription (Rossetto *et al.*, 2012). Phosphorylation of H3S10, T11 and S28 have been shown to be coupled with H3 acetylation, implicating phosphorylation in transcriptional activation. Indeed, phosphorylation of H3S10 promotes acetylation of H3K14 by Gcn5 *in vitro* and allows Gcn5-regulated gene transcription *in vivo* (Lo *et al.*, 2000; Zhong *et al.*, 2003). However, despite the association with transcriptional activation, H3S10 has also been associated with chromosome condensation and is required for proper chromosome segregation *in vivo* (Wei *et al.*, 1999) suggesting that the effect of this post-translational modification is context-dependent.

1.2.3 Ubiquitylation

Ubiquitylation, the addition of a 76 amino acid polypeptide ubiquitin, and sumoylation, the addition of the structurally related small ubiquitin-related modifier (SUMO) protein occurs on the ε amino group of lysine residues. Although histone proteins can be poly-ubiquitylated, the most prevalent form of the modification is mono-ubiquitylated lysine 119 of histone H2A and lysine 120 of histone H2B. Histone H2A mono-ubiquitylation is mediated by the Ring1b (E3 ligase), found within the polycomb repressive

complex 1 (PRC1), suggesting ubiquitylation is associated with transcriptional repression (Wang *et al.*, 2004). However, modification of histone H2B is correlated with the activation of HOX gene expression (Zhu *et al.*, 2005) suggesting that the modification is context dependent. In addition to this, core histone proteins H3 and H4 as well as linker histone H1 can also be modified. Reduction of histone H3 and H4 ubiquitylation impairs the recruitment of the repair protein XPC to damaged foci suggesting the modification participates in the cellular response to damage (Wang *et al.*, 2006).

1.2.4 Methylation

Methylation of histone proteins can occur on both lysine and arginine residues, and unlike phosphorylation and acetylation which both alter the charge of histone proteins, does not substantially alter the charge of the residue. Instead, methylation serves to provide binding sites for proteins containing chromatin-remodelling abilities, for example, H3K4 methylation marks can be recognised by the chromodomain-containing protein CHD1, an ATP-dependent remodelling protein. Lysines can be unmethylated (me0), mono-methylated (me1), di-methylated (me2) and tri-methylated (me3) whereas arginine residues can be mono-methylated (Rme1) or symmetrically (Rme2s) and asymmetrically (Rme2as) di-methylated. Catalysis occurs in a highly specific reaction by lysine (KMTs) and arginine methyltransferases (PRMTs) respectively.

All lysine methyltransferases, with the exception of DOT-1, contain a highly conserved SET (Su(var)3-9, Enhancer of Zeste and Trithorax) domain which is essential for enzymatic activity and catalyse the addition of S-adenosylmethionine (SAM) to the ε amino group of lysine residues (Dillon *et al.*, 2005; Shi *et al.*, 2004)ω-guanidino group of arginine.

Originally, the methylation status of histones was believed to be irreversible until the discovery of the first lysine demethylase, LSD1, in 2004 which catalyses the removal of methyl groups from H3K4me1/2 but

not H3K4me3 (Shi *et al.*, 2004). Following this, the identification of JMJD2, a member of the Jumonji-domain containing family of enzymes, which is responsible for the demethylation of tri-methyl lysine residues (Tsukada *et al.*, 2006), suggested that methylation of histone proteins is a dynamic process.

The transcriptional effect of lysine methylation is dependent on both the residue and number of methyl moieties present: transcriptional activation is associated with H3K4, H3K36 and H3K79 methylation, whereas H3K9, H3K27 and H4K20 methylation is associated with transcriptional repression. The association with both transcriptional activation and repression highlights the complexity of all the histone modifications which often work in a combinatorial fashion to reinforce their action (Strahl & Allis, 2000).

1.3 Histone deacetylases (HDACs)

HDACs were first identified in 1996 by Taunton *et al.* using the HDAC inhibitor trapoxin as an affinity tag (Taunton *et al.*, 1996). The protein was found to be an orthologue of the yeast protein Rpd3, which had previously been shown to be a global gene regulator, suggesting that HDACs themselves are involved in control of gene expression. Following this, the mammalian genome has been shown to encode 18 HDAC enzymes which can be classified into two groups: the “classical” HDAC family (Class I, Class IIa, Class IIb and Class IV) which are reliant on Zn^{2+} for their enzymatic activity, and the Sirtuins (Class III) which are NAD^{+} dependent. The work in this thesis will focus on the classical HDAC family, in particular the Class I HDAC family member HDAC3.

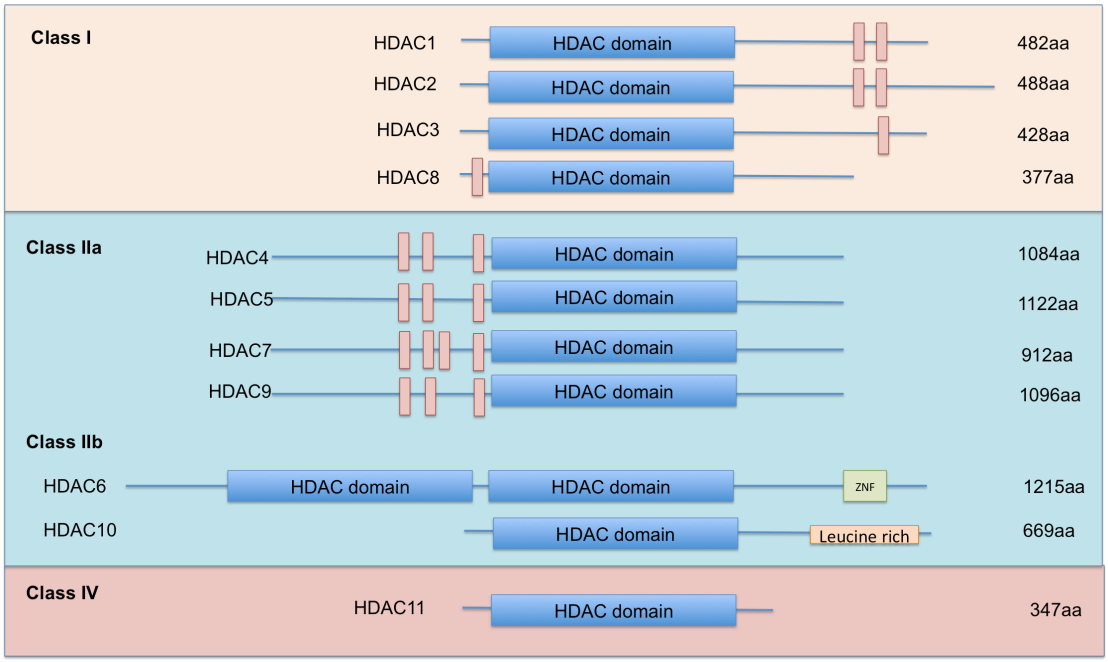

Figure 1.3 Classification of the classical histone deacetylase (HDAC) family. Mammalian HDACs are classified according to their homology to the yeast HDACs Hda1 and Rpd3. Dark blue bars represent the deacetylase domain and pink boxes denote serine phosphorylation sites. Also indicated are the leucine rich (orange) and zinc finger (green) domains in the class IIb HDACs HDAC6 and -10.

1.3.1 Classical HDAC family classification

The classical HDAC family is subdivided into four classes dependent on their homology with yeast deacetylases, Rpd3 (class I) and Hda1 (Class II) (FIGURE 1.3). Class I HDACs (HDAC1, 2, 3 and 8) are ubiquitously expressed nuclear enzymes. All Class I HDACs, except HDAC8 which is active in isolation, requires incorporation into a higher-order multi-protein complexes which are targeted to DNA in a sequence-specific fashion to achieve protein activation (Thiagalingam *et al.*, 2000). The catalytic domain of class I HDACs is highly conserved with yeast Rpd3 (greater than 80% sequence homology for HDAC1 and HDAC2 and greater than 65% sequence homology for HDAC3 and HDAC8). The domain is formed by a 390 amino acid sequence forming a tubular pocket containing evolutionarily conserved histidine, aspartic acid and tyrosine residues which form a charge relay mechanism requiring the presence of a Zn^{2+} atom which is located at the bottom of the pocket for catalysis (Finnin *et al.*, 1999).

HDAC1 and HDAC2 are highly conserved proteins with around 82% sequence similarity which arose due to the duplication of an ancestral gene (Brunmeir *et al.*, 2009). Due to a high level of sequence similarity, both enzymes exhibit functional redundancy in most instances with a compensatory effect observed in the absence of one or other of the enzymes; however, in certain physiological conditions, for example during embryogenesis (Lagger *et al.*, 2002) or the differentiation of embryonic stem cells (Dovey *et al.*, 2010), HDAC1 and 2 have highly specific functions independent of each other. HDAC3 shares 68% sequence homology with HDAC1 and -2 and is found exclusively in the SMRT/NCoR co-repressor complex (Guenther *et al.*, 2000; Li *et al.*, 2000) unlike HDAC1/2 which are found in 4 distinct co-repressor complexes: Sin3, NuRD, CoREST and MiDAC (Laherty *et al.*, 1997; Xue *et al.*, 1998; Bantscheff *et al.*, 2011). Finally, HDAC8 is most closely related to HDAC3 with 34% sequence identity and is fully functional in isolation (Hu *et al.*, 2000).

Class II HDACs are subdivided into two groups (IIa: HDAC4, -5, -7 and -9 and IIb: HDAC6 and -10) which share homology with the yeast deacetylase HDA1. Unlike class I HDACs which are found exclusively in the nucleus, localisation of class II HDACs is mediated directly through the binding of the chaperone 14-3-3 proteins upon phosphorylation by calcium/calmodulin-dependent kinase (CaMK) or protein kinase D (PKD). This blocks the nuclear localisation sites of the enzyme and shuttling to the cytoplasm (Grozinger & Schreiber, 2000); de-phosphorylation of the enzyme releases HDAC:14-3-3 binding exposing nuclear localisation sites and permits shuttling into the nucleus to modulate gene transcription. Similarly, the expression of class II HDACs is tissue-specific unlike class I HDACs with HDAC4, -5 and -9 being specifically expressed in the brain, muscle and heart whereas HDAC7 is expressed in thymocytes and endothelial cells (Zhang *et al.*, 2002; Vega *et al.*, 2004; Mejat *et al.*, 2005). HDAC6 is a cytoplasmic deacetylase which catalyses α-tubulin deacetylation. Uniquely, HDAC6 contains two deacetylase domains and a C-terminal zinc finger motif which can bind polyubiquitin (Hook *et al.*, 2002). HDAC10 is most similar to HDAC6 at its N terminus with its C terminus being leucine rich and exhibiting limited sequence similarity (Tong *et al.*, 2002; Guardiola & Yao, 2002).

HDAC11 is the sole member of class IV HDACs and contains a short N terminal domain and a deacetylase domain which is related to both class I and II HDACs (Gao *et al.*, 2002). Functionally, little is known about HDAC11 although recent work suggests that it negatively regulates expression of interleukin 10, and thus mediates immune system activation (Villagra *et al.*, 2009).

1.3.2 Class I HDAC co-repressor complexes

Due to a lack of a DNA-binding motif, all class I HDACs (except HDAC8) are targeted to DNA through incorporation into multi-protein co-repressor complexes (FIGURE 1.4). HDAC1 and HDAC2 are found as the catalytic component of the Sin3, NuRD, CoREST and MiDAC complexes

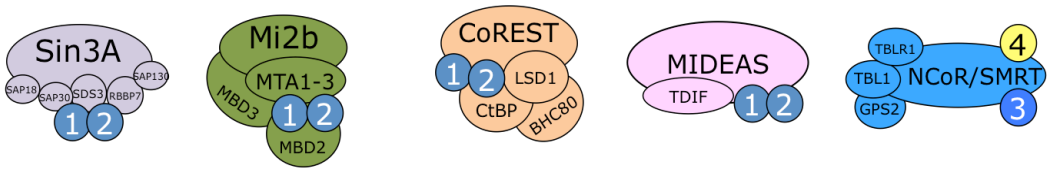

Sin3 Mi2/NURD CoREST MIDAC NCoR/SMRT

Complex	Component	Enzymatic activity/modification domain
SMRT/NCoR	**HDAC3**	deacetylase
	HDAC4	deacetylase
	SMRT/NCoR	ELM2-SANT domain
	TBL1/TBLR1	WD40 domain
	GPS2	
	Kaiso	Methyl CpG binding
	JMJD2A	PHD finger/Tudor domain
Sin3	**HDAC1**	deacetylase
	HDAC2	deacetylase
	RbAp46, RbAp48	WD40 domain
	Sin3A	PAH motifs
	SDS3	
	RBP1	
	SAP18	Ubiquitin fold
	SAP30	
	ING1/2	PHD finger
NuRD	**HDAC1**	deacetylase
	HDAC2	deacetylase
	RbAp46, RbAp48	WD40 domain
	Mi2α/β	ATP-dependent helicase
	MTA1/2/3	ELM2-SANT
	MBD2/3	Methyl CpG binding
	P66α/β	
CoREST	**HDAC1**	deacetylase
	HDAC2	deacetylase
	CoREST	ELM2-SANT domain
	LSD1	Histone lysine demethylase / SWIRM domain
	BHC80	PHD finger
	CtBP	Dehydrogenase
MiDAC	**HDAC1**	Deacetylase
	HDAC2	Deactylase
	MIDEAS	ELM2-SANT domain
	TDIF	SKI/SNO/DAC domain

Figure 1.4 Class I HDAC co-repressor complexes. Schematic shows core co-repressor components; tables shows detailed list of components and protein binding domains (Adapted from Yang, X and Seto, E., 2009).

(Laherty *et al.*, 1997; Xue *et al.*, 1998; Bantscheff *et al.*, 2011) whereas HDAC3 is found exclusively in the SMRT/NCoR complex (Li *et al.*, 2000).

1.3.2.1 SMRT/NCoR complex

HDAC3 interacts directly with silencing mediator of retinoid and thyroid receptor (SMRT) and nuclear receptor corepressor (NCoR), two homologous proteins containing nuclear receptor interaction domains as well as multiple repressor domains (Park *et al.*, 1999; Ordentlich *et al.*, 1999; Jepsen *et al.*, 2000; Jepsen *et al.*, 2007). Activation of HDAC3 is facilitated through the direct interaction of the deacetylase activation domain (DAD) found in SMRT/NCoR, composed of a 16 amino acid DAD-specific motif as well as a C terminal Swi3 ADA2 NCoR TFIIB (SANT)-like motif (Guenther *et al.*, 2001; Codina *et al.*, 2005). Also found within the complex are transducin β-like 1 (TBL1), TBL1-related protein (TBLR1) and G-protein pathway suppressor 2 (GPS2) in a 1:1 stoichiometric ratio which are critical for targeting the complex to chromatin (TBL1/TBLR1) and stabilisation of the complex (GPS2) (Yoon *et al.*, 2003; Guenther *et al.*, 2000; Zhang *et al.*, 2002).

1.3.2.1.1 Identification of HDAC3

HDCA3 was initially cloned based on the sequence similarity it shares with previous identified histone deacetylases, HDAC1 and -2 (Yang *et al.*, 1997; Dangond *et al.*, 1998). Functional analysis of the protein indicated that it shared common features with HDAC1 and -2, primarily through it was able to deacetylate histone substrates, bring about transcriptional repression when targeted to gene promoters and being able to physically interact with the transcription factor YY1 (Emiliani *et al.*, 1998) suggesting that the proteins was involved in the regulation of gene expression. Immunoaffinity purification studies indicated that the enzyme formed a stable ternary complex with SMRT and NCoR (Guenther *et al.*, 2001; Li *et al.*, 2000) and acts as the catalytic component of the complex.

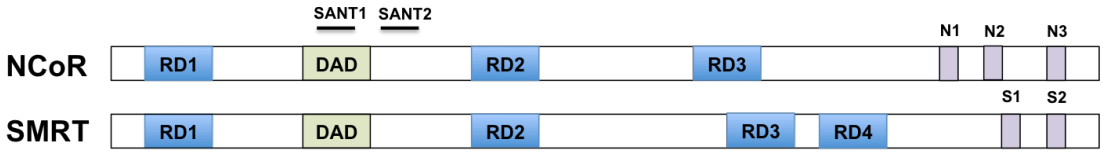

Figure 1.5 Schematic of the NCoR and SMRT co-repressor proteins. The primary structure of NCoR and SMRT are depicted with the locations of the repression domains (RD1-4; blue), the deacetylase activation domain (DAD; green), conserved SANT domains and the co-repressor motif (CoRNR; purple; N1-3 in NCoR and S1-2 in SMRT) shown.

1.3.2.1.2 SMRT and NCoR

SMRT and NCoR co-repressor proteins share approximately 45% amino acid sequence identity with each other with multiple isoforms being generated through alternative splicing (Privalsky, 2004). Structurally, they are highly similar, containing nuclear receptor interacting domains as well as multiple repressor domains (FIGURE 1.5). It is such domains that nucleate the assembly of the higher order co-repressor complex to bring about regulation of gene expression.

Both proteins are essential for embryonic development; however, although the proteins share many functions, they are not completely redundant. Indeed, homozygous deletion of both proteins is embryonic lethal. SMRT knockout mice exhibit lethality at e16.5 due to defects in cardiogensis including ventricular septation and hypoplasia of the ventricular chambers whereas NCoR knockout mice exhibit lethality a day earlier than SMRT-deficient embryos, typically by e15.5 (Jepsen *et al.*, 2000; Jepsen *et al.*, 2007). Embryos exhibit a wide variety of phenotypic defects including smaller livers, anaemia due to erythropoietic defects, defects in T-cell development, lower thymocytes counts and major aberrations in nervous

system development suggesting that NCoR regulates a number of essential developmental pathways independent of SMRT.

1.3.2.1.2 Co-repressor complex activity

Both the SMRT and NCoR complexes serve as key co-regulator complexes for a variety of transcription factors including nuclear hormone receptors, ETO1/2 and c-Jun, which recruit the complexes to modify chromatin and thereby regulate the transcription of key target genes. For example, in the absence of a ligand, SMRT and NCoR bind in the hydrophobic groove of the ligand binding domain of nuclear receptor proteins through a set of C-terminal LxxxIxxx(I/L) co-repressor motif (CoRNR) motifs (Hu & Lazar, 1999; Nagy *et al.*, 1999).

Activity of HDAC3 is dependant on the interaction of the protein with SMRT/NCoR. Recombinant HDAC3 is enzymatically inactive but interaction with its cognate co-repressor proteins potentiates HDAC3 activity confirming the role of both SMRT and NCoR is greater than the recruitment of HDAC3 to gene promoters (Wen *et al.*, 2000; Guenther *et al.*, 2001). Initial mapping of the HDAC3/SMRT binding site by Guenther *et al.* identified a highly conserved region present in both SMRT and NCoR, the DAD. This contains the first SANT motif found in the N-terminus of SMRT, which is also conserved in NCoR. Later, this region was found to form a unique four helical structure and undergo extensive conformational changes upon binding to HDAC3 such that the region wraps around the surface of the enzyme (Codina *et al.*, 2005; Watson *et al.*, 2012)

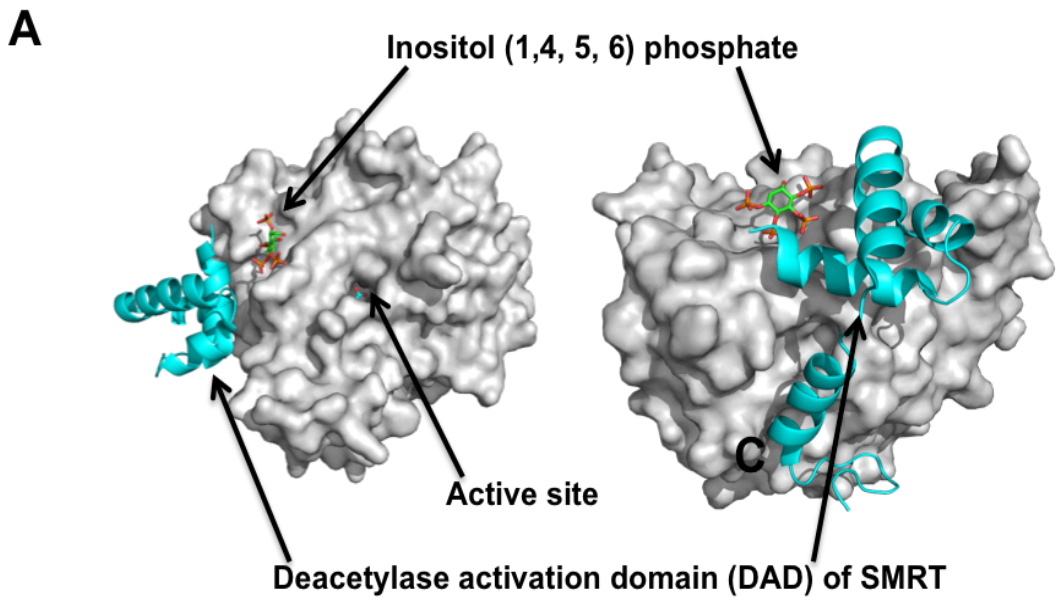

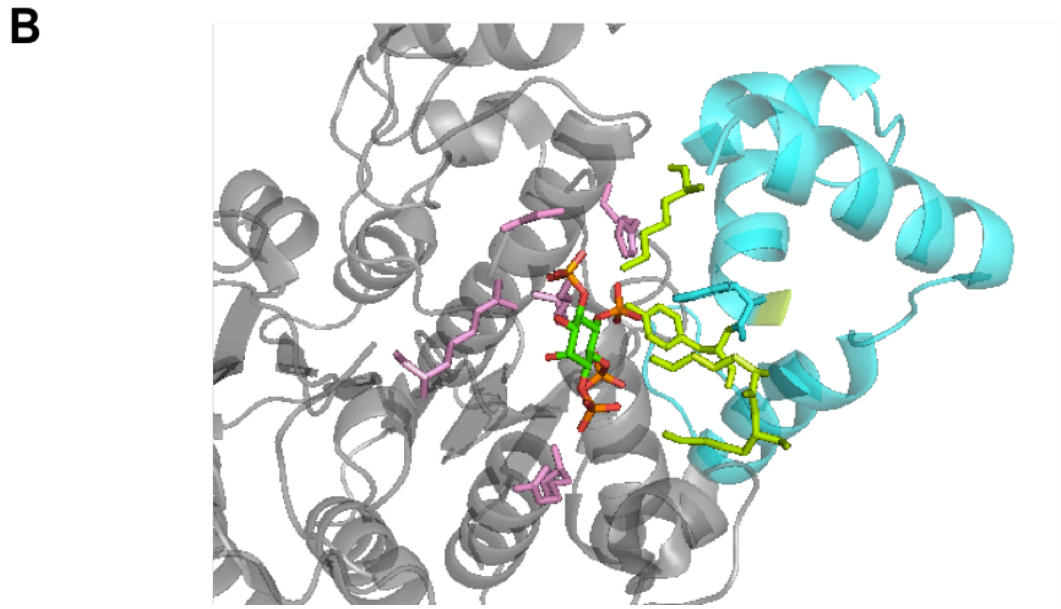

Figure 1.6 Structure of the HDAC3:SMRT complex. (A) Interaction of the DAD of SMRT (cyan; ribbon) with HDAC3 (grey; surface) with Ins (1, 4, 5, 6) P_4 at the protein interface (stick). (B) HDAC3 residues (pink; His 17, Gly 21, Lys 25, Arg 265, Arg 301) and SMRT (green; Lys 449, Tyr 470, Tyr 471, Lys 474 and Lys 475) that mediate the interaction are shown. PDB code: 4A69).

Structural studies also confirmed the presence of a molecule of inositol phosphate at the protein interface of the two proteins (Watson *et al.*, 2012). This could be unambiguously assigned as inositol 1, 4, 5, 6 tetrakisphosphate (Ins (1,4,5,6,) P_4) and binds in a highly basic pocket acting as a bridging molecule between the two complex components. Here, it makes extensive interactions with the two proteins (FIGURE 1.6B), each which contribute five hydrogen bonds and salt bridges to the Ins (1,4,5,6) P_4 molecule (His 17, Gly 21, Lys 25, Arg 265, Arg 301 of HDAC3 and Lys 449, Tyr 470, Tyr 471, Lys 474 and Lys 475 of SMRT). Enzyme activity is dependent on the presence of IP suggesting a potential regulatory mechanism of HDAC3 by IP (Watson *et al.*, 2012; Watson *et al.*, 2016).

HDAC3 activity has also been shown to be regulated by phosphorylation and de-phosphorylation. Serine 424, an unconserved residue among the class I HDACs, can be post-translationally modified by CK2, which induces the phosphorylation of the residue to upregulate HDAC3 activity. Conversely, HDAC3 has been shown to co-purify with the catalytic and regulatory subunits of the proteins serine/threonine phosphatase 4 complex which catalyses the removal of the modification (Zhang *et al.*, 2005).

1.3.2.2 Sin3 complex

The Sin3 complex was first identified by Ayer *et al.,* where it was found to mediate transcriptional repression via the basic region- helix-loop-helix-leucine zipper (bHLH-ZIP) protein Max, which heterodimerises with bHLH-ZIP family member Mad (Ayer *et al.*, 1995). Homologous to the yeast general transcriptional repressor, both mammalian isoforms, Sin3A and Sin3B, contain four highly conserved paired amphipathic helix (PAH) domains in addition to an HDAC interaction domain (HID) (Laherty *et al.*, 1997). It is the HID that facilitates binding of HDAC1/2 and is essential for

the repressive activity of the Sin3 complex. In addition to HDAC1/2 binding, the HID also potentiates binding of multiple other interacting proteins thus Sin3 acts as a central scaffold upon which different protein components are assembled (Grzenda *et al.*, 2009). The core complex components also contain Sin3 associated proteins (SAP) -18 and -30, suppressor of defective silencing 3 (SDS3) and retinoblastoma associated proteins, RbAp46/48 which are all involved in mediating the protein interactions within the complex as well as maintaining the integrity of the complex and stabilising the interaction with the nucleosome.

1.3.2.3 NuRD complex

The NuRD (nucleosome remodelling and histone deacetylation) complex functions to remodel chromatin in addition to directly modifying histones (Xue *et al.*, 1998). Several core components are shared with Sin3, namely HDAC1/2 and RbAp46/48 although other proteins are found exclusively within the complex (MTA and MBD proteins). MTA family members (MTA1, 2 and3) facilitate the interaction with HDAC1/2 through the presence of an ELM2-SANT domain which directly binds and activates the enzyme in an inositol phosphate dependent manner (Millard *et al.*, 2013). The MBD2/3 subunits belong to the methyl CpG binding domain family, suggesting that the complex is able to read the DNA methylation environment. Functional diversity of the complex is achieved through the presence of Mi2α/β, a member of the SWI/SNF family which promotes nucleosome remodelling in an ATP-dependent fashion (Bowen *et al.*, 2004). A variant of the NuRD complex which lacks MBD3 but also binds Oct4 and Nanog, the Nanog and Oct4-associated deacetylase (NODE) complex has been identified in ES cells, where it mediates repression of Oct4 and Nanog target genes. Knockdown of NODE components results in the spontaneous differentiation of ES cells to endodermal cells suggesting that NODE functions to repress developmental genes in undifferentiated cells (Liang *et al.*, 2008).

1.3.2.4 CoREST complex

CoREST was originally identified as a co-repressor of REST (RE-1 Silencing Transcription Factor), a transcription factor that plays a key role in the regulation of neuronal gene expression in non-neuronal cells (Andres *et al.*, 1999). It was subsequently found to be a component of an HDAC1/2- containing complex (You *et al.*, 2001) in which HDAC1/2 directly interact with the CoREST protein through the presence of an ELM2-SANT domain in the N-terminus of the protein. The complex is functionally diverse since it also contains demethylase activity due to the presence of LSD1 within the complex (Foster *et al.*, 2010), thus the complex functions to regulate neural gene expression through both the deacetylation and demethylation of histone proteins.

1.3.2.5 MiDAC complex

The mitotic deacetylase complex (MiDAC) is a novel HDAC-containing complex which was first identified in a chemoproteomics screen using a range of HDAC inhibitors as bait (Bantscheff *et al.*, 2011). The same study also showed that the complex is upregulated in cells arrested in mitosis and specifically associated with Cyclin A suggesting it is a mitotic-specific HDAC-containing complex. The complex is composed of three core proteins: the catalytic component HDAC1, Mideas, an ELM2-SANT containing protein which binds and activates the enzyme in an inositol phosphate dependent manner (analogous to the NuRD complex), and DNTTIP1, which contains a dimerization domain and DNA binding motif to target the complex to chromatin (Itoh *et al.*, 2015).

1.3.3 HDACs and transcription

It has been widely accepted that there is a correlation between local histone acetylation status and gene transcription. Deacetylation of histone tails by HDACs induces a closed conformation of chromatin and gene repression since the electrostatic potential of unacetylated lysine residues promotes inter-nucleosomal interactions (Luger & Richmond, 1998) whereas acetylation of histone tails by histone acetyltransferases (HATs)

promotes the relaxation of chromatin promoting gene expression. However, studies of the yeast deacetylase Rpd3, found that deletion of the enzyme resulted in the downregulation of more genes than were upregulated (Bernstein *et al.*, 2000). Analogously, treatment of yeast with the broad-spectrum HDAC inhibitor trichostatin A (TSA) also resulted in the down regulation of genes within 15 minutes, a trend that has been identified in other studies (Peart *et al.*, 2005). Furthermore, mapping of both Rpd3 and HDAC1 binding sites through chromatin immunoprecipitation experiments identified that both enzymes are predominantly bound at transcriptionally active genes (Kurdistani *et al.*, 2002; Wang *et al.*, 2009) suggesting that in addition to a traditional role in gene repression, HDACs also play a role in gene activation. Due to the association of HDACs with transcriptionally active genes, particularly with the co-localisation of HATs e.g. CBP, p300 at the same loci, it has been proposed that gene activation requires the actions of both enzymes in a cyclical fashion. The recruitment of HDACs to active genes is believed to reset chromatin state following transcription initiation by RNA polymerase II, in order to permit additional rounds of transcription (Dovey *et al.*, 2010).

1.4 HDAC knockout mice

In the mouse, the germline deletion of all of the classical HDAC family members (with the exception of HDAC10 and -11) has been assessed (summarised in TABLE 1.2). All class I HDACs results in embryonic lethality confirming an essential role for each enzyme in embryogenesis. Loss of HDAC1 results in embryonic lethality by embryonic day e10.5 as a result of growth retardation and proliferation defects (Lagger *et al.*, 2002). HDAC3 null animals also exhibit lethality around this time (embryonic day e9.5), close to the onset of gastrulation, suggesting that HDAC3 may play a role in gastrulation (Montgomery *et al.*, 2008; Bhaskara *et al.*, 2008). Conversely, loss of both HDAC2 and HDAC8 results in lethality later on in development. HDAC2 knockout animals exhibit lethality perinatally due to severe cardiac defects as the result of uncontrolled proliferation of ventricular cardiomyocytes (Montgomery *et al.*, 2007), or partial

embryonic lethality or death in adulthood (Trivedi *et al.*, 2007; Zimmermann *et al.*, 2007) depending on the knockout strategy utilised. Similarly, HDAC8 null animals results in perinatal lethality due to a highly specific deficiency of cranial neural crest cells (NCCs) resulting in skull instability and craniofacial defects (Haberland *et al.*, 2009); this result was phenocopied in a conditional knockout model of the enzyme in cranial neural crest cells and correlated with the de-repression of homeobox transcription factors Otx2 and Lhx1, found specifically in NCCs, which have been implicated in the patterning of the skull.

Class II HDAC knockout models have also been created. HDAC5, HDAC6 and HDAC9 null animals remain viable whereas loss of both HDAC4 and HDAC7 result in lethality. HDAC4 has been shown to play an essential role in the formation of the skeleton through negative regulation of Runx2, which regulates chrondocyte hypertrophy (Vega *et al.*, 2004). Loss of HDAC4 results in the premature ossification of developing bone and mice die by postnatal day 10. Conversely, HDAC7 null mice exhibit embryonic lethality at day e11 due to a failure in endothelial cell-cell adhesion resulting in dilation and rupture of the blood vessels due to de-repression of MMP10 (Chang *et al.*, 2006).

Class	Deacetylase	Lethality timing	Phenotype
I	HDAC1	E10.5	Proliferation defects
	HDAC2	Perinatal	Cardiac defects
	HDAC3	E9.5	Gastrulation defects
	HDAC8	Perinatal	Craniofacial defects
IIa	HDAC4	Perinatal	Chrondrocyte hypertrophy
	HDAC5	Viable	Stress-induced cardiac hypertrophy
	HDAC7	E11	Cardiovascular defects: impaired vascular integrity
	HDAC9	Viable	Stress-induced cardiac hypertrophy
IIb	HDAC6	Viable	Global α-tubulin hyperacetylation
	HDAC10	-	-
IV	HDAC11	-	-

Table 1.2: Summary of germline deletion of HDAC knockout mice. Adapted from Haberland, M. *et al*., 2009.

1.4.1 HDAC3 conditional knockout studies

To circumvent embryonic lethality and dissect the functional role of HDAC3 further, conditional knockout systems have been utilised in which HDAC3 has been deleted tissue specifically. Targeted deletion of HDAC3 in the liver resulted in hypertrophy of hepatocytes, which correlated with altered metabolism of both carbohydrates and lipids in addition to disruption in circadian rhythms (Knutson *et al.*, 2008; Montgomery *et al.*, 2008; Feng *et al.*, 2011). Similarly, cardiac-specific deletion of HDAC3 resulted in cardiomyocyte hypertrophy and the upregulation of genes associated with fatty acid uptake and oxidation (Montgomery *et al.*, 2008),

suggesting that HDAC3 plays a key role in the regulation of metabolic processes. HDAC3 has also been implicated in the regulation of the cell cycle. Loss of HDAC3 in mouse embryonic fibroblasts (MEFs) results in a delay in S-phase progression, cell-cycle dependent DNA damage and defective DNA double-strand break repair resulting in apoptosis (Bhaskara *et al.*, 2008). A similar defect in S-phrase progression was identified in $HDAC3^{-/-}$ haematopoietic stem cells which failed to efficiently replicate their DNA *in vitro* and subsequently failed to proliferate resulting in a dramatic loss of B and T cells (Summers *et al.*, 2013). Additionally, HDAC3 functions in macrophages to regulate inflammatory gene expression by binding to a subset of macrophage specific genes including interleukin 4 (IL-4) marked by the transcription factor Pu.1 where it deacetylates histone tails to prevent gene transcription (Mullican *et al.*, 2011). Loss of HDAC3 results in IL-4 expression and subsequent activation of macrophages.

1.5 Mouse embryonic stem (ES) cells

Mouse embryonic stem (ES) cells are derived from the inner cell mass (ICM) of the 32-64 cell stage pre-implantation embryo (blastocyst) (Evans & Kaufman, 1981). Ultimately, these cells will give rise to the embryo proper and trophectaderm which will form extra-embryonic tissue, including the placenta. Importantly, stem cells have two distinct properties that distinguish them from other cell types: firstly, cells retain the ability to self-renew and thus are capable of continually dividing indefinitely whilst maintaining a normal karyotype. Secondly, cells are pluripotent and can differentiate into all the cell types of an organism. Embryonic stem cells *in vitro* are able to differentiate readily into the three primary germ layers (mesoderm, endoderm and ectoderm), a highly controlled process influenced by cell-cell interaction and signalling known as gastrulation in the developing embryo (Tam & Behringer, 1997). Accordingly, ES cells are an ideal model system for examining the stage of early embryonic development and lineage induction (Smith, 2001).

1.5.1 Pluripotency

ES cell pluripotency was initially maintained *in vitro* through the co-culture of cells with mouse embryonic feeder cells (Evans & Kaufman, 1981). However, later studies identified that the signalling molecule, leukemia inhibitory factor (LIF), was essential for the maintenance of these cells *in vitro;* supplementation of recombinant LIF to culture media facilitates the growth of undifferentiated ES cells in the absence of feeder cells (Smith *et al.*, 1988; Williams *et al.*, 1988). LIF functions to initiate signalling via the gp130 receptor resulting in activation of the STAT3 pathway thereby promoting pluripotency (Niwa *et al.*, 1998). Pluripotency is also maintained through the BMP4-SMAD signalling pathway, resulting in the induction of the helix-loop-helix 'induction-of-differentiation' (Id) factors that suppress ectodermal differentiation (Ying *et al.*, 2003).

Both of these pathways override the MAPK and Wnt signalling pathways, which induce differentiation rather than self-renewal of ES cells which explains why there is always a heterogeneous population of cells in culture of both undifferentiated and partially differentiated ES cells (FIGURE 1.7). Autocrine production of fibroblast growth factor 4 (FGF4) by ES cells causes the activation of MAPK signalling. Loss of FGF4 in ES cells or treatment with FGF receptor inhibitors prevents both neural and mesodermal induction suggesting that FGF/MAPK signalling promotes differentiation of ES cells (Kunath *et al.*, 2007).

ES self-renewal can be maintained in culture through the addition of highly selective inhibitors (semi-defined 3i culture conditions), which block differentiation inducing signalling (Ying *et al.*, 2008). Addition of MEK (PD0325901), FGF (SU5402) and GSK (CHIR99021) inhibitors (3i) sustains ES self-renewal in the presence of LIF. Addition of a GSK inhibitor acts to promote the stabilisation of β-catenin and its translocation to the nucleus where it interacts with Tcf family member, Tcf3, which directly represses key pluripotency factors (Martello *et al.*, 2012). Interaction of the two proteins ablates repression by Tcf3 by dissociation of the repressor protein from its DNA binding sites thereby promoting ES

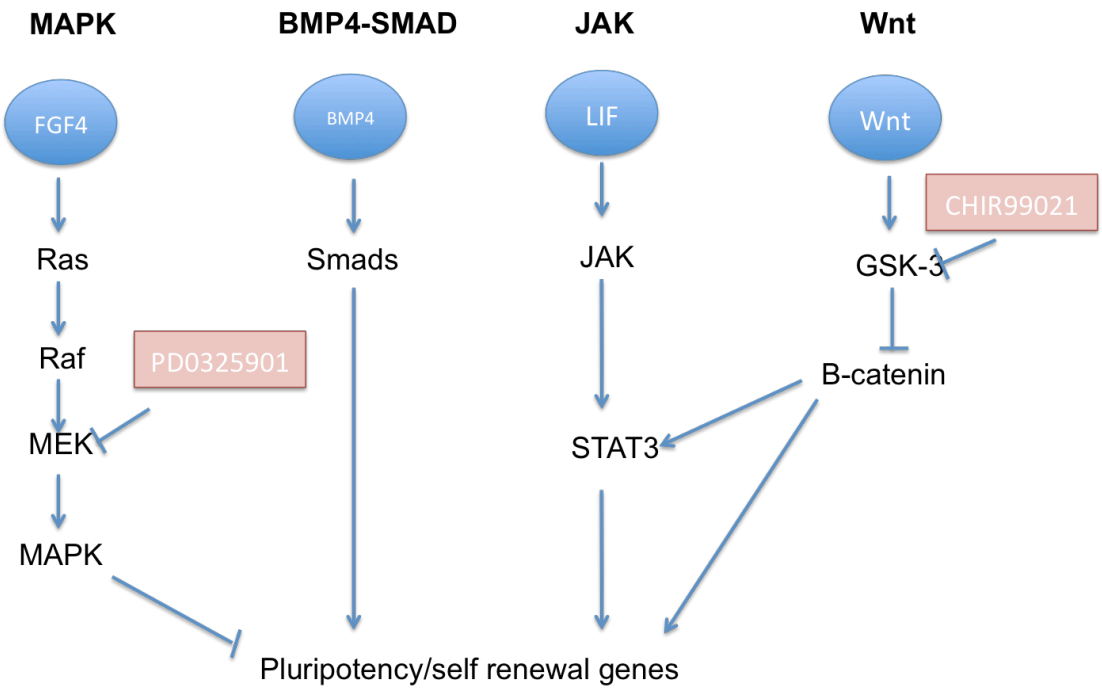

Figure 1.7: Signalling pathways involved in ES cell pluripotency. Pluripotency is maintained by BMP4-SMAD signalling and JAK pathways signalling whereas differentiation of ES cells is driven by MAPK and Wnt signalling.

cell self-renewal. More recently, cell culture conditions containing just MAPK and GSK3 inhibitors (2i) is sufficient to maintain the expansion of undifferentiated ES cells in the "naïve ground state" i.e. a homogenous population of ES cells exhibiting low levels of DNA methylation and the downregulation of *de novo* DNA methyltransferases Dnmt3a, Dnmt3b and Dnmt3l (Leitch *et al.*, 2010).

ES cell pluripotent identity is maintained transcriptionally through the expression of a group of key transcription factors including Oct4 (*Pou5f1*), Nanog and Sox2 (Niwa *et al.*, 1998; Nichols *et al.*, 1998; Avilion *et al.*, 2003; Rodda *et al.*, 2005). Oct4 is a member of the POU family and is an essential transcription factor during embryogenesis where expression is restricted to the inner cell mass and epiblast (Niwa *et al.*, 1998). Loss of Oct4 *in vivo* (in the epiblast) and *in vitro* (ES cells) causes pluripotent cells

to revert to the trophoblast lineage, whereas overexpression above endogenous levels results in differentiation towards extra-embryonic and mesodermal lineages, suggesting the balance of Oct4 expression is essential for ES cell pluripotency and cell fate decisions. Nanog, a homeodomain-containing protein, is also critical for the maintenance of pluripotency; loss of the protein results in the generation of cells that initially are pluripotent but then immediately differentiate into endodermal cells (Chambers *et al.*, 2003). Finally Sox2, a member of the SRY-related HMG box family, works in conjunction with Oct4 to maintain pluripotent identity through control of FGF4 expression (Avilion *et al.*, 2003).

Genome-wide analysis of these key transcription factors highlighted that many of their target genes are shared and form a network of auto-regulatory and feed-forward loops (Boyer *et al.*, 2005; Loh *et al.*, 2006). In mouse ES cells, Oct4 and Nanog bind 1083 and 3006 genes respectively, of which 345 genes are shared. Typically, these genes encode transcription factors, including themselves, as well as STAT3 responsive genes to drive pluripotency. In addition to this, core pluripotency factors regulate the repression of differentiation programmes through either direct gene repression, or regulating the expression of other downstream factors including Esrrb, Rif1 and REST that mediate gene repression (Loh *et al.*, 2006).

1.5.2 Differentiation of ES cells

The ability of ES cells to differentiate readily *in vitro* means that they are a powerful tool to assess the changes in gene expression associated with early embryogenesis. Differentiation of ES cells can be stimulated through LIF withdrawal, which removes the inhibitory actions of STAT3 leading to mesodermal and endodermal differentiation. LIF removal prompts the spontaneous differentiation of ES cells as embryoid bodies (EBs), defined initially through an outer layer of primitive endoderm with other lineages being derived from the inner core of the aggregate (Keller, 1995).

Other methods of ES cell differentiation include the culture of ES cells on stromal cells where differentiation is stimulated by cell-cell contact (Nakano *et al.*, 1994), culturing ES cells in collagen-coated dishes (Nishikawa *et al.*, 1998) or differentiation of ES cells in serum-free N2B27 media. This promotes the neuroectodermal differentiation of ES cells due to loss of serum BMP4 that relieves the inhibitory effect of Id proteins.

Differentiation of ES cells into EBs mimics the changes in gene expression associated with the generation of the three primary germ layers *in vivo*, which occurs during gastrulation. Gastrulation occurs around embryonic day 6.5-7.0 and involves the gross re-organisation of the epiblast and the generation of the mesoderm, endoderm and ectoderm which go on to form all tissues in the body. Gastrulation occurs in response to signalling pathways, primarily Nodal, Wnt and BMP, and initiates through the formation of a transient structure known as the primitive streak, to form the mesoderm and definitive endoderm. Cells found at the most anterior region of the epiblast do not move through the primitive streak and ultimately form ectoderm (Tam & Behringer, 1997). Temporal expression of key drivers determines lineage specification: development of the mesendoderm (from which mesoderm and endodermal lineages will be derived) is dependent on the expression of *brachyury* whereas ectodermal formation is dependent on the expression of *Fgf* family members. Loss of function studies results in lethality at gastrulation indicating the importance of these factors throughout the process (Lolas *et al.*, 2014; Deng *et al.*, 1994; Hebert *et al.*, 1991; Deng *et al.*, 1994).

1.6 Inositol phosphates

Since their initial discovery, inositol phosphates (IPs) have been identified as biologically significant molecules, participating in a wide range of processes including mRNA export, apoptosis, DNA repair and chromatin remodelling (Resnick *et al.*, 2005; Leyman *et al.*, 2007). Inositol phosphate signalling pathways are activated by the hydrolysis of the membrane phospholipid phosphatidylinositol 4,5-bisphosphate (PIP_2), by

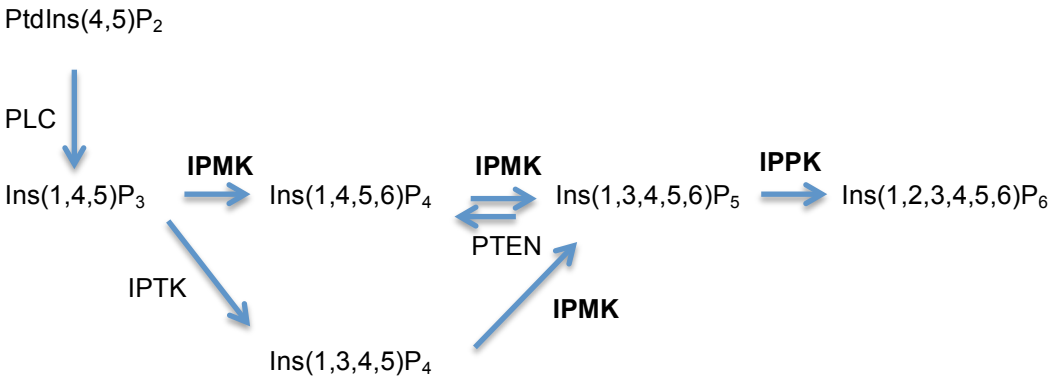

Figure 1.8: Inositol phosphate metabolism. Upon hydrolysis of PIP2 by phospholipase C to diacylglycerol and IP_3, IP_3 is sequentially phosphorylated by IPMK to generate IP_4 and IP_5. This is subsequently phosphorylated by IPPK to generate IP_6, the precursor of inositol pyrophosphates.

phospholipase C (PLC) to diacylglycerol and inositol 1,4,5-trisphosphate (IP_3), a precursor in the generation of higher order inositol phosphates (FIGURE 1.8).

Key to this metabolic pathway are two enzymes: inositol polyphosphate multikinase (IPMK) and inositol polyphosphate kinase (IPPK). IPMK is a pleiotropic enzyme with both inositol phosphate kinase (IP_3-kinase) and phosphatidylinositol kinase (PI3-kinase) activities. Through its IP_3-kinase function, IPMK acts to sequentially phosphorylate IP_3 to generate inositol 1,4,5,6-tetrakisphosphate (IP_4) and inositol 1,3,4,5,6-pentakisphoshate (IP_5). Subsequent phosphorylation of IP_5 by IPPK generates inositol hexakisphosphate (IP_6).

Homozygous deletion of IPMK is embryonic lethal in mice at embryonic day e9.5, whilst deletion of IPPK is embryonic lethal between day e8.5 and e9.5, indicating that both enzymes play an essential role in embryogenesis. Indeed, deletion of IPMK abolishes the formation of IP_4

and all other higher phosphorylated inositol phosphate species whereas loss of IPPK results in the loss of IP_6 and its downstream metabolites, inositol pyrophosphates (Verbsky *et al.*, 2005; Frederick *et al.*, 2005). Taken together, the knockout phenotypes for both enzymes indicate that inositol phosphate molecule signalling is essential for embryonic development.

1.6.1 Inositol phosphates and gene transcription

A role for IPs in the regulation of gene expression was first implicated by the IPMK yeast homologue, *Arg82*, which is involved in arginine and phosphate responsive transcriptional regulation. Arg82 is an essential component of the Arg:Mcm1 complex where it functions as an inositol phosphate kinase which catalyses the conversion of IP_3 to IP_4 (Odom *et al.*, 2000). Deletion of *Arg82* in yeast activates a subset of genes that are transcriptionally inactive in high phosphate conditions and restricts growth compared to wild-type suggesting that IPMK and its downstream metabolite Ins-(1,4,5,6)-P_4 have a role in transcriptional repression (El Alami *et al.*, 2003).

Recent work by Watson *et al.,* 2012 further identified a transcriptional repressive function for IP_4. The crystal structure of HDAC3 and the deacetylase activation domain (DAD) of SMRT identified that upon binding to HDAC3, the DAD undergoes extensive conformational rearrangements as compared to previously published structure of the DAD alone (Codina *et al.*, 2005). This acts to facilitate a greater interaction of the N-terminal α-helix of the DAD and HDAC3. Additionally, IP_4 was identified at the interface of the two proteins laying in a highly basic pocket, making extensive contact with both proteins where it acts as a bridging molecule between the two proteins (Watson *et al.*, 2012). Of particular importance is the interaction of Arg265 (loop 6 of HDAC3) which is in direct contact with the 4-phosphate group of IP_4 (FIGURE 1.9); mutation of this residue not only abolishes interaction of HDAC3:SMRT but also results in loss of

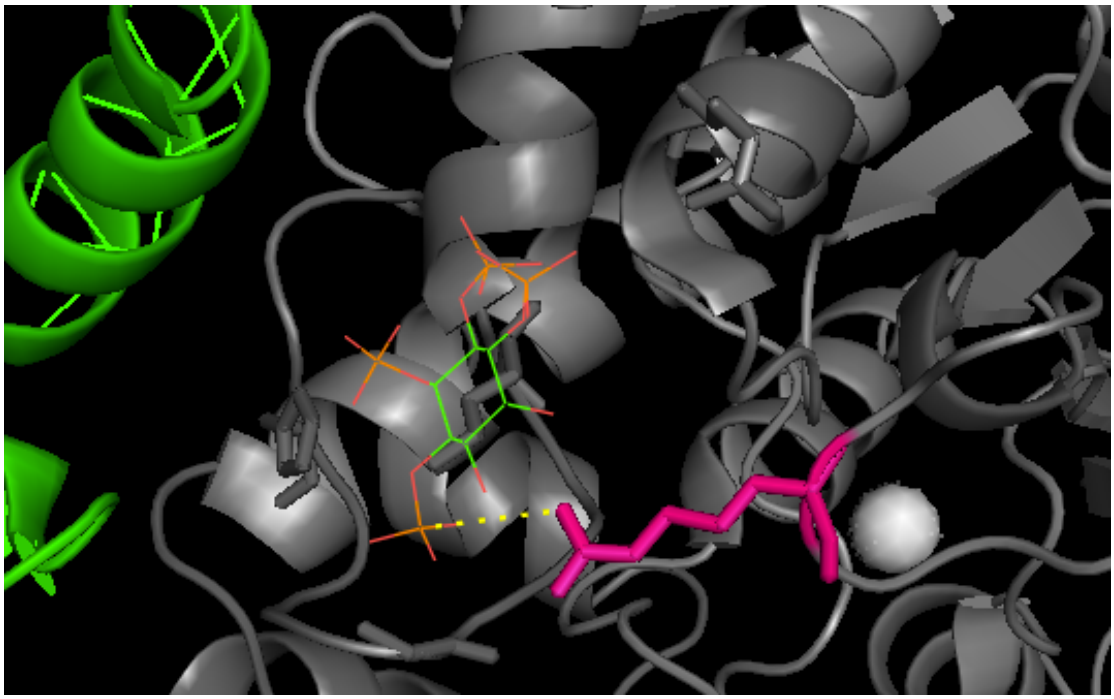

Figure 1.9 Key interactions between inositol phosphate and R265 of HDAC3. Crystal structure (PDB code: 4A69) showing electrostatic interaction of inositol (1, 4, 5 6) tetraphosphate (stick model) and R265 (pink) of HDAC3 (remainder of the protein shown in grey). Mutation of R265 abolishes enzyme activity indicating it is a key residue in mediating HDAC3 activity. PDB code: 4A69.

deacetylase activity thereby implicating IP_4 to act as both a structural and activator capacity.

Conversely, IPMK has also been implicated in transcriptional activation. Studies by Xu *et al.* and Kim *et al.* identified that IPMK functioned in a non-catalytic capacity as a transcriptional co-activator for p53 and serum response factor (SRF) to cause the induction of cell cycle arrest and apoptotic p53 targets and families of immediate early genes respectively (Xu & Snyder, 2013; Kim *et al.*, 2013). However, exactly how IPMK alternates between transcriptional co-activation and co-repressive functions remains unknown.

1.7 Aims of the project

Knockout studies of Class I HDACs demonstrate that the enzymes are critical for embryogenesis. HDAC3 knockout mice themselves are embryonic lethal prior to day e9.5 confirming HDAC3 as an essential gene. Additionally, recent studies suggest that the HDAC3:SMRT complex is regulated *in vivo* by inositol phosphates. In this project, we used two models systems, a conditional knockout ES cell line and transcriptional reporter assays in human embryonic kidney (HEK) 293T cells to:

- Interrogate the physiological requirement of the HDAC3:SMRT co-repressor complex
- Assess the role of HDAC3 in cell proliferation and differentiation of ES cells
- Understand the role of inositol phosphate in the regulation of HDAC3 activity.

Chapter 2: Materials and methods

2.1 Culture of mouse embryonic stem cells (mESCs)

The E14 Cre-ER mouse embryonic stem cells used all experimental work described in this thesis were a kind gift from David Adams and Jos Jonkers.

2.1.1 Thawing of mESCs

Individual vials of mESCs were thawed rapidly at 36.8°C and seeded onto a 100mm culture plate pre-coated in 0.1% gelatin solution in PBS for cell adherence; cells are maintained in a 5% CO_2 incubator at 36.8°C. Cells were monitored with daily changes of fresh mES culture medium (M15+LIF or 2i media).

2.1.2 Passage of mESCs

Upon reaching 80-90% confluency, cells were passaged. Culture medium was aspirated and cells were washed twice at room temperature with PBS. Dissociation of cells was achieved through incubation for 5 minutes with TrypLE Express dissociation reagent (ThermoFisher Scientific) at 36.8°C. Neutralisation of the reaction was achieved through addition of standard mESC culture medium and cells were suspended as single cells by pipetting multiple times. Cells were pelleted by centrifugation at 1200rpm for 3 minutes and re-suspended in fresh culture medium for re-seeding onto fresh pre-gelatinised culture plates.

For passaging of 96 well plates, cells were washed with PBS as before, and dissociated with addition of 50 µl/well of TrypLE Express reagent. Inactivation occurred with addition of 130 µl/well of ES culture medium following incubation at 36.8°C for 5 minutes. Cells were re-suspended through pipetting and an equal volume of the cell suspension being split between three 96 well plates pre-covered in gelatin with the addition of 140 µl/well M15+LIF (total volume/well of 200 µl).

2.1.3 Freezing and storage of mESC stocks

ES cells were frozen from an 80% confluent 100 mm cell culture plate, typically yielding $3x10^7$ cells. Cells were washed and dissociated as previously described in 2.1.2 and re-suspended in 1ml of 1x freezing media before being transferred into 1.5ml cryovials. Vials were transferred to a cryopreservation pot containing isopropanol and placed at -80°C; after 24 hours, cells were transferred to liquid nitrogen for long-term storage.

For cells grown in 96 well plates, cells were washed and dissociated as previously described before the addition of 50 µl of 2x freezing media. Cells were re-suspended by pipetting, the plate sealed with autoclave tape and wrapped in cling film and several layers of blue roll. The plates were then placed at -80°C for storage.

2.1.4 Genomic DNA extraction

For Southern blotting screening, cells grown in 96 well plates were grown beyond confluency. Cells were washed twice with PBS and incubated overnight re-suspended in 50ul of cell lysis buffer containing 200 µg/ml proteinase K. An equal volume of isopropanol was added to each well and the plate was placed on a plate shaker at 200 rpm for 30 minutes to allow precipitation of DNA. Plates were spun at 1200 rpm for 5 minutes before washing twice with 200 µl of 70% ethanol. DNA was air-dried and re-suspended in 50 µl TE buffer.

2.1.5 Media and reagents for culture of ES cells

M15+LIF ES cell medium

Knockout DMEM (Gibco, Life Technologies, Paisley)	500ml
Foetal Bovine Serum (Seralab)	90ml
100X Penicillin/Streptomycin/Glutamine (Gibco)	6ml
100mM β-mercaptoethanol	600µl
Leukaemia Inhibitory Factor (LIF, synthesised in house)	25µl

2i media

Knockout DMEM (Gibco, Life Technologies, Paisley)	500 ml
Leukaemia Inhibitory Factor (LIF, synthesised in house)	25 µl
100X Penicillin/Streptomycin/Glutamine (Gibco)	6ml
100mM β-mercaptoethanol	600µl

Per 50ml aliquot of stock media:

100X N-2 supplement (Invitrogen)	500 µl
50X B-27 supplement (Invitrogen)	1 ml
CHIR99021 (3uM; GSKi; Sigma Aldrich)	6 µl
PD0325901 (1uM; MEKi; Sigma Aldrich)	10 µl

Differentiation media

DMEM/F12 (Gibco, Life Technologies, Paisley)	500 ml
Foetal Bovine Serum (Seralab)	56.2ml
100X Penicillin/Streptomycin/Glutamine	6 ml
100mM β-mercaptoethanol	600 µl

0.1% gelatin

PBS	500 ml
2% gelatin solution	25 ml

2X freezing media

Knockout DMEM (Gibco, Life Technologies, Paisley)	60%
Foetal Bovine Serum (Seralab)	20%
DMSO	20%

Cell lysis buffer

50 mM Tris-HCl
100 mM NaCl
10 mM EDTA
1% SDS

2.2 Generation of conditional HDAC3 knockout ES cell line

Specific details of the *Hdac3* gene targeting strategy, enzymes and PCR primers used are described in detail in Chapter 3 in addition to Southern blot screen strategies (PCR primers and enzymes used see Appendix One).

2.2.1 Targeting vector electroporation

60 µg of targeting vector plasmid DNA was linearized by restriction enzyme digest, electrophoresised and visualised on a 1% agarose gel. The linearized DNA was then precipitated through addition of 20 µl sodium acetate and 3X volume 100% ethanol, mixed by pulse vortexing for 30 seconds and left overnight at -20°C. The following day, the precipitated DNA was centrifuged at 14,000 rpm for 30 minutes at 4°C, washed once in 70% ethanol and centrifuged for 15 minutes at 14,000rpm 4°C. DNA was washed twice more with 70% ethanol and left to air dry for 5 minutes before being re-suspended in 150 µl PBS and left at 60°C for 2 hours to ensure it had fully re-dissolved. To check the purification of plasmid DNA, 1 µg purified vector was diluted in 50 µl TE and 20, 40, 80 and 160 ng of plasmid DNA was run on a 1% agarose gel.

Two aliquots of $1x10^7$ E14 CreER-T mES cells were washed twice in PBS, re-suspended in 800 µl PBS and added to 0.4cm mammalian electroporation cuvettes. 10 and 20 µg of linearized targeting vector were added to the cells and left to incubate at room temperature for 10 minutes. Electroporation was performed using a Biorad GenePulser at 0.23V and 500µF with a routinely recorded time constant of 9.0 and above. The cuvette was placed on ice for 10 minutes before cells were re-suspended in 20 ml warm ES cell culture media and seeded onto 100 mm cell culture plates; cells were cultured for 24 hours before drug selection was started.

2.2.2 Transient transfection of ES cells by lipofection

Transfection of pCAGGS-FlpO plasmid was used to remove the selection cassettes of the doubly target clones; this was achieved with

Lipofectamine 2000 (Invitrogen, Life Technologies, Paisley) and performed as per the manufacturers instructions. Briefly, $1x10^6$ cells were seeded in a 6 well plate 24 hours prior to transfection. The following day, the culture media was replaced and transfection reagents were set up: 10 µl of Lipofectamine2000 was added to 250 µl OptiMEM reduced serum medium (Gibco, Life Technologies, Paisley) in a 1.5ml tube and incubated for 5 minutes. Meanwhile, 5 µg of plasmid DNA was added to 250 µl OptiMEM medium in a separate 1.5 ml tube. The diluted DNA was combined with the Lipofectamine (total volume: ≈500 µl) and mixed by pipetting up and down multiple times; lipofection complexes were left to form over 20 minutes at room temperature before the mixture was added drop-wise into culture media. 24 hours post-transfection, cells were washed, dissociated and plated at 1000 and 500 cells per 100mm plate.

2.2.3 Targeted ES cell selection

Following electroporation with targeting vectors, cells were subjected to positive drug selection for 10 days to enrich for successfully targeted events; cells electroporated with Hdac3-cKO-Neo or Hdac3-cKO-Hyg targeting vectors were selected using G418 (200 µg/ml) and Hygromycin B (100 µg/ml) respectively (Invitrogen, Life Technologies, Paisley). After 10 days, colonies were of sufficient size for picking: plates were washed twice in PBS and 96 individual colonies were picked in 50 µl TryPLE Express reagent in a 96-well round-bottomed plate. Cells were incubated at 36.8°C for 10 minutes before the addition of 150 µl/well M15+LIF culture medium and cells re-suspended by pipetting up and down several ties. The total volume of each well was transferred to a 96-well flat-bottomed plate for culture. Selected clones were grown for 3 days until replica plated onto three 96-well plates: two plates were grown until fully confluent and used for screening by Southern blotting to identify correctly targeted alleles; the final plate was frozen down at 80% confluency to be revived appropriately when targeted clones had been identified.

2.2.4 Recombineering of Hdac3-cKO-Neo targeting vector

In order to generate the second targeting vector, Hdac3-cKO-Hyg, required for the generation of doubly targeted ES cells, the –pgkHyg cassette was PCR amplified using 15 ng of pSC5 plasmid DNA which introduced 5' and 3' 66bp arms of homology to the –pgkNeo selection cassette of the initial Hdac3-cKO-Neo targeting vector. The PCR product was purified using MinElute columns (Qiagen, Life Technologies, Paisley) and purified product was *Dpn* I treated in a 100µl reaction left overnight at 37°C before being run on a 1% agarose gel and gel purified.

Meanwhile, 5 ml overnight culture of the recombineering strain SW102 were grown at 30°C in an orbital shaker. The following morning, 500 µl of overnight culture was used to inoculate a larger 25ml culture (25ml LB, 10 µl tetracycline, 500 µl overnight culture); this was cultured at 30°C for 3 hours until the OD_{600} reached 0.6. 10 ml of culture was then heat-shocked and grown at 45°C to induce expression of recombineering genes (*exo, bet* and *gam*). The bacterial culture was then rapidly cooled in iced water and left for 5-10 minutes and spun at 4°C at 4000rpm for 5 minutes. Supernatant was removed and the pelleted bacterial washed three times in 1ml 10% glycerol spinning at 4°C 13,000 rpm for 20 seconds between washes. Cells were then transferred to a pre-chilled 1.5ml tube and mixed with 10ng circular Hdac3-cKO-Neo and 5 µl purified linear –pgkHyg cassette, mixed by pipetting up and down several times. The bacteria/DNA mix was then transferred to a pre-chilled 0.4 cm electroporation cuvette and electroporated at 1.8kV, 200Ω, 25 µF using a BioRad GenePulser. Bacteria were immediately recovered in 1 ml LB media and incubated for 2 hours at 30°C in an orbital shaker before streaking onto an LB agar plate containing 100 µg/ml Hygromycin B. Plates were incubated overnight at 37°C before multiple colonies were picked, mini-prepped and sequenced to confirm the recombined fragment was in the correct orientation and matched the predicted sequence.

2.2.5 LoxP recombination

The two Hdac3$^{L/L}$ clones identified by Southern blotting were revived in 96-well plates and cultured for the generation of stocks. Cells were plated in 6-well tissue culture plates and the induction of LoxP recombination achieved through the addition of 1 μM 4-hydroxytamoxifen (4-OHT) to culture media over a period of 5 days. Protein was harvested from cells every 24 hours and screened by western blotting for deletion of HDAC3.

2.2.6 Screening by Southern blotting

Southern blotting was routinely used for the identification of gene targeting events, the specifics of which are detailed in Chapter 3. Details of PCR primers used to generate Southern blot probes can be found in Appendix One Table 2.

2.2.6.1 Gel electrophoresis

Genomic DNA extracted from 96-well plates was digested overnight at 37°C using the appropriate restriction enzyme (total reaction volume 50 μl). 5 μl 10X DNA loading dye was added to each sample and loaded onto a 0.8% agarose gel; gels were ran overnight at 20V. The following day, the gel was visualised on a UV transilluminator to assess the digestion of all DNA samples and was washed twice in alkaline transfer buffer.

2.2.6.2 Transfer to Hybond XL membrane

After washing, the DNA was transferred to a charged membrane, Hybond XL (GE Healthcare Life Sciences, Buckinghamshire), via capillary transfer overnight. The membrane was first equilibrated in alkaline transfer buffer. The following day, the membrane was washed twice for 15 minutes in neutralisation buffer and then dried for 30 minutes at 37°C. The membrane was the pre-hybridised using 10ml Rapid-Hyb buffer (GE Healthcare Life Sciences, Buckinghamshire) in glass roller bottles, constantly rotated.

2.2.6.3 Probe labelling

25 ng of double-stranded probe DNA was radiolabelled through the incorporation of $dCTP^{32}$. The probe was diluted in 45 µl TE, boiled for 5 minutes at 95°C to ensure denaturation of DNA and immediately chilled for 5 minutes. The DNA was centrifuged briefly, transferred to an aliquot of Ready-To-Go DNA Labelling Beads (GE Healthcare Life Sciences, Buckinghamshire) and 1.85 Bq (5 µl) of $dCTP^{32}$ was added to the mix which was thoroughly mixed by pipetting up and down multiple times. The probe was labelled for 1 hour at 37°C before purification using Illustra Microspin S-200 HR columns (GE Healthcare Life Sciences, Buckinghamshire) to remove unincorporated nucleotides. The purified probe was boiled for 5 minutes at 95°C before being added to the 10ml Rapid-Hyb in the glass roller bottle and incubated at 65°C overnight.

2.2.6.4 Membrane washing and development

The following day, the buffer was removed and the membrane washed twice in pre-warmed 2X SSC/0.1% SDS buffer and twice with 0.2X SSC/0.1% SDS buffer at 65°C. Membranes were exposed to x-ray film in a cassette placed at -80°C overnight before being developed.

2.2.7 Buffers

Alkaline transfer buffer

1 M NaCl

0.4 M NaOH

Neutralisation buffer

1 M NaCl

0.5 M Tris-HCl pH 6.8

2.3 Analysis of ES cell pluripotency and differentiation

2.3.1 Colony formation assay

To assess the clonogenicity of HDAC3$^{L/L}$ knockout cells, 7x10^2 cells were plated in triplicate in 6 well plates and cultured for 7 days. Colonies were stained with methylene blue (VWR) in 70% ethanol to aid identification of colonies and counted by eye.

2.3.2 Proliferation assay

The proliferative capacity of HDAC3$^{L/L}$ knockout cells was assessed by plating 5x10^4 cells in triplicate in a 12 well plate; total and live cell counts were taken daily using an automated cell counter BioRad TC-10 for a 7 day period and population doubling was calculated by:

Population doubling = log**T**/[log(**Total**)-log(**Initial**)]

T: time (hours) between seeding and counting of cells
Total: Total cell count on a given day
Initial: Initial number of cells seeded

2.3.3 Alkaline phosphatase staining

5x10^2 cells per well were seeded onto 6 well plates in the presence of LIF. Following 24 hours of culture, cell were there cultured in the presence (M15+LIF) or absence (DMEM/F12) for 6 days to allow colonies to form. Colonies were then fixed for 2 minutes in 4% paraformaldehyde (Alfa Aesar), washed twice in PBS containing 0.1% Tween and then stained with a commercial Alkaline Phosphatase dectection kit (Millipore, Watford) containing Fast Violet Red, Napthol and water in a ratio 2:1:1. Colonies were incubated for 15 minutes in the dark at room temperature, washed in PBS+0.1% Tween and visualised by light microscopy. There were scored depending on staining: undifferentiated (dark purple staining), mixed population (intermediate purple staining) and differentiated (absence of purple staining).

2.3.4 *In vitro* differentiation of mESCs as embryoid bodies (EBs)

Differentiation of HDAC3$^{L/L}$ knockout cells was induced by plating 5x10^2 cells per well in Corning Costar Ultra Low attachment round bottom 96 well plates (Sigma Aldrich) in 100ul of DMEM/F12 differentiation media. EBs were visualised daily by light microscopy and diameters were measuring using the Leica Application Suite software.

2.3.5 Differentiation of mESCs using retinoic acid (RA)

To induce monolayer differentiation of knockout cells, 1.5x10^5 cells were seeded in triplicate in 6 well plates and treated for up to 4 days with DMEM/F12 differentiation media supplemented with 1 μM retinoic acid. Cells were counted daily for a 4 day period using an automated cell counter BioRad TC-10 before pooling for PI analysis.

2.4 Protein and enzymatic analysis

2.4.1 Total RNA extraction

All reagents and equipment used were treated with RNase Zap (Ambion, Life Technologies, Paisley) to ensure removal of RNase contaminants. ES cells were harvested from 60mm tissue culture plates and EBs were collected in 1.5ml tubes. To isolate RNA from ES cells, cells were washed twice with PBS. 1ml of TRIreagent (Zymo Research) was added directly to the plate to lyse cells and the mix was pipetted until a homogenous solution was achieved; this was then transferred to a 1.5ml tube. For RNA isolation from EBs, EBs were collected and washed twice with PBS. Depending on the size and number of EBs collected, between 500-1000 μl of TRIreagent was added and the mix pipetted up and down multiple times to achieve a smooth consistency. Samples were either stored at -80°C or immediately processed.

RNA was extracted using a Direct-zol RNA MiniPrep Kit (Zymo Research). An equal volume of 100% ethanol was added to samples and mixed by vortexing. Samples were loaded onto a Zymo-Spin IIC Column and

centrifuged for 30 seconds. Columns were washed with 400 µl RNA wash buffer and centrifuged for 30 seconds. Samples were treated with DNase I reaction mix (5 µl DNase I, 75 µl DNA digestion buffer) and incubated at room temperature for 15 minutes. Samples were washed twice with 400 µl Direct-zol RNA PreWash and centrifuged for 30 seconds. Following this, 700 µl RNA wash buffer was added to the columns, centrifuged for 2 minutes to ensure complete removal of the buffer. The column was then transferred to a RNase/DNase free tube and RNA eluted with 25 µl DNase/RNase free water and centrifuged for 30 seconds. The concentration of RNA was quantified using a NanoPhotometer (Implen) and stored at -80°C.

2.4.2 Protein extraction

ES cells were cultured to 80% confluency, media was aspirated and cells washed twice with PBS. Cells were scraped in 1ml of PBS before being transferred to 1.5ml tubes. Samples were pelleted by centrifugation at 1200rpm for 2 minutes. Whole cell extracts (WCE) of samples were prepared by re-suspending cell pellets in 50-500 µl whole cell extract buffer depending on the size of the pellet supplemented with 1X protease inhibitor cocktail and placed on a rotator at 4°C for 30-60 minutes. Extracts were spun at 14,000rpm for 20 minutes to pellet debris and the supernatant transferred to a fresh 1.5ml tube. Protein concentration was quantified using Bradford reagent (BioRad) and absorbency at 595 nm was read.

2.4.3 Western blotting

Protein samples were prepared for electrophoresis by combining 25 µg protein with an equal volume of 2X protein loading buffer. Samples were boiled for 5 minutes to denature protein and were resolved on a 4-12% gradient SDS-PAGE gel and ran for 1 hour at 150V. Following transfer to a nitrocellulose membrane, the membrane was blocked for 1 hour with Odyssey Blocking Buffer (Li-COR) and then incubated for one hour with antibody (Appendix Two Table 1). The membrane was washed three times

for 10 minutes with PBS-T (PBS/0.1% Tween) and incubated for one hour with the appropriate IRDye conjugated secondary antibodies). Following this, the blot was washed three times for 10 minutes with PBS-T and once with PBS. Membranes were scanned using the Odyssey Infrared Imaging System (Li-COR Biosciences).

2.4.4 Histone extraction

Cells were harvested and whole cell extracted was performed as described in 2.4.2. Acid extraction of histones was achieved through the addition of an equal volume of 0.2 M H_2SO_4 as was used to create WCE to the pellet and incubated overnight on a rotator at 4°C. The following day, extracts were spun at 4°C for 15 minutes at 14,000rpm with the supernatant then transferred to a fresh 1.5ml tube. 25 µg of histone extract was resolved by 4-12% SDS-PAGE and membranes were probed with antibodies raised against the histone modification indicated in Appendix Two Table 2. Membranes were scanned using the Odyssey Infrared Imaging system and quantification of proteins achieved using the appropriate IRDye conjugated secondary antibodies (Li-COR Bioscience, Nebraska, USA).

2.4.5 Histone deacetylase assay

The histone deacetylase activity of extracts was assayed using a commercially available colorimetric kit (Active Motif, La Hulpe, Belgium), which contains a short peptide substrate, BoC-Lys(Ac)-AMC, containing an acetylated lysine residue. Upon deacetylation, the lysine residue reacts with the developing solution and releases the chromaphore from the substrate, producing a yellow colour that absorbs at 405nm.

30 µg of protein extract was measured in triplicate in a 96-well plate combined with 10 µl of the substrate (500 µM) and the volume made to 50 µl with assay buffer. Samples were mixed for 30 minutes on a flat rotating platform at 37°C before the reaction was stopped through addition of 50 µl

of the HDAC assay developing solution, incubated at room temperature for 10 minutes.

2.4.6 Buffers used for protein and enzymatic analysis

Whole cell extract buffer

50 mM Tris-HCl
250 mM NaCl
0.5% Igepal
0.5% Triton
1X Protease inhibitor cocktail (Sigma Aldrich)

1X running buffer for western blotting

192 mM glycine
25 mM Tris-base
0.1% SDS

1X transfer buffer for western blotting

192 mM glycine
25 mM Tris-base
10% ethanol

Protein loading buffer

70 mM Tris-HCl
200 mM β-mercaptoethanol
2% SDS
20% glycerol
Bromophenol blue

HDAC assay buffer

50 mM Tris-HCl pH7.5
50 mM NaCl

HDAC assay developing solution

50 mM Tris-HCl pH7.5

100 mM NaCl

2 µM Trichostatin A

10 µg/µl trypsin

2.5 Molecular biology

2.5.1 Reverse transcription and quantitative real-time PCR.

Total RNA was isolated outlined in 2.4.1 and quantified using a NanoPhotometer (Implen). 0.5µg total RNA was reverse transcribed using Q-Script cDNA Supermix (quanta Biosciences, Gaithersburg, MD, USA): to each sample, 4 µl of Q-Script cDNA Supermix was added and DNase/RNase free water to a final volume of 20 µl. cDNA synthesis was carried out in a thermocycler with the following conditions:

25°C 5 minutes

42°C 30 minutes

85°C 5 minutes

4°C Hold

cDNA was quantified using a NanoPhotometer and diluted to 100ul DNase/RNase free water before being used for quantitative real-time PCR experiments.

Multiplex assays, using GAPDH as an internal control to normalise the target gene Ct value, were designed using the Universal Probe Library Assay Design Centre (www.roche-applied-science.com, see Appendix One Table 3 for primers and probes). Probes consist of Lock Nucleic Acid technology, which upon binding of the reaction amplicon and polymerase elongation, release a HEX or FAM fluorophore. For each reaction (done in triplicate), 2ul of diluted cDNA was used with the multiplex reaction mix made using the LightCycler Probes Master (Roche Applied Science).

Reactions were performed in LightCycler 480 Multiwell 96-well plates under the following conditions:

94°C 10 minutes
94°C 10 seconds
55°C 20 seconds
72°C 5 seconds
] 40 cycles
4°C Hold

Advanced relative quantification analysis using the Roche LightCycler software generated a relative expression value based on the comparative Ct calculations ([delta][delta] Ct = [delta] Ct,sample - [delta] Ct,reference).

2.5.2 Polymerase chain reaction (PCR)

PCR was used to amplify DNA fragments for the generation of Southern blot probes and molecular cloning. High fidelity KOD Hot Start DNA Polymerase (Merck Millipore, Watford) was used in all cloning. A typical PCR reaction is outline below:

95°C 15 minutes
92°C 10 seconds
55°C 30 seconds
72°C 30 seconds
] 30 cycles
72°C 10 minutes
4°C Hold

A typical 50 µl reaction mix consisted of:

10X buffer	5 µl
25 mM $MgSO_4$	3 µl
dNTPs	5 µl
5’ primer	1.5 µl
3’ primer	1.5 µl
Template DNA	2 µl
KOD hot start DNA polymerase	1 µl
ddH_20	31 µl

2.5.3 Bacterial cultures

DH5α competent cells (Bioline) were used for transformation and propagation of plasmids.

2.5.3.1 Storage and revival of bacterial strains

Transformed bacterial strains were prepared as glycerol stocks for long term storage at -80°C. 500 µl of bacteria grown overnight in LB media supplemented with the appropriate antibiotic was added to 500 µl of 50% glycerol in a 1.5ml tube. The mix was vortexed briefly and stored at -80°C. Revival of bacterial strains was achieved by picking a small quantity of bacterial glycerol stock with a pipette tip and inoculating an overnight culture at 37°C.

2.5.3.2 Culturing bacterial cells for mini and maxiprep

Bacterial colonies were picked from agar plates with a sterile pipette tip and used to inoculated 5ml starter LB culture containing the appropriate antibiotic. These were incubated overnight in a 37°C shaking incubator either harvesting plasmid for miniprep or used to inoculate a starter culture volume for plasmid maxiprep.

2.5.3.3 Plasmid purification and gel extraction

All extraction methods are adapted from the original alkaline lysis plasmid purification method described in Birnboim, H.C. and Doly, J., 1979, followed by binding of DNA to an anion-exchange resin under appropriate salt and pH conditions and subsequent elution in ddH_2O or T.E. Minipreps and endotoxin-free maxipreps were prepared using Qiagen Plasmid Miniprep or Maxiprep kits respectively as per manufacturer's instructions (Qiagen, Crawley). Gel extraction of DNA was performed using a QIAEX II Gel Extraction Kit (Qiagen, Crawley) as per the manufacturers instructions.

2.6 Fluorescent activated cell sorting (FACS)

2.6.1 Isolation of SSEA1^{+} HDAC3$^{L/L}$ clones

HDAC3$^{L/L}$ clones C1 and D6 were stained for SSEA1 (stage-specific embryonic antigen-1), a cell surface marker expressed in murine ES cells to identify the most pluripotent ES cells. Cells were washed twice with PBS prior to dissociation using Tryple dissociation reagent, incubated at 36.8°C for five minutes and neutralised using mES culture medium. 5x10^{6} cells were washed in 1% BSA in PBS, pelleted through centrifugation at 1200rpm before incubation in a 1:100 dilution of anti-SSEA1 antibody (MAB4301 clone MC-480; Merck Millipore) at 4°C for 30 minutes. After being washed in 1% BSA solution, SSEA1 was detected by goat anti-mouse IgM conjugated with Alexa Fluor 488 (A11029; ThermoFisher Scientific) diluted 1:100 in 1% BSA solution for 15 minutes at 4°C in the dark. Cells were washed once in 1% BSA solution, transferred to standard FACS tubes and resuspended in 1% BSA. Samples were immediately processed for FACS analysis using a BD FACSCanto II flow cytometer (BD Biosciences). SSEA1+ cells were collected into standard mES culture medium (0.5x10^{6} and 1x10^{6} cells for clones C1 and D6 respectively) and were plated on pre-gelatinised culture dishes.

2.6.2 EdU replication assay

Between 0.5 and 1x10^{6} cells were plated per well of a 6 well plate. Following overnight culture, cells were treated with a commercial Click-iT EdU Flow Cytometry Assay Kit (Invitrogen). Briefly, cells were cultured in the presence of 10 μM EdU for 45 minutes before the culture media was collected from each sample and cells were harvested and counted using an automated BioRad TC-10 automated cell counter. Cells were washed once in 1% BSA (Sigma Aldrich) in PBS and were fixed for 15 minutes in 4% paraformaldehyde protected from light. Cells were washed, pelleted and re-suspended in 1X Click-iT saponin-based permeabilisation buffer and mixed for 15 minutes. The Click-iT reaction cocktail was prepared as follows and added to cells for 30 minutes in the dark at room temperature:

PBS	438 µl	
$CuSO_4$	10 µl	
Fluorescent dye azide	2.5 µl	
Reaction buffer additive	50	µl

Cells were then washed in 1x Click-iT saponin-based permeabilisation buffer and were immediately processed for FACS analysis using a BD FACSCanto II flow cytometer (BD Biosciences).

2.7 Global transcriptome analysis

Comparative gene expression profiles of control (-OHT) and knockout (OHT-4) cells and day 3, 5 and 7 EB differentiation time course was compared to that of wild type controls using the SurePrint G3 Mouse Gene Expression v2 8x60K microarray (Agilent Technologies UK Limited, Stockport). Total mRNA was isolated as in 2.4.1 and quality control of total mRNA was performed using a 2100 Bioanalyser (Agilent). Samples with a RNA integrity number (RIN) of 7.0 and above were selected from processing and array hybridisation.

2.7.1 RNA labelling and amplification

RNA labelling and amplification was performed using a One-colour Low Input Quick Amp Labelling Kit according to manufacturers instructions. This process uses T7 RNA polymerase blend which simultaneously amplifies target material and incorporates Cyanine 3-CTP to label RNA. This was then purified using an RNeasy mini kit (Qiagen) before being quantified using a nanodrop.

2.7.2 Array hybridisation

Hybridisation was performed using the SurePrint G3 Mouse Gene Expression v2 8x60K microarray according to the manufacturers protocol. The Agilent 8x60K array contains 8 identical subgrids of 60,000 probes

covering over 27,000 transcripts and 4,500 long non-coding RNAs separated into 8 chambers thus 8 samples can be simultaneously examined on a single slide. 600 ng of Cy-3 labelled cRNA for each sample was hybridized to the probes on the chip for a minimum of 17 hours at 65°C at 10rpm. The arrays were washed twice before being scanned with an Agilent microarray scanner.

2.7.3 Analysis of microarray

Raw microarray image files were analysed using Feature Extraction and processed using GeneSpring v12.5 software packages (Agilent Technologies) which performed percentile normalisation and identified the top differentially expressed genes for each using the Benjamini and Hochberg correction. Analysis of functionally related gene groups among samples was performed using the Database for Annotation, Visualisation and Integrated Discovery (DAVID; v6.7). Principal component analysis (PCA), using 3 principal components (or eigenvectors) to capture the largest amount of variation within the dataset, was also performed using GeneSpring to assess data quality and separation between groups of replicates.

2.8 Luciferase reporter assay

HEK293T cells were thawed, passaged and frozen as described in 2.1.1-2.1.3. They were maintained in M10 (Dulbecco's modified Eagle's medium (DMEM) supplemented with 10% foetal bovine serum (FBS), Penicillin/Streptomycin/Glutamine and β-mercaptoethanol at 37°C in a 5% CO_2 atmosphere.

2.8.1 Transfection of HEK293T cells

For transient transfection, $5x10^5$ cells were seeded per well in a 48-well plate 24 hours prior to transfection. Cells were co-transfected with 0.23 ug of Gal4 upstream activation sequence (UAS)-thymidine kinase (Tk)-luciferase reporter, 0.18 ug β-galactosidase expression vector and 0.1ug

of Gal4DBD-fusion protein constructs using Lipofectamine 2000 (Invitrogen) according to manufacturer's instructions. The cells were cultured in complete medium for 48 hours prior to assaying for luciferase and β-galactosidase activity. For RNAi knockdown experiments, HEK293T cells were co-transfected with either non-targeting short-hairpin RNA constructs (GFP) or shRNA-targeting IPMK or IPPK (0.1ug or 0.357ug; see Appendix Three for detailed information) purchased from Sigma Aldrich using Lipofectamine 2000 and were cultured for either 48 or 74 hours prior to assaying for luciferase and β-galactosidase activity. For chemical inhibition of IPMK, chlorogenic acid (CHA; $C_{16}H_{18}O_9$; MW 354.3) and aurintricarboxylic acid (ATA; $C_{22}H_{14}0_9$; MW 422.34) were purchased from Sigma. Following transfection of Tk luciferase reporter, β-galactosidase expression vector and Gal4-fusion protein constructs for 24 hours, the medium was removed and varying concentrations (0, 1, 10 and 100 µg/ml CHA or 1, 10 and 50 µM ATA) were added in triplicate and cells were cultured for an additional 24 or 48 hours prior to assaying for luciferase and β–galactosidase activity.

2.8.2 Beta-galactosidase and luciferase assay

Culture medium was removed and cells were washed twice with PBS. 140 µl/well of cell lysis buffer was added to cells and the plate was left at room temperature for 2 hours at room temperature on a rotating platform. The plate was then sealed and placed at -80°C for minimum of 30 minutes prior to processing.

A commercially available luciferase assay kit (Biovision) was used to determine relative levels of the luciferase gene product. Briefly, 20 µl of cell lysate was incubated in a microtitre plate with 100 µl of Substrate A. Within 10 minutes, 100 µl of Substrate B was added to the well and the signal was immediately read using a plate reader. To determine relative levels of the β-galactosidase vector, 80 µl of cell lysate was incubated with 100 µl of β-galactosidase stock solution and incubated at 37°C for around

5 minutes until a yellow colour was observed. Absorbance was then read using a plate reader at 420 nm. Light units were normalised to the co-transfected β–galactosidase expression vector. Repression was calculated relative to the Tk luciferase reporter and results of triplicate samples were plotted.

2.8.3 Buffers

5X Lysis buffer

0.5M Tris-HCl pH7.8	1.25 ml
1M DTT	1 ml
0.1M EDTA	10 ml
Glycerol	50 ml
Triton X-100	5 ml
ddH_20	32.75 ml

B-galactosidase stock solution

0.1M Na_2HPO_4	120 ml
1M KCl	2 ml
0.1M $MgCl_2$	2 ml
0.1M NaH_2PO_4	80 ml

B-galactosidase substrate

B-galactosidase stock solution	10 ml
ONPG	20 mg
B-mercaptoethanol	35 µl

Chapter Three: Generation of HDAC3 conditional knockout mouse ES cell line

3.1 Introduction

Unlike HDAC1 and HDAC2 which are incorporated into multiple co-repressor complexes, HDAC3 is exclusively recruited to the SMRT/NCoR complex. Germline deletion of the enzyme triggers embryonic lethality prior to embryonic day e9.5 indicating that HDAC3 is an essential enzyme for embryogenesis (Bhaskara *et al.*, 2008). Although the exact cause of lethality is unknown, its proximity to gastrulation suggests that HDAC3 may play an important role in early development.

To understand the physiological role of HDAC3 in embryogenesis, we designed a gene targeting strategy that permits the conditional inactivation of the enzyme using E14 mouse embryonic stem cells expressing Cre-ER fusion protein and floxed (flanked by LoxP sites) alleles of HDAC3. The *in vitro* differentiation of embryonic stem (ES) cells into embryoid bodies (EBs), generating the three primary germ layers (mesoderm, endoderm and ectoderm), mimics the changes in gene expression of early embryogenesis thus this system allows us to further understand the developmental role of HDAC3 *in vivo* whilst circumventing embryonic lethality (Smith, 2001).

3.2 Gene targeting strategy for conditional deletion of HDAC3

To generate a conditional knockout (cKO) of *Hdac3* in ES cells, a critical exon that is shared between all transcripts, exon 3, was identified to become the floxed exon. Deletion of exon 3 induces a frame shift mutation resulting in the generation of a premature stop codon in exon 5, with the transcript subjected to nonsense-mediated decay (FIGURE 3.1).

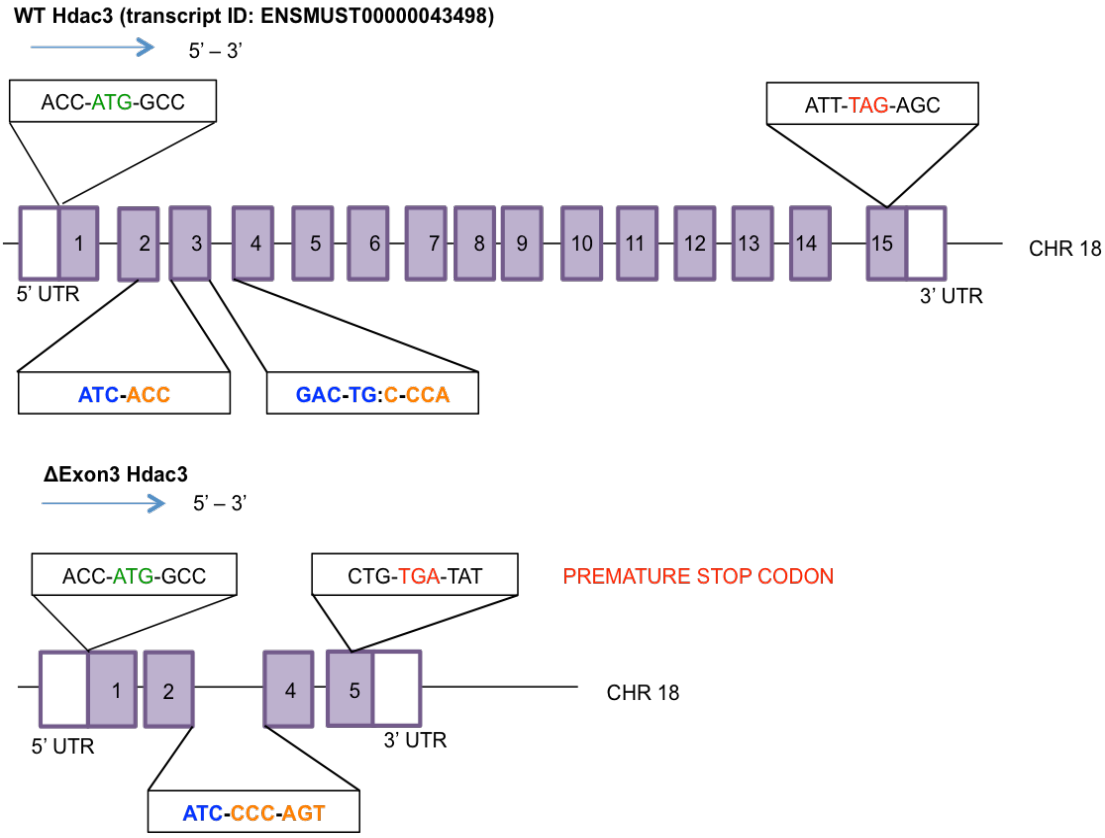

Figure 3.1 Overview of HDAC3 deletion strategy through loss of exon 3. Removal of exon 3 causes the indication of a premature stop codon in exon 5 and loss of Hdac3 by nonsense mediated decay. Start (green) and stop (red) codons are denoted.

To achieve conditional gene targeting of HDAC3, a two-step targeting strategy was used in an E14 ES cell line containing an inducible Cre recombinase fused to a mutated oestrogen receptor ligand binding domain (LBD) (Vooijs *et al.*, 2001). The strategy required sequential gene targeting of each allele via homologous recombination using a targeting vector which were electroporated in ES cells.

Selection of successfully targeted clones was achieved in each instance through positive drug selection since each targeting vector also contains a selection cassette, -pgkNeo and -pgkHyg respectively for the first and second allele, flanked by FRT sites; removal of these cassettes is facilitated by FlpO recombinase which catalyses recombination between

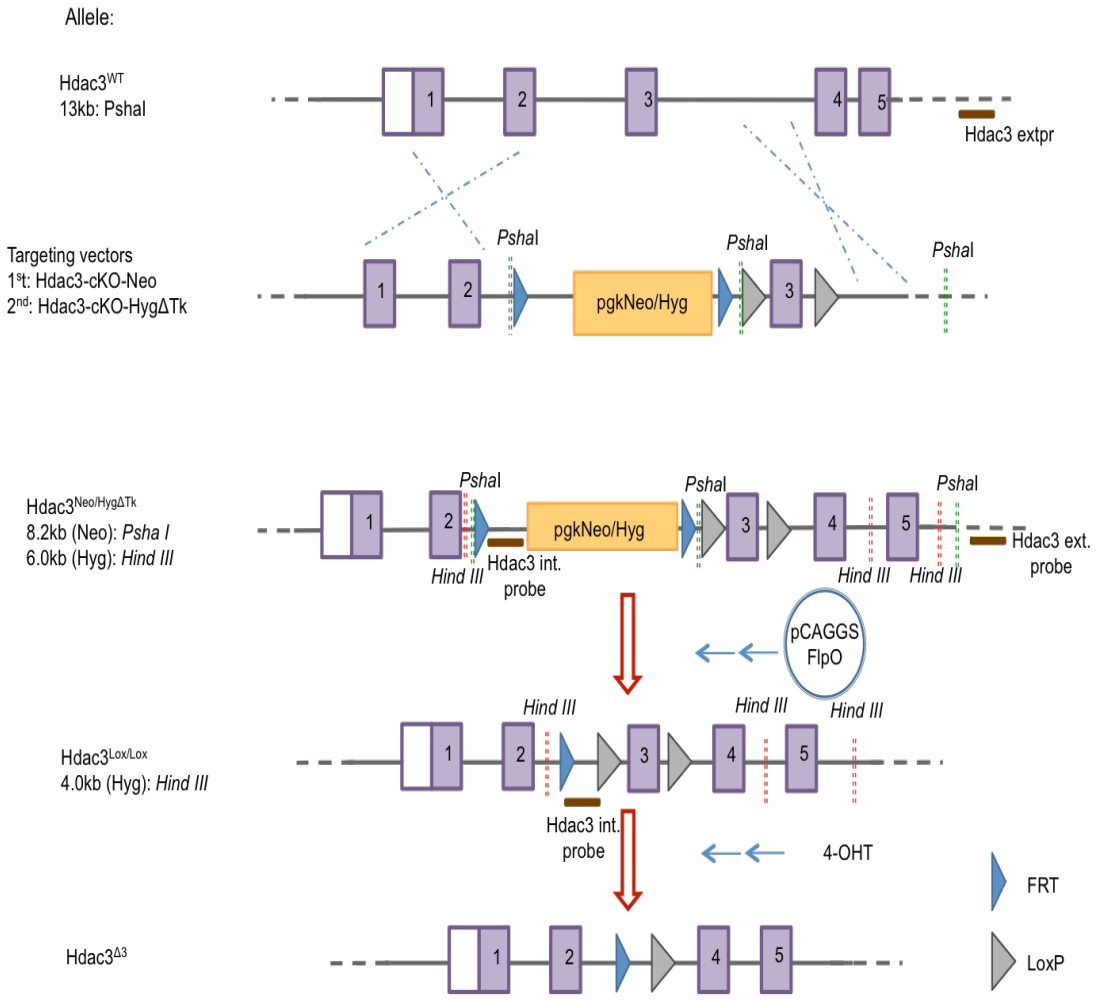

Figure 3.2 Southern blotting screening strategy for HDAC3 conditional knockout ES cell line. Gene targeting of the endogenous HDAC3 locus requires a two step sequential targeting strategy with detection by Southern blotting to confirm success integration of targeting vectors and removal of selectable cassettes. Probes (brown box), digests (red and green dashed lines) and expected fragment sizes are outlined.

FRT sites. Similarly, following addition of 4-hydroxytamoxifen (4-OHT) to cell media, Cre-ER recombinase translocates into the nucleus where it mediates recombination between the exon 3 flanked LoxP sites, resulting in removal of exon 3 and deletion of the *Hdac3* protein.

3.2.1 Targeting the first allele

The linearized HDAC3-cKO-Neo targeting vector (see Chapter 2.3.7 for map) was electroporated into E14^{CreER} ES cells to target the first *Hdac3* allele. Following selection of the cells with G418 supplemented media to identify clones in which integration of the vector had occurred, colonies were screened for successful targeting via Southern blotting following genomic DNA digestion by *Psha I* enzyme (FIGURE 3.2). The 3' external probe detects either a wild-type 13kb fragment (Hdac3^{WT}) or a 8.2kb targeted fragment (Hdac3^{Neo}) (FIGURE 3.3). Following recombination, successful targeting was identified in 7 clones, 2 of which were selected for further gene targeting.

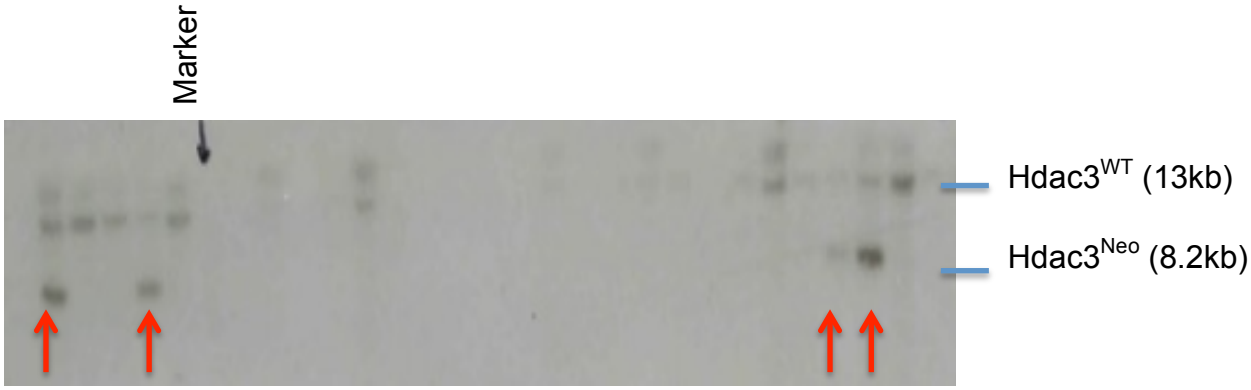

Figure 3.3 Successful targeting of the first allele of HDAC3. Successful integration of the HDAC3-cKO-Neo targeting vector was confirmed via Southern blotting. Using the HDAC3 external probe hybridised to *Psha I* digested genomic DNA, either a wild type band (13kb) or targeted Hdac3^{Neo} was identified (8.2kb). Representative blot of at least 96 individual clones grown under G418 positive selection. Red arrows denote successfully targeted clones.

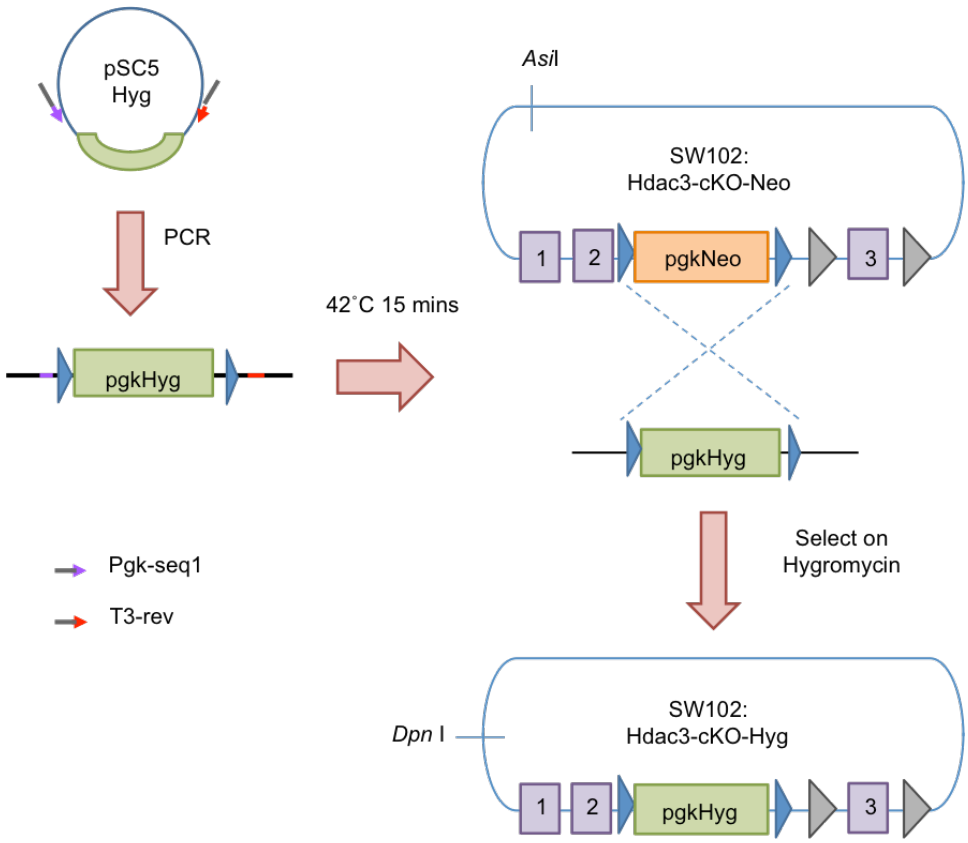

Figure 3.3 Generation of the HDAC3-cKO-Hyg targeting vector. Schematic of the strategy used to generate the HDAC3-cKO-Hyg targeting vector from the HDAC3-cKO-Neo targeting vector using recombineering methodologies. The –pgkHyg cassette was PCR amplified from pSC5 using Pgk-seq1 and T3-rev primers (grey denotes 60bp region of homology with 5' and 3' target Hdac3-cKO-Neo; red and purple denotes sequence used to permit amplification of the –pgkHyg cassette). Following linearization and gel purification, the DNA fragment was electroporated into SW102 alongside the HDAC3-cKO-Neo targeting vector, heat shocked to induce recombination and selected on hygromycin plates.

3.2.2 Generation of the HDAC3-cKO-Hyg targeting vector

In order to generate homozygous floxed cells, the second allele of HDAC3 was targeted with a second targeting vector containing an alternative selectable marker. Accordingly, the –pgkNeo cassette from the original Hdac3-cKO-Neo targeting vector was replaced using recombineering (FIGURE 3.3) (Liu *et al.*, 2003).

Firstly, the hygromycin cassette was PCR amplified from pSC5 using the pgk-Seq1 and T3 primer pairs which contain a 60bp sequence homologous to the 5' and 3' sequence flanking the –pgkNeo selection cassette of Hdac3-cKO-Neo and a smaller 20bp sequence used to amplify the –pgkHyg fragment from pSC5 to generate a 2.9kb fragment. The fragment was then digested with *Dpn* I (to remove any contaminating parental vector) and gel purified. In order for recombineering to proceed, electrocompetent SW102 bacterial cells were heat-shocked allowing the induction of *gam, bet* and *exo* genes and the cassette was electroporated alongside the Hdac3-cKO-Neo targeting vector. Selection on Hyg containing LB agar plates was used to select for the exchange of Neo and Hyg cassettes before genomic DNA was extracted from positively selected clones and sequenced to ensure that the recombined cassette was in the correct orientation.

3.2.3 Targeting the second allele

Targeting of the second wild type allele of HDAC3 was achieved by a similar process to that described above. The HDAC3-cKO-Hyg targeting vector was linearized with *Not I* and then electroporated into singly targeted $Hdac3^{Neo/WT}$ ES identified in Fig.3.3. Clones were drug selected with hygromycin B for 10 days; individual colonies were isolated and then double targeted events ($Hdac3^{Neo/Hyg}$) were identified by Southern blotting. To detect successful targeting, the *Hind III* digested genomic DNA was hybridised to the internal probe to identify a wild-type 9kb ($HDAC3^{WT}$) fragment or a 6kb targeted fragment ($Hdac3^{Neo/Hyg}$) (FiGURE 3.4A); successful targeting occurred in 2 out of 96 clones which were both taken

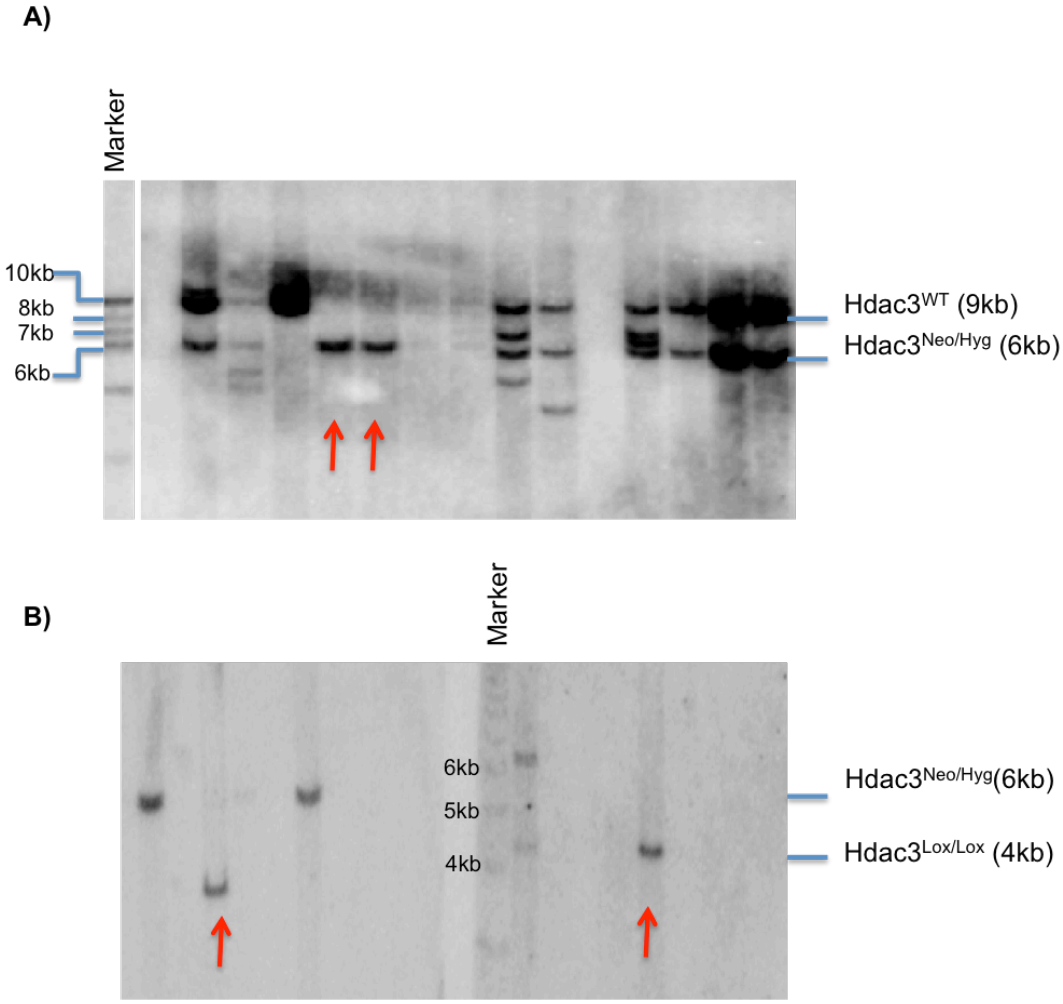

Figure 3.4 Successful targeting of the second *Hdac3* allele (A) and removal of neomycin and hygromycin selectable markers (B). (A) Confirmation of successful targeting of the second Hdac3 allele. Representative Southern blotting using the HDAC3 internal probe hybridised to *Hind III* digested genomic DNA yields a 9kb wild-type fragment or a 6kb targeted fragment ($Hdac3^{Neo/Hyg}$). Additional bands detected due to non-specific hybridisation of internal probe. (B) Confirmation of FlpO mediated excision of selectable cassettes from homozygous $HDAC3^{Neo/Hyg}$ cells assessed by Southern blotting. Using the HDAC3 internal probe on *Hind III* digested genomic DNA yields a 6kb targeted fragment ($Hdac3^{Neo/Hyg}$) or a 4kb FlpO recombined fragment ($Hdac3^{Lox/Lox}$).

forward for further testing and removal of selectable markers.

3.2.4 Removal of selection cassettes in HDAC3$^{Neo/Hyg}$ double targeted cells

Selectable markers are associated with promoter and enhancer sequences which may interfere with the expression of genes at the targeted locus (Lakso *et al.*, 1996; Buchholz *et al.*, 1998). Consequently, the cassettes were flanked with FRT sites to permit the removal of the selectable markers via homologous recombination following transfection of a codon optimised version of the yeast recombinase, FlpO.

Double targeted Hdac3$^{Neo/Hyg}$ cells were transiently transfected with a pCAGGS-FlpO plasmid and plated at low density (approx. 500cell/100mm plate) to allow individual clones to grow. Due to the efficiency of the FlpO plasmid, no selection was applied. To detect successful removal of selectable markers in targeted Hdac3$^{Neo/Hyg}$ ES cells, *Hind III* digested genomic DNA was hybridised with the internal probe to identify either a 6kb fragment (Hdac3$^{Neo/Hyg}$) or the 4kb FlpO recombined fragment (Hdac3$^{Lox/Lox}$) (FIGURE 3.4B); of 19 clones screened, 2 positive clones were identified in which the selectable markers had been removed which were taken forward for characterisation.

3.2.5 Deletion of exon 3 from Hdac3$^{L/L}$ ES cells

Removal of exon 3 from the *Hdac3* allele is mediated by Cre/LoxP recombination. The E14 cells used in this study express a Cre recombinase fused to a mutated oestrogen receptor ligand binding domain (Cre-ER) in which glycine 521 has been mutated to arginine. This mutation renders the LBD insensitive to 17 β-estradiol, but activated in the presence of its analogue, 4-hydroxytamoxifen (4-OHT) (Feil *et al.*, 1996; Feil *et al.*, 2009). In the absence of 4-OHT, Cre-ER is sequestered in the cytoplasm by the chaperone protein Hsp90; upon addition of 4-OHT to cell culture

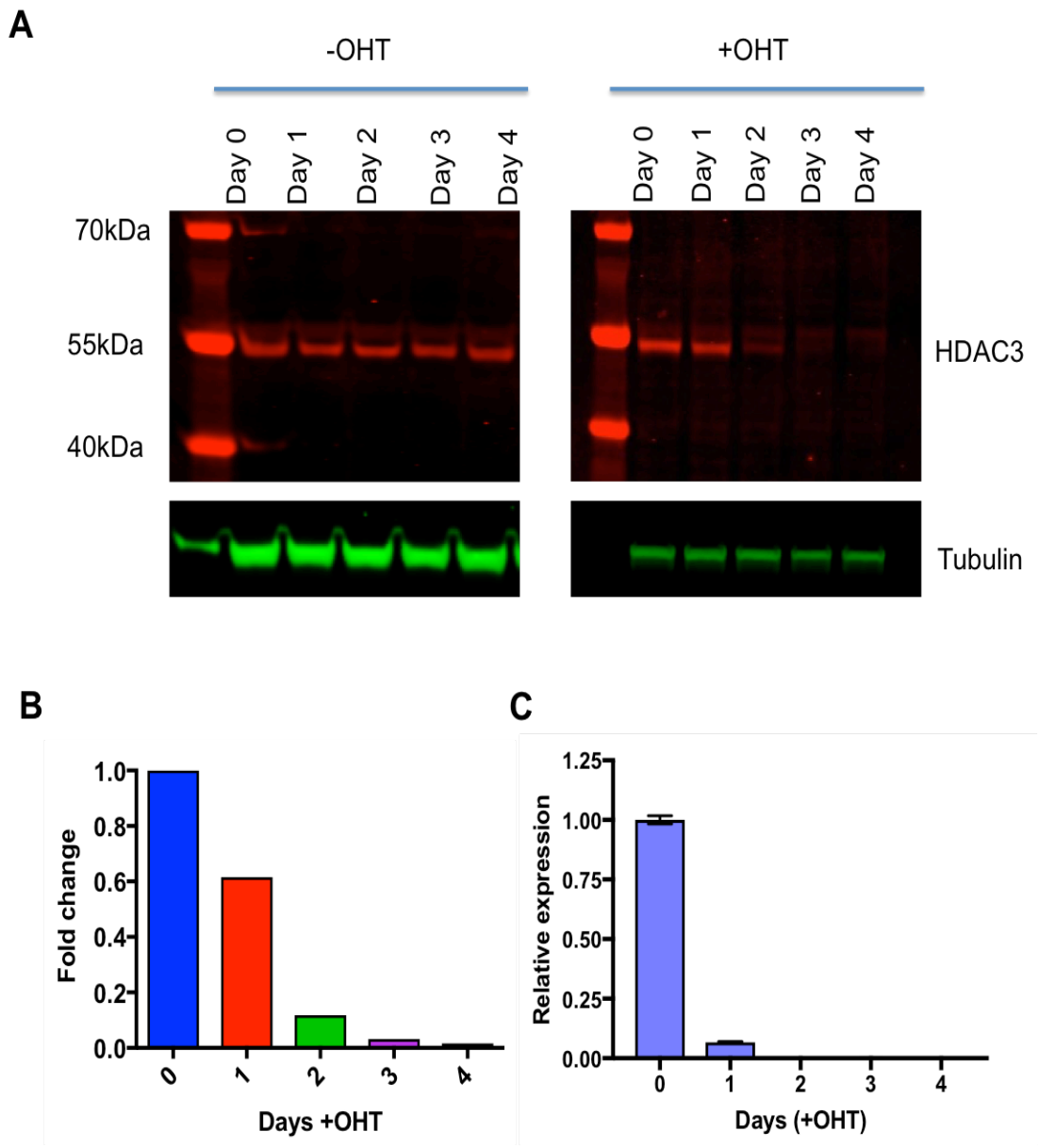

Figure 3.5 Confirmation of inducible HDAC3 conditional knockout ES cell line. (A) Quantitative Western blot showing control (-OHT; left) and 4-OHT inducible degradation of HDAC3 protein (right) upon addition to cell culture media. Cells were cultured for 4 days; α-tubulin was used to normalise protein loading. (B) Fold change of HDAC3 protein (bottom) following gene inactivation shows a total absence of protein within 72 hours. Blot was visualised and quantified using a LiCOR scanner. (C) Quantitative RT-qPCR of HDAC3 transcript in knockout cells. All values are mean (n=3) ± SEM. Values indicate expression of gene relative to the *Gapdh* reference gene

media, the enzyme is released from Hsp90 and translocates to the nucleus where recombination occurs to remove the DNA sequence between LoxP sites (exon 3 of HDAC3). Upon recombination, the open reading frame of HDAC3 is disrupted and a frameshift mutation occurs, inducing a premature stop codon in exon 5. Consequently, Hdac3 protein is degraded by nonsense mediated decay.

Following addition of 0.1 μM 4-OHT to cell culture media, progressive loss of HDAC3 is observed over 3 days (FIGURE 3.5A and B) as analysed by Western blotting. There is rapid degradation of the protein with a 40% reduction in protein within 24 hours and a total loss within 72 hours indicating that the protein has a half-life of around 24 hours, similar to other class I HDAC enzymes (Jamaladdin *et al.*, 2014). HDAC3 transcript was also dramatically reduced after 24 hours and absent within 48 hours of OHT treatment confirming that the protein was degraded by nonsense-mediated decay (FIGURE 3.5C).

3.3 Analysis of undifferentiated HDAC3 knockout cells

3.3.1 HDAC3 contributes to HDAC:SMRT complex stability

HDAC3 is specifically recruited to the SMRT/NCoR complex which facilitates the activation of the enzyme (Wen *et al.*, 2000; Guenther *et al.*, 2000; Li *et al.*, 2000). Following the deletion of HDAC3, the protein levels of other core complex components, TBL1X and NCoR, were analysed through Western blotting of control (untreated) and knockout cells (+OHT) cells to assess the integrity of the complex in the absence of HDAC3. As shown in FIGURE 3.6, we identified a decrease in both TBL1X (top band) and NCoR1 protein levels suggesting that HDAC3 may contribute to the structural integrity of the HDAC3:SMRT complex. Interestingly, while there was a decrease in protein level of NCoR1, there was a concomitant increase in transcript levels of both NCoR1 and NCoR2 (SMRT). This suggests that there may be compensation at the transcript level, perhaps to counteract a decrease in protein levels.

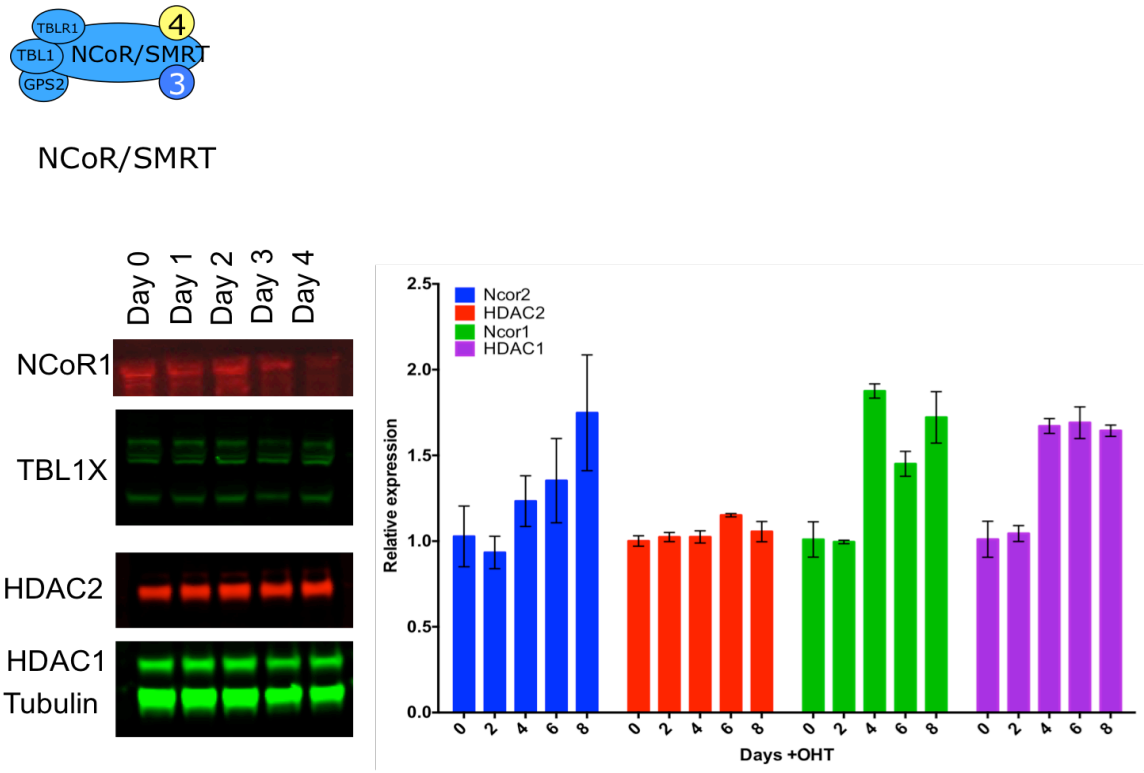

Figure 3.6 Reduction in NCoR1 and TBL1X protein levels in HDAC3 knockout cells. (Left) Quantitative Western blot of indicated proteins indicates a reduction in endogenous levels of key HDAC:SMRT co-repressor complex components TBL1 and NCoR1 in the absence of HDAC3. Levels of other Class I HDACs HDAC1 and HDAC2 remain constant. α-tubulin was used to normalise protein loading. (Right) Quantitative RT-qPCR data of indicated mRNA transcripts in the absence of HDAC3. All values are mean (n=3) ± SEM. Values indicate expression of gene relative to the *Gapdh* reference gene; measured using Universal Probe Library hydrolysis probes.

Additionally, unlike other Class I HDAC knockout models which identifies a compensation of other HDAC proteins in the absence of an individual protein, there was no increase in either HDAC1 or HDAC2 protein levels when HDAC3 has been deleted. However, there was a slight increase in HDAC1 transcript levels suggesting there may be a limited amount of compensation by HDAC1 for the loss of HDAC3 at the transcriptional level.

3.3.2 Loss of HDAC3 has a minimal effect on global deacetylase activity.

Since loss of HDAC3 appears to contribute to the integrity of the HDAC3:SMRT complex, we next examined the effect of HDAC3 loss on the total cellular HDAC activity. HDAC activity was assessed for up to 7 days post 4-OHT treatment i.e. when all HDAC3 protein had been lost. Surprisingly, we observed only a slight decrease in total deacetylase activity at day 4, although this decrease is no longer significant by day 7. In contrast, cells lacking HDAC1 and HDAC2 show a significant decrease in activity (~53% of wild-type deacetylase activity) (FIGURE 3.7).

This suggests that the HDAC3:SMRT complex only contributes a minor proportion of total deacetylase activity in ES cells compared with HDAC1/2-containing complexes suggesting that HDAC1 and -2 are the dominant deacetylases in ES cells and that the individual co-repressor complexes have different functionalities within cells.

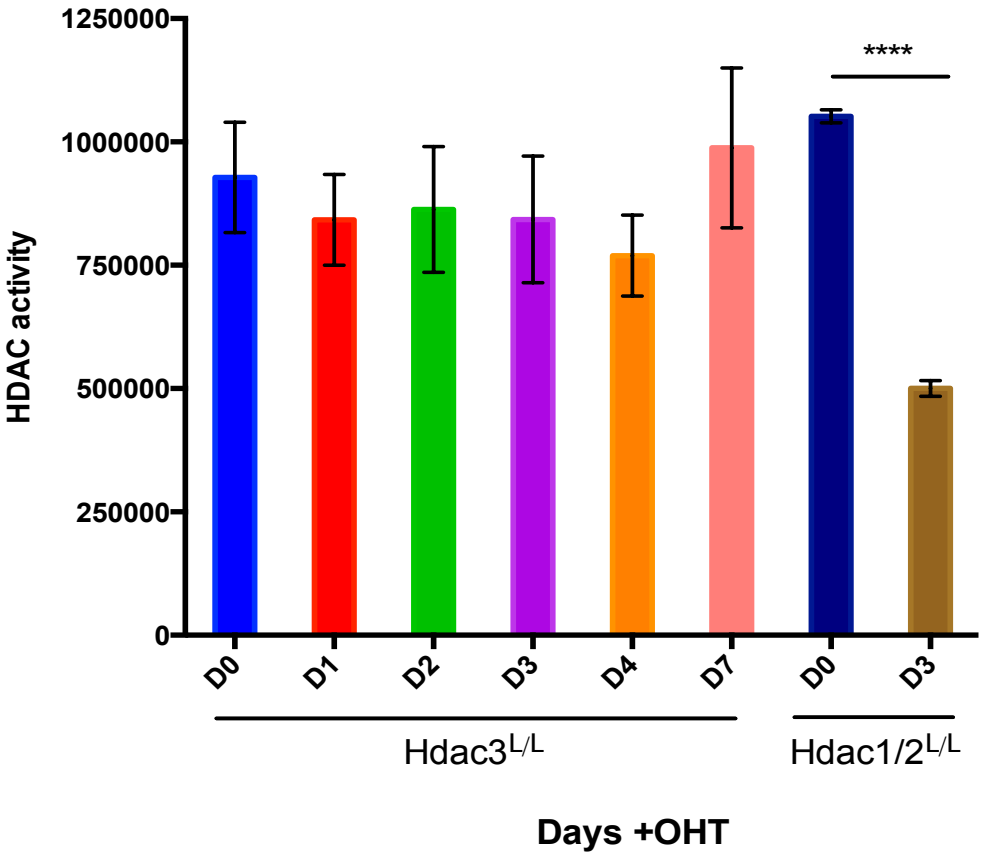

Figure 3.7 Limited effect of HDAC3 loss on total deacetylase activity in HDAC3 knockout ES cells. Deactylase activity was measured in whole cell extract up to 7 days following gene inactivation using a commercially available kit. All vales are means (n=3) ± SEM. The significance (P value) was calculated using a two-tailed t test (**** <0.00001).

Next, the levels of histone H3 acetylation were analysed in the absence of HDAC3 (FIGURE 3.8). Since ES cells have a highly plastic chromatin structure, they consequently have a high basal level of histone acetylation (Dovey *et al.*, 2010). Nevertheless, we detected a modest 1.5-fold increase in H3K18 and H3K27 acetylation suggesting these sites are targets of HDAC3. Both H3K18ac and H3K27ac are known to be associated with enhancers (Creyghton *et al.*, 2010; Calo & Wysocka, 2013) thus HDAC3 may be functioning in a gene-specific context to bring about gene repression.

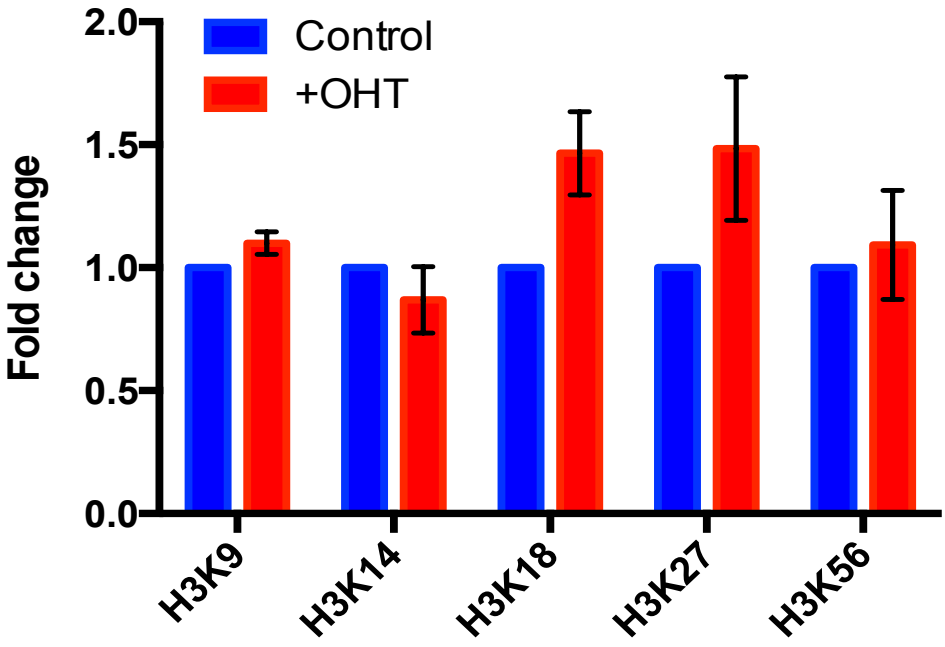

Figure 3.8 Increase in global histone acetylation levels of histone H3. Quantitative Western blotting was used to determine the acetylation status of indicated marks in histone H3. Histones were acid extracted from untreated (control) cells and OHT-treated (knockout cells) 4 days following gene inactivation. Signal of acetylated lysine was normalised to the total amount of H3 using an Odyssey scanner. All values are means ± SEM.

3.3.3 Proliferation capacity of ES cells is inhibited by loss of HDAC3.

HDAC3 has been implicated in cell cycle progression since HDAC3 knockout MEFs exhibited proliferation defects (Bhaskara *et al.*, 2008; Bhaskara *et al.*, 2010) thus the growth rate and population doubling time of HDAC3 knockout ES cells was assessed compared to controls (untreated). Loss of HDAC3 had a direct impact on both the proliferative capacity and doubling time measured over a 7 day period. As shown in FIGURE 3.9 (left), the growth rate of knockout cells was reduced beyond day 3 when HDAC3 protein is lost. This disparity increases along the duration of the time-course with both total number and live counts reduced in knockout cells by approximately 40% at each time point. Additionally, the population doubling was delayed by 5 hours in knockout cells (19 hours in control versus 24 hours in knockout cells; FIGURE 3.9 (right)).

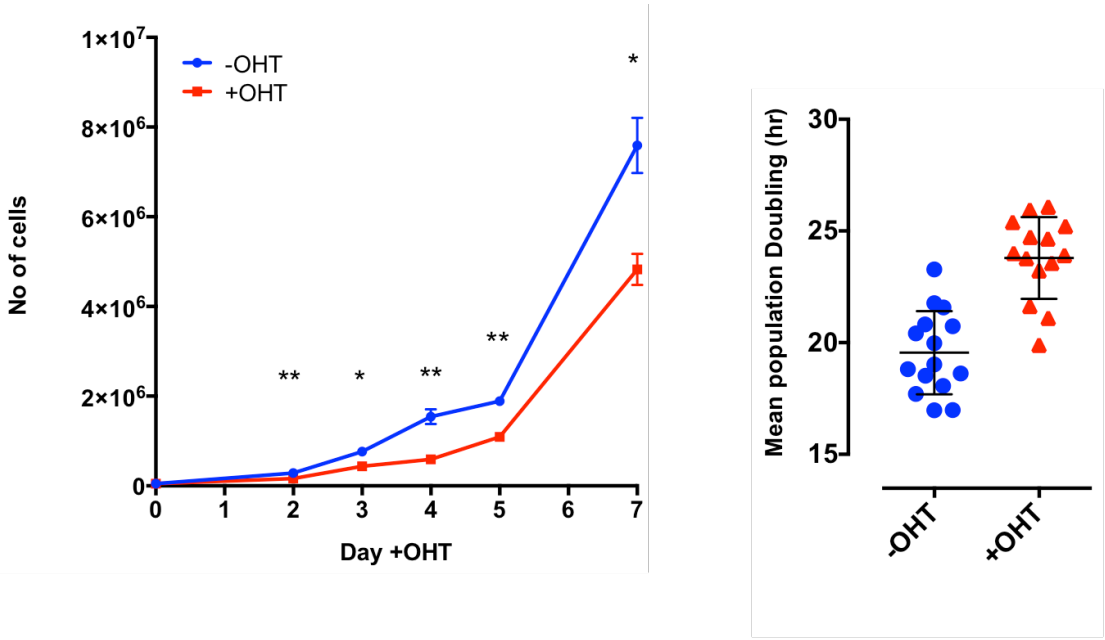

Figure 3.9 Proliferative capacity of HDAC3 knockout cells is inhibited. Growth rate of untreated (-OHT control) and HDAC3 knockout (+OHT) cells following gene inactivation was assessed by counting cells over a 7 day period (left). Population doubling was delayed in HDAC3 knockout cells (+OHT) compared to untreated controls (-OHT). All values are means ± SEM. The significance (P value) was calculated using a two-tailed t test (* <0.01, ** <0.001).

A role for HDAC3 in cell cycle progression was further suggested when HDAC3 knockout cells were treated with EdU, a nucleoside analogue which becomes incorporated into DNA during DNA synthesis thereby allowing us to examine the percentage of actively proliferating cells. Following treatment, there was a significant reduction in the number of EdU-positive cells in OHT-4 and OHT-8 treated knockout cells (cells which had been treated with 4-OHT 4 and 8 days prior thus had no HDAC3 protein present) (FIGURE 3.10). In both knockout conditions, there was both a shift to the left and a broadening of the S phase peak suggesting that not only were there fewer S-phase cells present but that there was also a delay in cells reaching S-phase. Indeed, compared to control cells in which 60.5% were EdU-positive and actively cycling, only 21.6% and 29.0% of cells were EdU-positive for OHT-4 and OHT-8 treated cells respectively. This result may explain the growth disparity observed between knockout and control cells and confirms that HDAC3 plays a key role in the cycling of cells.

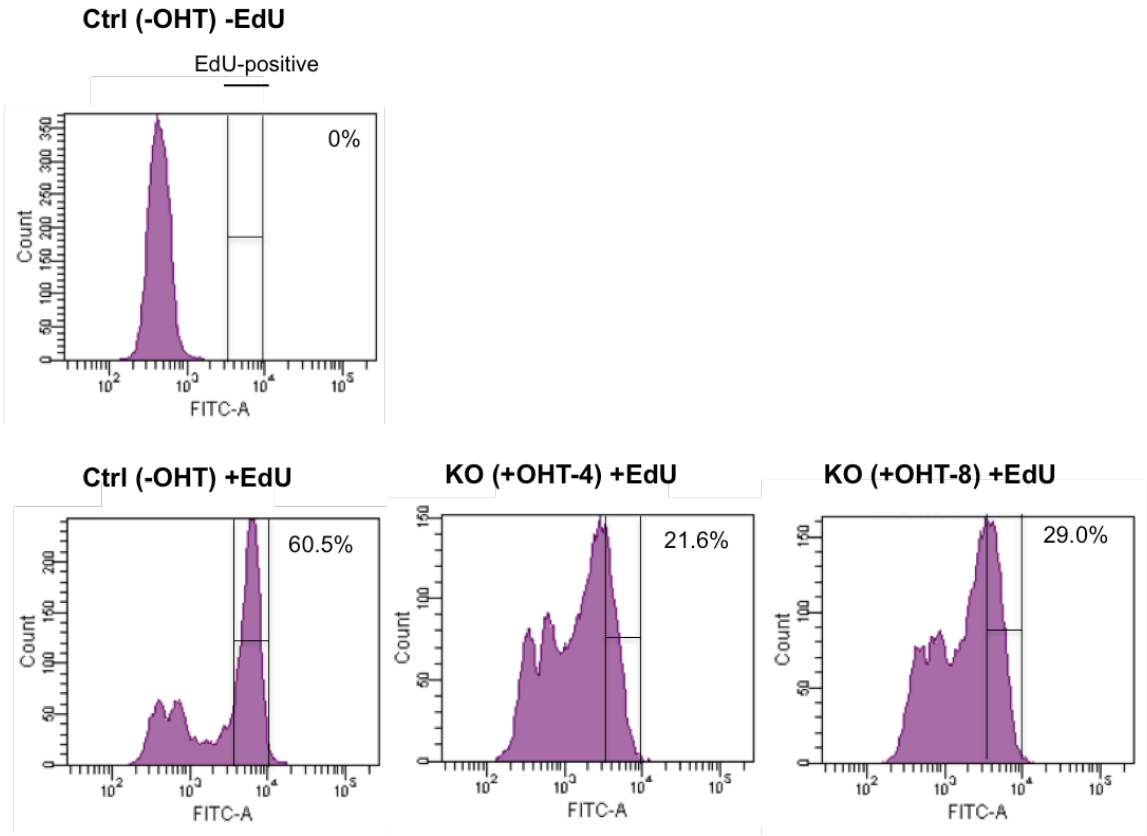

Figure 3.10 HDAC3 knockout cells show a delay in S-phase progression. EdU-incorporation following 45 minutes of treatment in untreated –OHT (left) and +OHT treated knockout cells (-4 treated cells: middle, -8 treated cells: right). (Left) Addition of EdU to untreated cells generates a sharp S-phase peak (60.5% cells). (Middle) and (right) Knockout cells (OHT-4 and OHT-8 days respectively) shows a broadening and shift of the peak indicating reduction and delay of cells to reach S-phase.

To further evaluate changes in growth ability of HDAC3 knockout cells, cells were plated at low density to assess the clonogenicity of cells; loss of HDAC3 resulted in 2-fold less colonies which were much smaller and irregularly shaped in both cells in which HDAC3 had already been deleted (HDAC3 KO; +OHT-4) and cells in which induction of HDAC3 deletion occurred on the day of plating (+OHT) (FIGURE 3.11A) which again may indicate a cell cycle defect or loss of self-renewal.

Next, the ability of HDAC3 knockout cells to retain pluripotency when grown in the presence of LIF and their ability to differentiate in the absence of LIF was assessed (FIGURE 3.11B). Control (untreated), knockout (OHT-4) and cells in which loss of HDAC3 was induced on day of plating (+OHT) were plated at low density and cultured for 6 days in the presence and absence of LIF prior to assaying for alkaline phosphatase, a stem cell marker. In the presence of LIF, colonies derived from control (-OHT) and knockout cells (+OHT and +OHT-4) showed comparable levels of alkaline phosphatase staining indicating that cells retained pluripotency in the presence of LIF. In the absence of LIF, cells were able to spontaneously differentiate; there was a comparable reduction in the percentage of undifferentiated colonies, although the proportion of mixed and differentiated colonies was altered between controls and treated cells. Compared to control colonies of which 80% were differentiated, the number of colonies from cells treated with 4-OHT on the day of plating (+OHT) or knockout cells (treated with 4-OHT four days prior; +OHT-4) was substantially reduced: in both instances, around 30% of colonies were mixed and only 60% of colonies were differentiated. This suggests that while cells are able to differentiate, there may be a defect in differentiation in the absence of HDAC3. Overall, this data suggests that the proliferation and differentiation capacity of *Hdac3* knockout cells is inhibited and further differentiation experiments were required to understand the effect of HDAC3 loss.

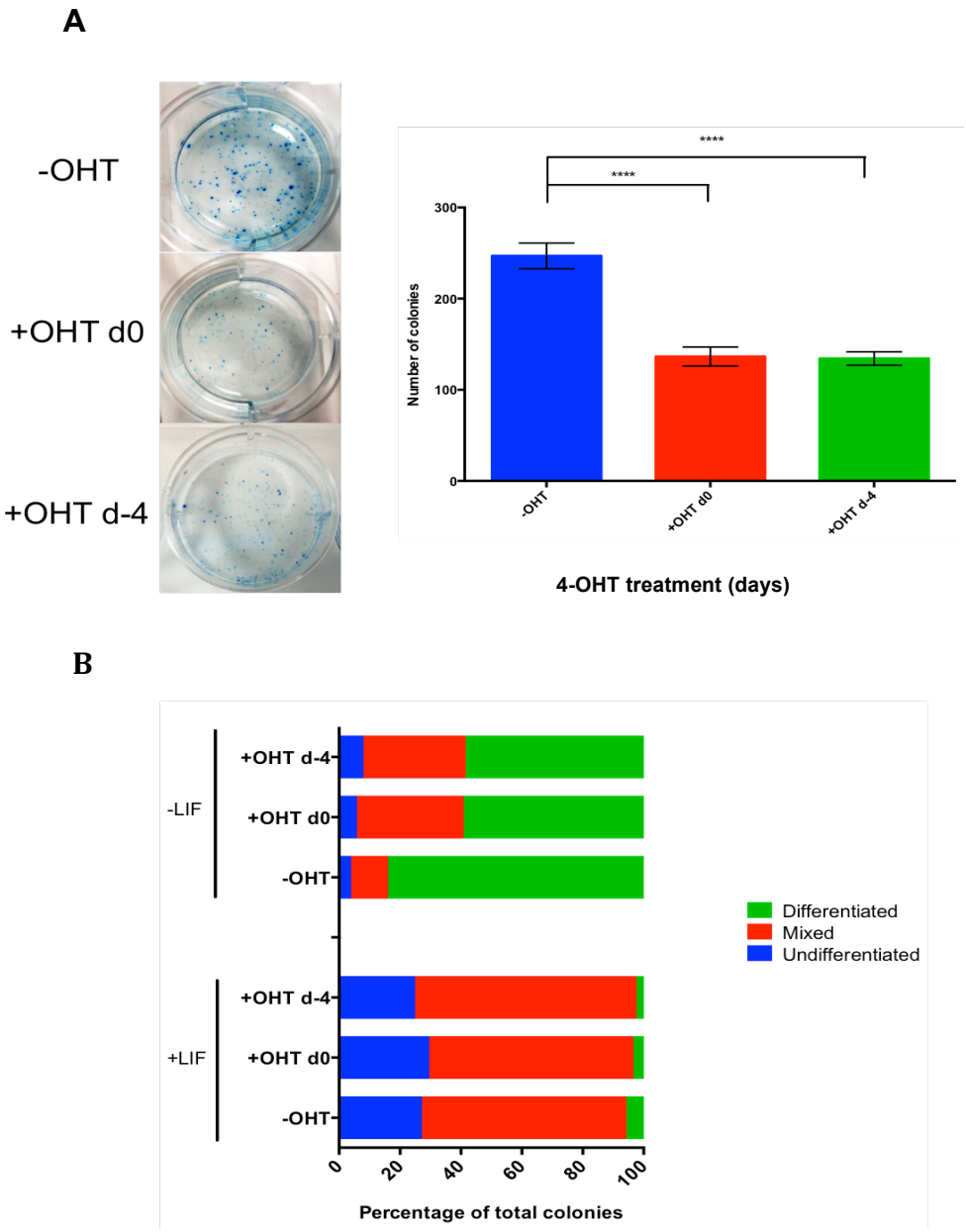

Figure 3.11 Loss of HDAC3 inhibits the growth and the differentiation potential of ES cells. (A) Colony formation assay of control untreated (-OHT), induced on day of plating (+OHT d0) and knockout (+OHTd-4; treated with OHT 4 days prior) cells plated at low density and stained with methylene blue. Means (n=3) ± SEM are plotted in the right panel. The significance (P value) was calculated using a two-tailed t test (**** <0.00001). (B) Cell types indicated were plated at low density and cultured in the presence and absence of LIF for 6 prior to assaying for alkaline phosphatase. Colonies were scored as undifferentiated (blue), differentiated (green) or mixed (red).

3.5 Conclusions

Sections 3.2.1-3.2.5 outlines the generation of a HDAC3 conditional knockout mouse embryonic stem cell line as confirmed at each stage of gene targeting by Southern blotting. Selectable markers for gene targeting events were also successfully removed through the transient transfection of FlpO to mediate excision by FRT recombination. Finally, Western blotting confirms that the conditional inactivation of the enzyme is achieved through addition of 4-OHT to cell culture media with a rapid protein loss of 90% within 48 hours and complete protein loss within 72 hours.

Initial analysis of the knockout cells indicates that absence of HDAC3 impacts on the growth rate of cells with population doubling time delayed by 5 hours, delay in S phase progress and reduced clonogenicity (FIGURES 3.9-3.11) although the differentiation potential of cells was not inhibited as they were able to exit the pluripotent state in the absence of LIF (FIGURE 3.11). We also observed a decrease in co-repressor complex components in the absence of HDAC3 indicating that HDAC3 is essential for maintaining the structural integrity of the HDAC:SMRT/NCoR complex (FIGURE 3.6).

Chapter Four: Understanding the role of HDAC3 in embryonic development

4.1 Introduction

HDAC3 knockout mice exhibit embryonic lethality prior to embryonic day 9.5 (e9.5 days) suggesting possible defects in gastrulation. Using the HDAC3 conditional knockout ES cell line generated in Chapter 3, we aimed to further examine the role of HDAC3 in embryonic development through the differentiation of ES cells into embryoid bodies (EBs).

4.2 *In vitro* differentiation analysis of *Hdac3*$^{L/L}$ mouse ES cells

4.2.1 ES cells depleted in HDAC3 exhibit morphological defects as embryoid bodies (EBs).

During mouse embryogenesis, in the epiblast, a transient structure known as the primitive streak develops just prior to gastrulation at embryonic day e6.5-7.0, which gives rise to the mesoderm, endoderm and ectoderm, the three primary germ layers (Tada *et al.*, 2005). The generation of spheroid aggregates known as embryoid bodies (EBs) from ES cells mimic the changes of early gastrulation, allows further examination of the role of HDAC3 in embryogenesis *in vitro*.

Control (-OHT) and knockout cells (+OHT-4) cells were cultured in the absence of LIF for 8 days in ultra-low attachment 96 well plates which allowed the generation of uniform size EBs and were visualised and measured every 2 days. Initial culture of HDAC3 knockout EBs showed that they were able to form aggregates similar to control EBs until day 4 of culture (FIGURE 4.1). However, extended culture beyond this timepoint revealed that EBs lacking HDAC3 are morphologically abnormal, becoming irregularly shaped rather than uniformly spherical. In addition to this, knockout EBs are significantly smaller; at day 4 of culture, both control and knockout EBs are comparable in

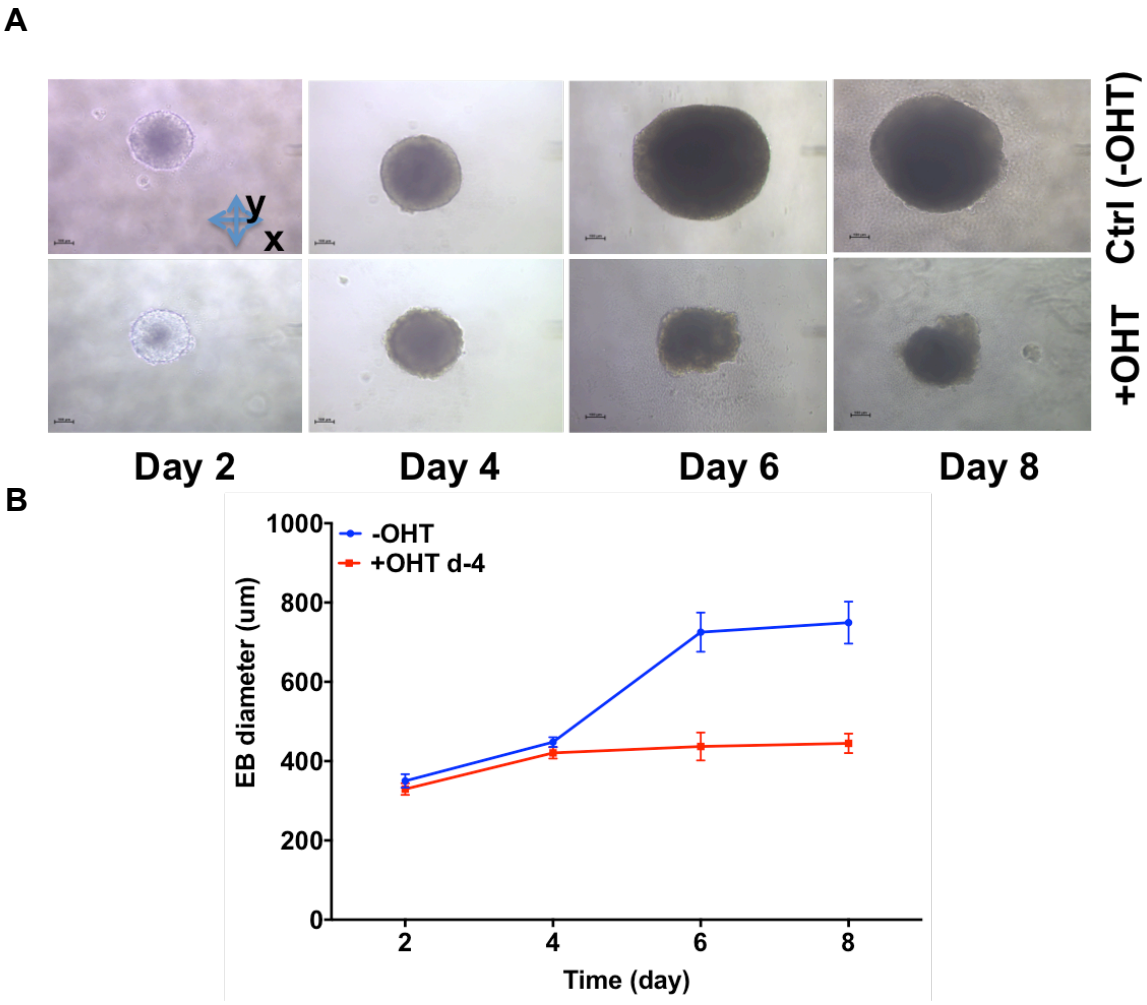

Figure 4.2 Loss of HDAC3 affects embryoid body differentiation. (A) Representative images of EBs at the indicated timepoint reveals a reduction in size and irregular shape of EBs lacking HDAC3. (B) Mean size of EBs during a 8 day experiment. Mean values (n=3) ± SEM are plotted.

size (420 μm and 448 μm respectively). However, subsequent culture beyond this time point reveals that growth of knockout EBs stalls and there is no further increase in size. By day 6 of culture, knockout EBs are around 40% smaller than controls indicating a possible defect in differentiation.

4.2.2 Experimental design of HDAC3 microarray

The HDAC3:SMRT complex acts as a transcriptional repressor which regulates gene expression. In order to fully understand the abnormal phenotype of EBs lacking HDAC3, gene expression analysis using microarray was performed on control and knockout EBs at day 3, 5 and 7 days of EB development to assess the effect of HDAC3 loss on gene expression. These time points were selected for a number of reason; firstly, knockout EBs appear to mimic control EB development until 4 days of culture beyond which knockout EBs do not increase in size. As such, day 4 of culture appears to be a significant timepoint at which knockout EBs diverge from their counterpart and are no longer able to differentiate further, perhaps due a block in development or due to cell death. By choosing time points either side of this critical timepoint, we hoped that we would understand the changes in gene expression associated with this defect. Similarly, by choosing a timepoint at which the EBs are most dissimilar (day 7), we aimed to understand the effect of HDAC3 loss later on in differentiation.

RNA was isolated from control and knockout EBs (day 0: ES cells through to day 7 EBs) and used for comparative analysis through hybridisation to an Agilent SurePrint G3 Mouse Gene Expression microarray which covers more than 27,000 transcripts and 4,500 long non-coding RNAs. Quality control of RNA was assessed using a Nanodrop spectrophotometer followed by analysis on an Agilent Bioanalyser; robust rRNA peaks confirmed the integrity of the RNA and only samples with an RNA integrity number (RIN) of 7.0 and above were selected from processing and array hybridization.

Principal component analysis (PCA) using GeneSpring software (detailed in Chapter 2.7.3) allowed us to initially group samples and look at intra- and inter-sample variation which can skew downstream analysis (Ringner, 2008). Greatest variability was identified between time points (FIGURE 4.2); as would be expected, the largest variation between data sets was between D0 and D7 samples (red and green compared to dark blue and grey: control and untreated, respectively). Although there are differences in variation between conditions (treated (+OHT; denoted T followed by time point number in days in figure e.g. T3: +OHT day 3 EBs) compared to untreated control; denoted C in figure), at day 0, these are still similar enough to be grouped near each other suggesting similar gene expression profiles. As the EB differentiation time course progresses, there is increased variation between the conditions such that their position in 3-dimensional space is increased, becoming more separated from the day 0 control samples suggesting larger variation between samples (inter-sample variability) and the greatest differences in gene

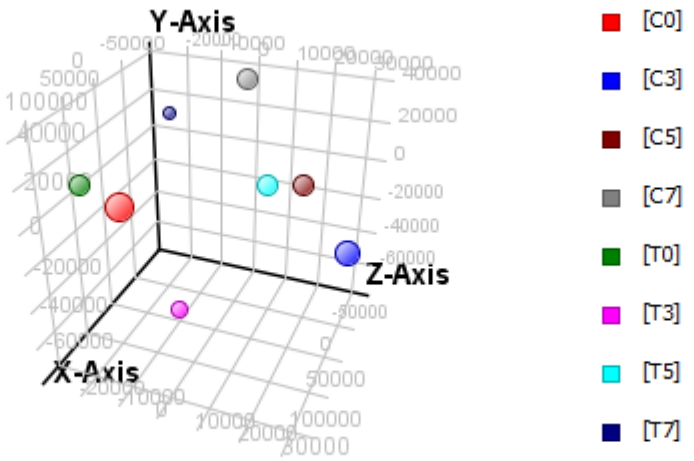

Figure 4.2 Principal component analysis (PCA) of EB differentiation time course. 3D PCA score plot of all differentiation time course samples suggests greater variability between later time points compared to respective controls (red (control) and green (+OHT (T))).

expression patterns. PCA analysis of each of the individual timepoint replicates revealed tight grouping of each of the three independent samples used for each timepoint indicating that there was limited intra-sample variability.

4.2.3 Initial differentiation of HDAC3 knockout EBs is unaffected.

Transcripts that were up- or down-regulated by greater than 1.5 fold (p value <0.05) across three independent experiments were identified using GeneSpring analysis software. As expected, there was a correlation between the duration of EB differentiation and the number of deregulated genes (FIGURE 4.3). On day 0 (control compared to knockout cells), there were 870 de-regulated genes (546 up-regulated compared with 324 down-regulated transcripts) with increasing numbers of differentially expressed genes over the duration of the time course (2591 on day 3, 2265 on day 5

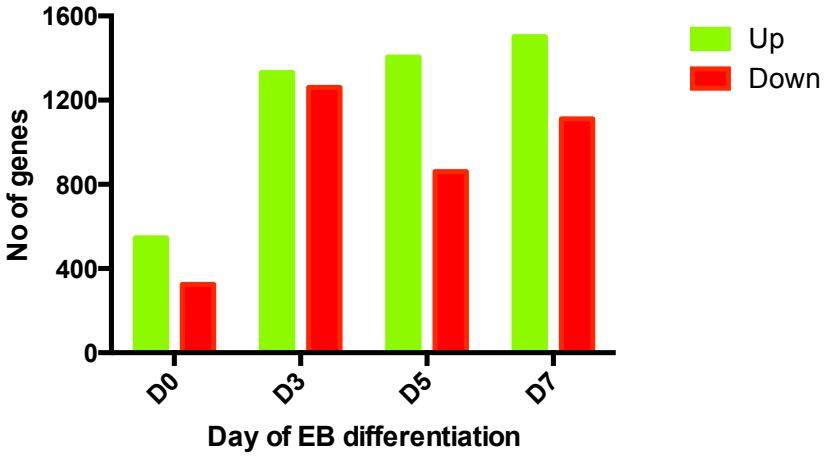

Figure 4.3 Differential expression of gene in the absence of HDAC3. Number of genes differentially expressed (FC >1.5) at the indicated days (compared with control -OHT) over EB differentiation time course; up indicates gene that are upregulated, down indicated genes that are downregulated.

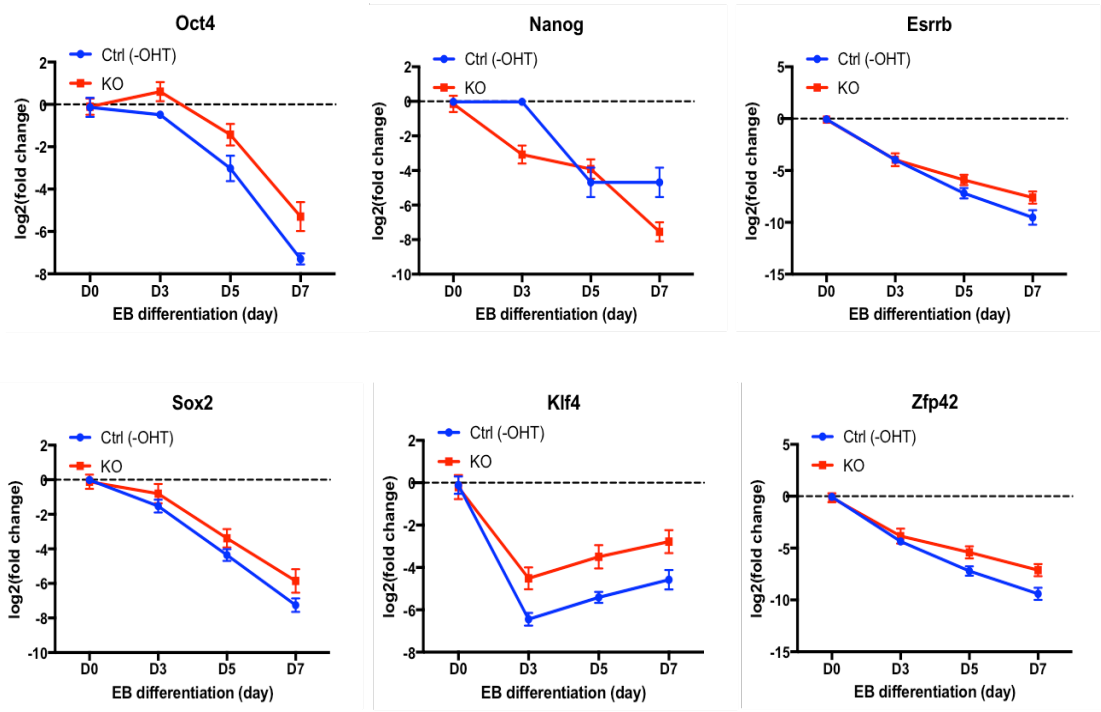

Figure 4.4 HDAC3 knockout cells can exit pluripotency. Expression of key pluripotent genes *Oct4, Nanog, Sox2 and Klf4* show a reduction in expression in the absence of HDAC3 comparable to control cells. Fold change was calculated using raw microarray data, scale is log2.

and 2613 on day 7). There were consistently more up-regulated genes in the absence of HDAC3, (1405 up-regulated and 860 down-regulated on day 5 and 1502 up-regulated and 1111 down-regulated on day 7) consistent with a role of HDAC3 in transcriptional repression.

Further analysis indicated that key pluripotency factors including *Pou5f1 (Oct4)* and *Nanog* as well as other factors associated with pluripotency, *Sox2*, *Klf4*, *Rex1 (Zfp42)* and *Essrb* were significantly reduced by day 7 of EB differentiation (FIGURE 4.4) confirming that cells have successfully exited from the pluripotent stem cell programme.

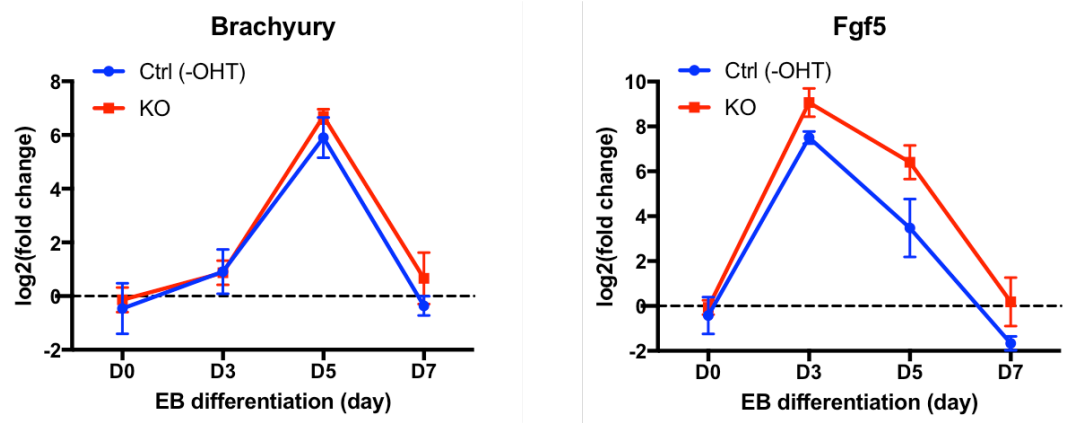

Figure 4.5 Initial ectoderm and mesendoderm differentiation is not affected by HDAC3 loss. Expression of key drivers of mesendoderm (*brachyury*) and ectoderm (*Fgf5*) differentiation shows similar patterns of expression between control and knockout EBs. Fold change was calculated using raw microarray data, scale is log2.

As previously discussed, EB differentiation mimics the changes in gene expression associated with gastrulation, culminating with the generation of the three primary germ layers, mesoderm, endoderm and ectoderm. Accordingly, gastrulation is a highly organised and tightly controlled process that requires the interaction of both intrinsic (transcription factors, chromatin remodellers and epigenetic regulators) and extrinsic (Nodal, Wnt and BMP) factors. Each germ layer is specified through the expression of a key driver whose specific expression is required for downstream differentiation. For example, primitive streak formation and the subsequent development of the mesoderm and endoderm from the intermediate mesendoderm (ME), requires the expression of *brachyury (T),* which is expressed throughout the primitive streak. Loss-of-function studies indicate *T* plays an essential role in gastrulation since there is a complete failure of gastrulation and primitive streak formation during mouse embryogenesis (Lolas *et al.*, 2014). Similarly, ectoderm formation is dependent on FGF signalling with loss-of-function of FGF receptor 1 (*Fgfr1)* and other FGF family members resulting in lethality at gastrulation (Deng *et al.*, 1994; Hebert *et al.*, 1991).

We assessed the expression of these key factors over the duration of the 7 day EB differentiation time course and noted that knockout EBs show a similar induction (day 5) and repression (day 7) of *Brachyury* and *Fgf5* (induced day 3 and repressed by day 7) (FIGURE 4.5) suggesting that loss of HDAC3 does not affect the initial differentiation of either mesendoderm or ectoderm lineages.

4.2.4 HDAC3 loss impacts mesoderm and endoderm differentiation.

Since the initial specification of the primary germ layers is not affected by HDAC3 loss, we next looked at specific lineage markers from each germ layer. Ectoderm gives rise to the formation of the neural tube, neural crest and the epidermis. Accordingly, expression of early neuronal cell markers *Nestin and Pou3f2* as well as *Map2* and *Pax6* (FIGURE 4.6) which are expressed later in the neuronal differentiation pathway all exhibit similar patterns of induction in knockout EBs compared to controls suggesting that ectodermal differentiation is unaffected by HDAC3 loss.

Expression of brachyury indicated that initial mesendodermal differentiation was unaffected; however, endodermal and mesodermal specification appears to be altered downstream of *brachyury* expression. Both lineages are derived from the mesendoderm, with the mesoderm giving rise to bone, heart, haematopoietic cells, muscle and kidney whereas the endoderm differentiates into liver, kidney, pancreas, lung and intestine (Wang & Chen, 2016).

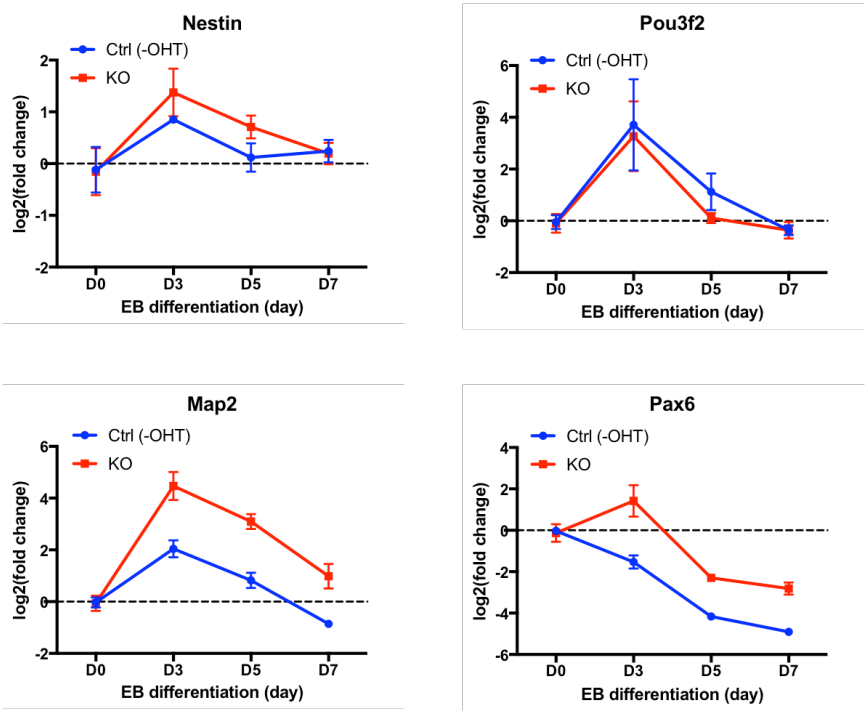

Figure 4.6 HDAC3 loss does not affect differentiation of the ectodermal germ layer. Markers of ectodermal differentiation show similar patterns of expression between control and knockout EBs. Fold change was calculated using raw microarray data, scale is log2.

Unlike HDAC1 knockout EBs which develop a spontaneous "beating" phenotype and concomitant increase in cardiomyocyte specific markers (Dovey *et al.*, 2010), HDAC3 knockout EBs exhibit a decrease in several cardiomyocyte markers (FIGURE 4.7A). Essential for cardiomyocyte differentiation and vasculature formation, *Mef2c* shows a similar pattern of induction (day 3) and repression (from day 5) between knockout and control EBs. However, whilst the early cardiomyocyte markers *TBX5* and *TBX20* both exhibit the same pattern of induction as control EBs, expression is markedly reduced in knockouts by day 5 of differentiation suggesting that cardiomyocyte specification is directly affected by HDAC3 loss.

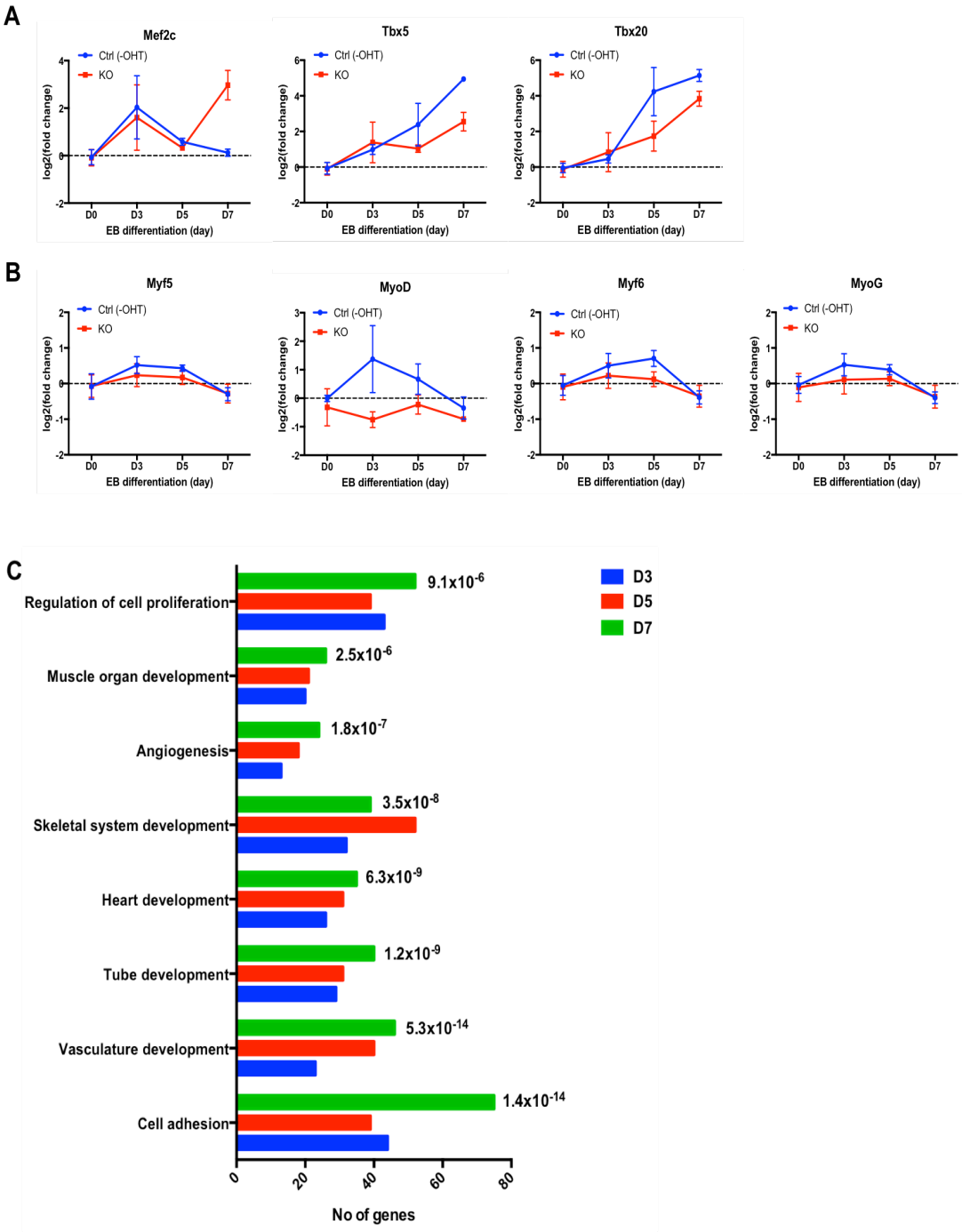

Figure 4.7 Mesodermal differentiation is reduced in HDAC3 knockout EBs. Reduction in expression of (A) cardiomyocyte specific markers and (B) muscle specific markers throughout the EB differentiation time course is shown in knockout EBs. Fold change was calculated using raw microarray data, scale is log2. (C) Functional annotation clustering of genes down-regulated in HDAC3 knockout EBs. Represented are the top statistically enriched biological function gene ontology terms (BF-GO terms) and the number of deregulated genes of each cluster.

Muscle differentiation (myogenesis) is specified through the expression of myogenic regulatory factor (MRF) genes, including *Myf5, Myf6, MyoD1* (encoding MyoD) and *MyoG (*encoding myogenin) (Rohwedel *et al.*, 1994). *Myf5* is the earliest MRF gene to be expressed in the developing embryo prior to the sequential expression of other MRF family members. From day 3 of EB differentiation, *Myf5* shows a reduction in expression which continues for the duration of the time course before expression in both control and knockout EBs is repressed by day 7 (FIGURE 4.7B). However, all downstream MRFs are markedly affected by HDAC3 loss. *Myf6, MyoD and MyoG* all show negligible induction throughout the duration of the EB time course unlike control EBs which all show expression by day 3 and subsequent repression suggesting that myogenic differentiation is lost in HDAC3 knockout EBs.

An analysis of functionally related gene groups among the genes that are down-regulated in knockout EBs using Database for Annotation, Visualisation and Integrated Discovery (FIGURE 4.7C) revealed that there was enrichment for genes involved in muscle organ development ($2.5x10^{-6}$), heart ($6.3x10^{-9}$) and vasculature development ($5.3x10^{-14}$) as well as skeletal system development ($3.5x10^{-8}$), again suggesting that mesodermal differentiation, particularly of cardiomyoctye and muscle lineages, is affected in HDAC3 knockout EBs.

Conversely, there is an increase in markers associated with endodermal differentiation. During mouse development, endoderm can be divided into two classes: visceral (primitive) endoderm which derives directly from the inner cell mass and gives rise to extra-embryonic endoderm or definitive endoderm which gives rise to the epithelium of the gastrointestinal and respiratory systems (Lu *et al.*, 2001). Forkhead transcription factors of the FoxA family (primarily *FoxA2)* and GATA factors (primarily *Gata4* and *Gata6)* as well as the SRY-related HMG-box family member *Sox17* are all essential for endodermal development (Kanai-Azuma *et al.*, 2002; Ang *et al.*, 1993; Jacobsen *et al.*, 2002). Microarray analysis indicates that there

A

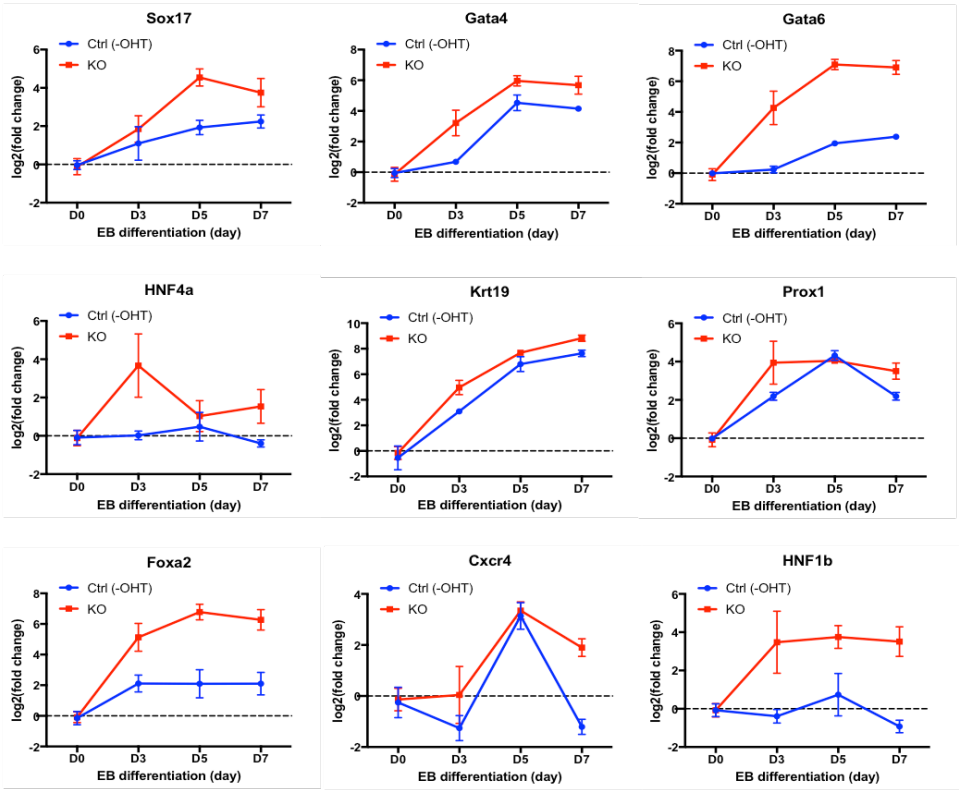

B

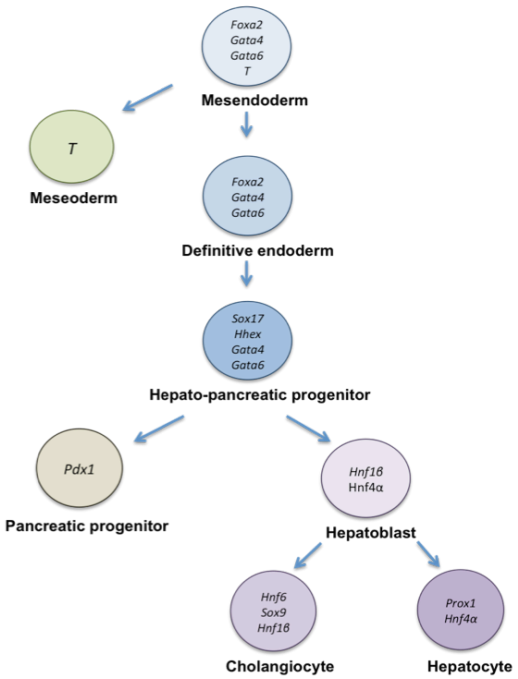

Figure 4.8 HDAC3 loss affects differentiation of the hepatic lineage. (A) Increase in expression of endodermal markers in HDAC3 knockout EBs. Fold change was calculated using raw microarray data, scale is log2. (B) Schematic of hepatic differentiation with associated markers denoted.

is a marked increase in expression of each of these factors suggesting that there is increased endodermal expression in HDAC3 knockout EBs (FIGURE 4.8A).

Downstream targets of these genes including hepatocyte nuclear factor (HNF) family members *HNF1β* and *HNF4α* as well as cytokeratin family member *Krt19* are also upregulated. Taken together, this data suggests that HDAC3 knockout EBs preferentially differentiate towards endodermal specification at the expense of mesoderm whilst ectodermal differentiation is unaffected.

4.2.5 HDAC3 loss impacts hepatic differentiation

During embryogenesis, multipotent progenitors require commitment at each stage of differentiation to give rise to terminally differentiated cells. Interestingly, each of the genes highlighted above are essential for hepatic development (FIGURE 4.8B). For example, *FoxA2, Gata4 and -6* and *brachyury* are all widely expressed in the mesendoderm at the onset of gastrulation. Loss of *brachyury* but maintenance of *Gata4/6* and *Foxa2* is indicative of definitive endoderm formation which occurs 8 to 10 hours following the onset of gastrulation (Lawson *et al.*, 1991). Following this, foregut definitive endoderm gives rise to a bipotent hepato-pancreatic progenitor expressing *Sox17, Hhex, Gata4* and *Gata6;* downstream of this either pancreatic progenitors (*Pdx1*$^{+}$*)* or hepatoblasts (*Hnf1β*$^{+}$ *Hnf4α*$^{+}$*)* are produced, which ultimately give rise to terminally differentiated cholangiocytes or hepatocytes (Gordillo *et al.*, 2015).

Each of these hepatic-specific genes are mis-regulated in HDAC3 knockout EBs at day 3 of EB differentiation despite the pioneer factor of mesendoderm formation, *brachyury*, exhibiting a normal pattern of expression. Notably, expression of *Hnf1β* and *Hnf4α,* factors that are both essential for the onset of hepatic gene expression during differentiation and liver bud formation, were both already highly expressed at day 3 whereas control EBs did not show induction until day 5 of EB formation.

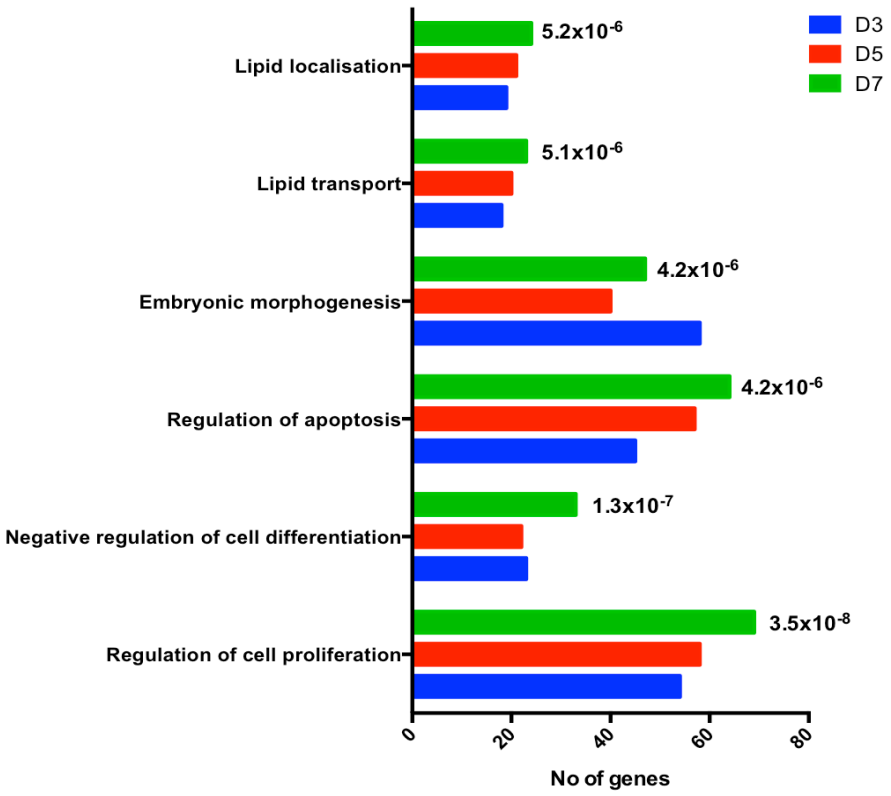

Figure 4.9 Downregulation of liver-specific functions in HDAC3 knockout EBs. Functional annotation clustering of genes up-regulated in HDAC3 knockout EBs. Represented are the top statistically enriched biological function gene ontology terms (BF-GO terms) and the number of deregulated genes of each cluster.

Allied to this, analysis of functionally related gene groups among deregulated genes using DAVID (FIGURE 4.9) indicated that there was an enrichment of genes involved in lipid localisation ($p= 5.2x10^{-6}$) and lipid transport ($p=5.1x10^{-6}$), both liver-specific functions, among genes that are expressed at a higher level in HDAC3 knockout EBs. These results suggest that HDAC3 may play a role in regulating hepatic cell fate.

4.3 Conclusions

Initial differentiation studies in Chapter Three suggested that, although knockout cells were able to spontaneously differentiate in the absence of LIF, there were reduced numbers of differentiated colonies in the absence of HDAC3 suggesting a possible defect in differentiation. Thus, HDAC3 knockout ES cells were differentiated into EBs to further understand the role of HDAC3 in embryonic development. Knockout cells were able to exit the pluripotent stem cell programme and form EB aggregates over a two day period, but then became morphologically abnormal and smaller in size compare to controls (Figure 4.1). Global transcriptome analysis revealed that downstream lineage differentiation is affected in knockout EBs although validation of the microarray either through quantitative RT-qPCR or Western blotting has yet to be performed. However, due to the design of the Agilent microarray, multiple probes per gene were present on the array, all of which exhibit the same pattern of gene expression which suggests the observed differences in gene expression are bone fide. There was a decrease in the expression of mesodermal markers, particularly those associated with cardiac and skeletal muscle (Figure 4.6), and an increase in endodermal markers, particularly those associated with hepatic differentiation (Figure 4.7). Together, this data shows that knockout cells show a propensity to differentiate towards endodermal lineages at the expense of mesodermal lineages.

Chapter Five: Understanding the physiological role of inositol phosphates in the HDAC3:SMRT complex

5.1 Introduction

Recent work by Watson *et al.* identified that at the core of the HDAC3:SMRT crystal structure, inositol 1,4,5,6-tetrakisphosphate (IP_4) was bound in a highly basic pocket at the interface between the enzyme and its cognate co-repressor protein. Phosphates from the IP molecule make extensive intermolecular interactions with both proteins (His17, Gly21, Lys25, Arg265 and Arg301 of HDAC3 and Lys449, Tyr470, Lys474 and Lys475 of the deacetylase activation domain (DAD) in SMRT). These residues are evolutionarily conserved in other Class I HDAC-containing complexes suggesting that these complexes may also be activated by inositol phosphates. Indeed, exogenous application of IP_4 to purified HDAC3:SMRT, HDAC1:MTA1 or MiDAC complexes results in robust activation of the complex suggesting that IP_4 and other inositol phosphates may act as regulators of HDAC activity *in vivo* (Millard *et al.*, 2013; Itoh *et al.*, 2015; Watson *et al.*, 2016).

To further understand whether IP regulates HDAC3:SMRT mediated repression *in vivo*, I utilised a luciferase transcriptional reporter assay system. Mutations were made to key IP_4 interacting residues in both HDAC3 and SMRT and their effects on reporter gene transcription were assessed. Once established, I attempted to manipulate the endogenous levels of inositol phosphates through short hairpin RNA (shRNA) mediated gene knockdown and chemical inhibition of IPMK and IPPK, two enzymes key to the generation of inositol phosphates, to determine whether modifying inositol phosphate levels directly impacts on the repressive ability of the HDAC3:IP_4:SMRT complex.

5.2 Transcriptional repression by the HDAC3:SMRT complex

In isolation, HDAC3 is enzymatically inert (Guenther *et al.*, 2001). It is the proteins incorporation into large, multi-protein complexes with either silencing mediator for retinoid and thyroid hormone receptors (SMRT) or its homologue nuclear co-repressor (NCoR), transducin β-like 1 (TBL1), TBL1-related protein (TBLR1) and G-protein pathway suppressor 2 (GPS2) in a 1:1 stoichiometric ratio that allows for the activation of the enzyme (Li *et al.*, 2000; Wen *et al.*, 2000; Guenther *et al.*, 2001; Oberoi *et al.*, 2011; You *et al.*, 2013). Activation of HDAC3 is facilitated through direct interaction with the deacetylase activation domain (DAD) of NCoR/SMRT proteins: this is found in the N-terminus of the co-repressors and is composed of a 16 amino acid DAD-specific motif as well as a C terminal SANT-like motif (Guenther *et al.*, 2001; Codina *et al.*, 2005). Upon formation of a functional complex with HDAC3, there are gross conformational rearrangements in the structure of the DAD such that it lies along the surface of the enzyme making extensive intermolecular interactions (Watson *et al.*, 2012)

At the protein-protein interface, it has been identified that a potential regulatory molecule, inositol tetrakisphosphate (IP_4), is bound. It has previously been demonstrated *in vitro* that the enzymatic activity of HDAC3 is dependent on the presence of IP_4 at the interface between the HDAC enzyme and its cognate co-repressor (Watson *et al.*, 2012; Watson *et al.*, 2016)Whilst the repressive abilities of the HDAC3:SMRT complex have long been identified, it is unknown whether the transcriptional repression mediated by the complex *in vivo* is IP_4 dependent.

HDACs function as transcriptional co-repressors and associate with repressed genes where they mediate transcriptional repression through the deacetylation of histone proteins in the vicinity of target gene promoters. Consequently, if inositol phosphate modulates the enzymatic activity of HDAC3, the repression of a reporter gene would be affected. To demonstrate the repressive role of the HDAC3:SMRT complex, a

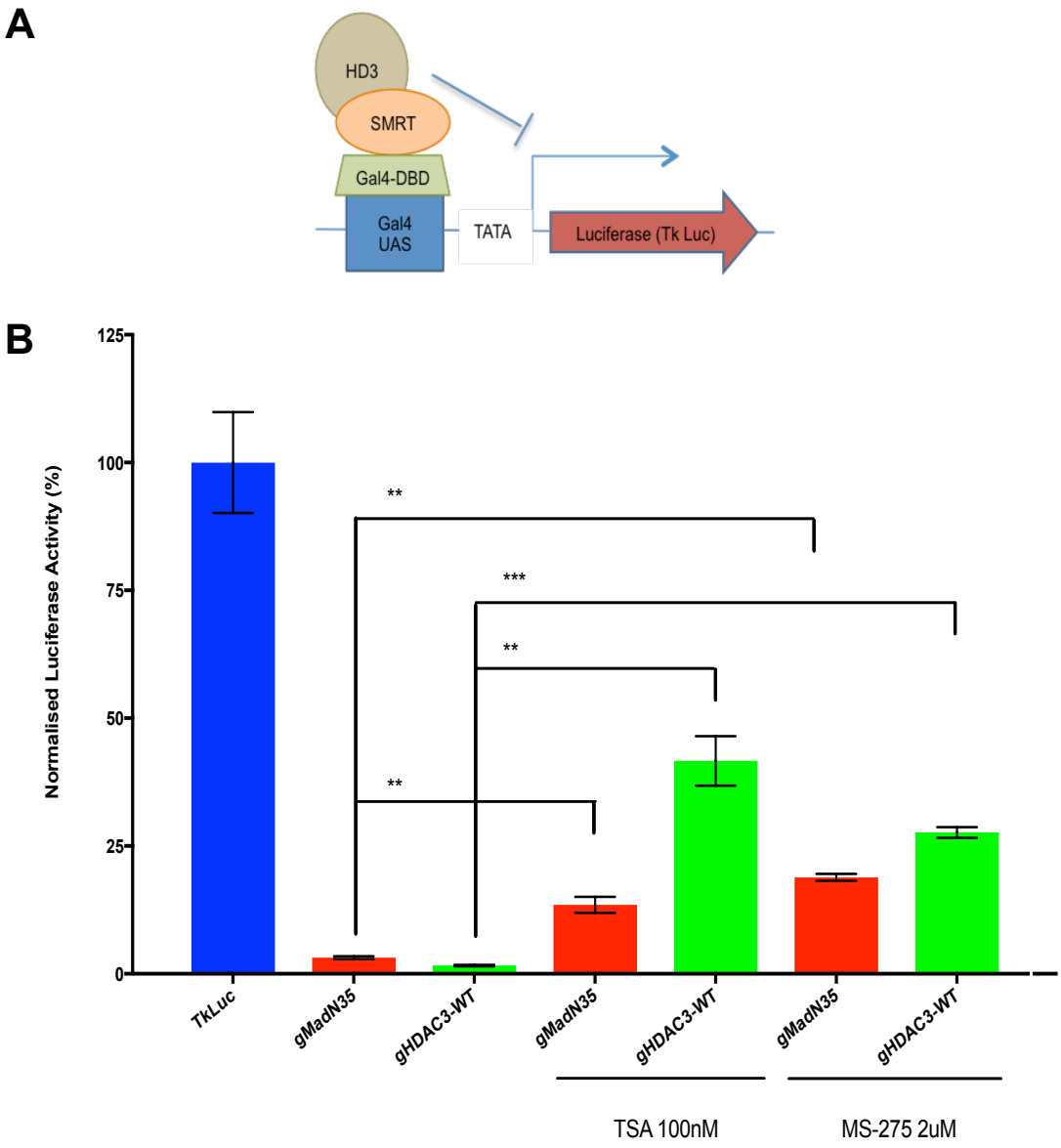

Figure 5.1 Transcriptional repression of luciferase reporter gene is HDAC dependent. (Top) Schematic of luciferase reporter assay: repression is mediated through recruitment of Gal4-DBD fusion proteins to drive repression of thymidine kinase (TK) luciferase gene construct. (Bottom) Repression of luciferase reporter gene is HDAC-dependent as treatment with HDAC inhibitors TSA and MS-275 induces a relief in repression in both Gal4-DBD MadN35 and HDAC3 fusion proteins. Mean luciferase values (n=3) ± SEM is shown.

conventional luciferase reporter assay was utilised. Here, HEK293T cells were transient transfected with a luciferase reporter gene which becomes chromatinised (Wells & Farnham, 2002). The plasmid contains multiple Gal4-DNA binding domain (DBD) binding sites upstream of the human simian virus thymidine kinase (TK) promoter which drives high levels of basal transcription of the luciferase reporter plasmid. As such, expression of the plasmid can be modulated through tethering of SMRT or HDAC3 to the promoter through their fused Gal4-DBD (FIGURE 5.1: top).

Accordingly, luciferase expression is robustly repressed by a Gal4-fusion protein of HDAC3 (FIGURE 5.1 bottom; lane 3) indicating that endogenous HDAC3:SMRT complex components are able to be recruited to the promoter to drive repression of the reporter gene. As a control for HDAC dependent repression, we also used Gal4-MadN35, the N-terminal 35 amino acids of the Mad1 protein, a robust repressor of transcription. Repression is similarly induced by the MadN35 construct (FIGURE 5.1 bottom; lane 2); this N-terminal region contains the Sin3-interaction domain (SID) which is necessary and sufficient for Mad transcriptional repression is an mSin3:HDAC1/2-dependent manner (Ayer *et al.,* 1996).

To confirm repression is dependent on histone deacetylation of the chromatinised reporter gene plasmid, two HDAC inhibitors, the pan HDAC inhibitor trichostatin A (TSA) and HDAC1-3 selective inhibitor MS275, were added to media for 24 hours prior to assaying luciferase expression. As expected, culture with either HDAC inhibitors resulted in a loss of ability of HDAC3 and Mad proteins to repress the reporter gene i.e. a relief in repression is shown (FIGURE 5.1) thereby indicating that the deacetylation of the histone tails in the region of the TK promoter is necessary for reporter gene repression and thus confirming the suitability of this system for assessing the transcriptional effects of the HDAC3:SMRT complex.

5.3 Mutational analysis of the HDAC3 and SMRT IP_4 binding residues.

Upon binding of HDAC3 to SMRT, there are gross conformational changes to the proteins' structure such that the co-repressor protein wraps along the surface of the enzyme (Watson *et al.*, 2012; Millard *et al.*, 2013). Previous mutagenesis studies indicate that mutations to the DAD (primarily Lys449, Tyr470 and Tyr471) impaired both the ability of the two proteins to interact as well as activation of HDAC3 (Codina *et al.*, 2005), which could be a consequence of impaired IP_4 binding.

The crystal structure of HDAC3:IP:SMRT (FIGURE 5.2, top) by Watson *et al.* was used as a basis for designing mutations to key IP interacting residues in both HDAC3 and SMRT (detailed in table in Figure 5.2). In order to identify whether transcriptional repression mediated by the HDAC3:SMRT complex *in vivo* is inositol phosphate dependent, these mutations would be expected to impair IP_4 binding and consequently impair the ability of the complex to repress transcription of the thymidine kinase reporter gene.

Initial experiments by Watson *et* al., 2013 confirmed expression of all protein constructs. As a control experiment, each of the mutants were transfected in HEK293T cells in isolation (FIGURE 5.3). All of the HDAC3 mutants showed little ability to modulate transcription of the luciferase reporter construct. This was to be expected since they lack a Gal4-DBD and as such, cannot be targeted to the promoter of the reporter gene. However, unlike Gal4-HDAC3, which was shown to be a potent repressor, Gal4-SMRT fusion proteins (gXtDAD; extended deacetylase activation domain; wild-type (lane 7) and mutants (lanes 8 and 9)) were also unable to repress transcription when expressed in isolation, indicating that they are unable to recruit endogenous complex components to the promoter and bring about repression.

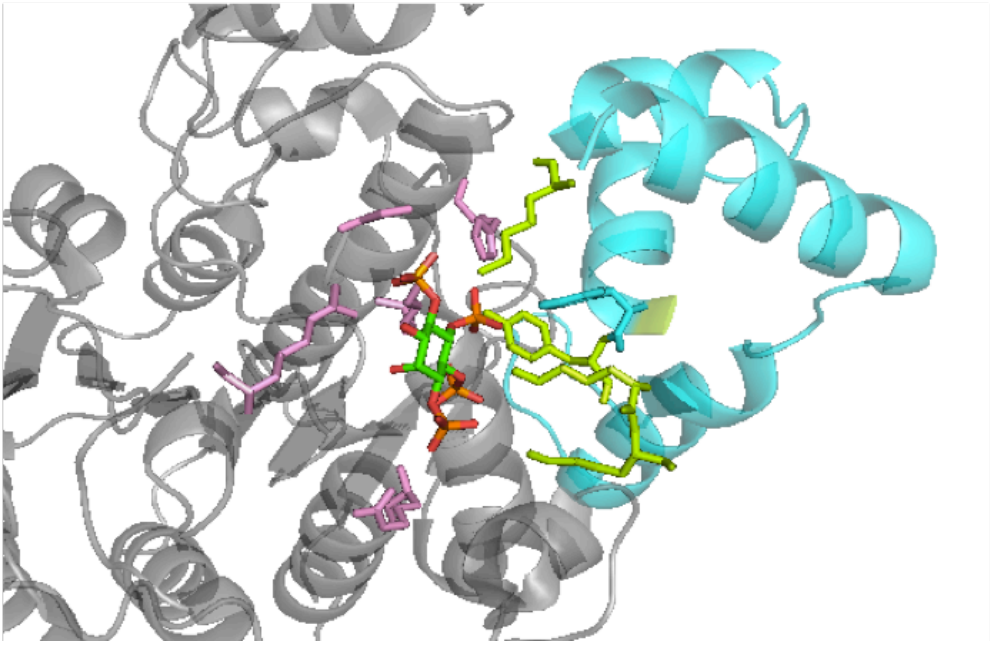

Protein	Mutation	Information
HDAC3	**uHDAC3 IP4-HDAC8** (H17C G21A K25I R265P R301A)	All IP_4 binding residues mutated to corresponding residues in HDAC8
	uHDAC3 Loop 6 (R265P/L266M)	Loop 6: binding surface for DAD and IP_4
	uHDAC3 R265P	IP_4 binding residue; key interaction
	uHDAC3 R265A	IP_4 binding residue; key interaction
	gHDAC3-mut (H17C G21A K25I R265P L266M R301A)	All IP_4 binding residues mutated to corresponding residues in HDAC8 AND Loop 6 mutant
SMRT	gXtDAD K474A K475A	
	gXtDAD Y470A Y471A	Failure to activate HDAC3.

Figure 5.2 Crystal structure of HDAC3:SMRT complex. (Top) At the interface of HDAC3 (grey) and deacetylase activation domain (DAD) of SMRT (green), IP_4 is bound in a highly basic pocket. HDAC3 (pink) and SMRT (green) residues that mediate the interaction with IP are shown. (Bottom) mutant HDAC3 and SMRT (XtDAD; extended deacetylase activation domain) constructs used in luciferase reporter gene transcription assay. "u" refers to untagged proteins, "g" refers to Gal4-DBD fusion proteins. PDB code: 4A69.

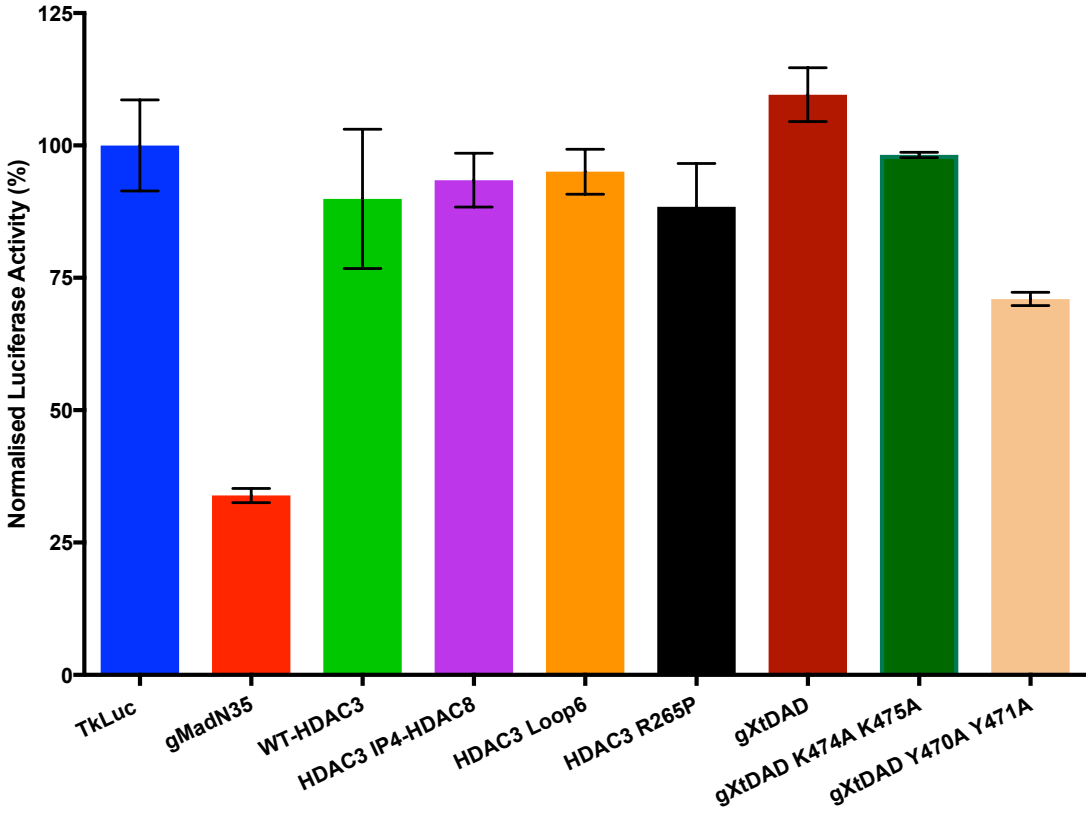

Figure 5.3 Transcription is unaffected by IP_4 HDAC3 and SMRT constructs in isolation. Untagged wild-type HDAC3, mutant HDAC3 (IP4-HDAC8, Loop 6 and R265P) and Gal4-XtDAD constructs were co-transfected into HEK293T wells; luciferase activity was not impacted upon transfection of the constructs in isolation. Details of all mutants can be found in table in FIGURE 5.2. The means luciferase activity (n=3) ±SEM is shown.

To investigate whether IP_4 HDAC3 mutants (FIGURE 5.4) retained their ability to repress transcription in a more physiological setting, the two most severe mutant constructs were co-transfected with a Gal4-XtDAD fusion protein. The first mutant selected was IP_4-HDAC8, in which all IP_4 interacting residues have been mutated to the equivalent residues in HDAC8. HDAC8 is the only Class I HDAC that is active in isolation and is not reliant on the presence of IP_4 for its enzymatic activity thus such mutations should render the mutant inactive and unable to interact with IP_4. The mutant was unable to drive repression of the reporter gene construct (FIGURE 5.5; lane 7) compared to wild type repression (lane 5). Similarly the second mutant in which Loop 6, the binding surface for the DAD and IP_4 in HDAC3 has been mutated, was also unable to bring about repression of the reporter construct (lane 9). This inability to impact on repression of the luciferase reporter is indicative of a lack of HDAC3 activity, presumably resulting from an impaired ability of IP_4 binding in the complex.

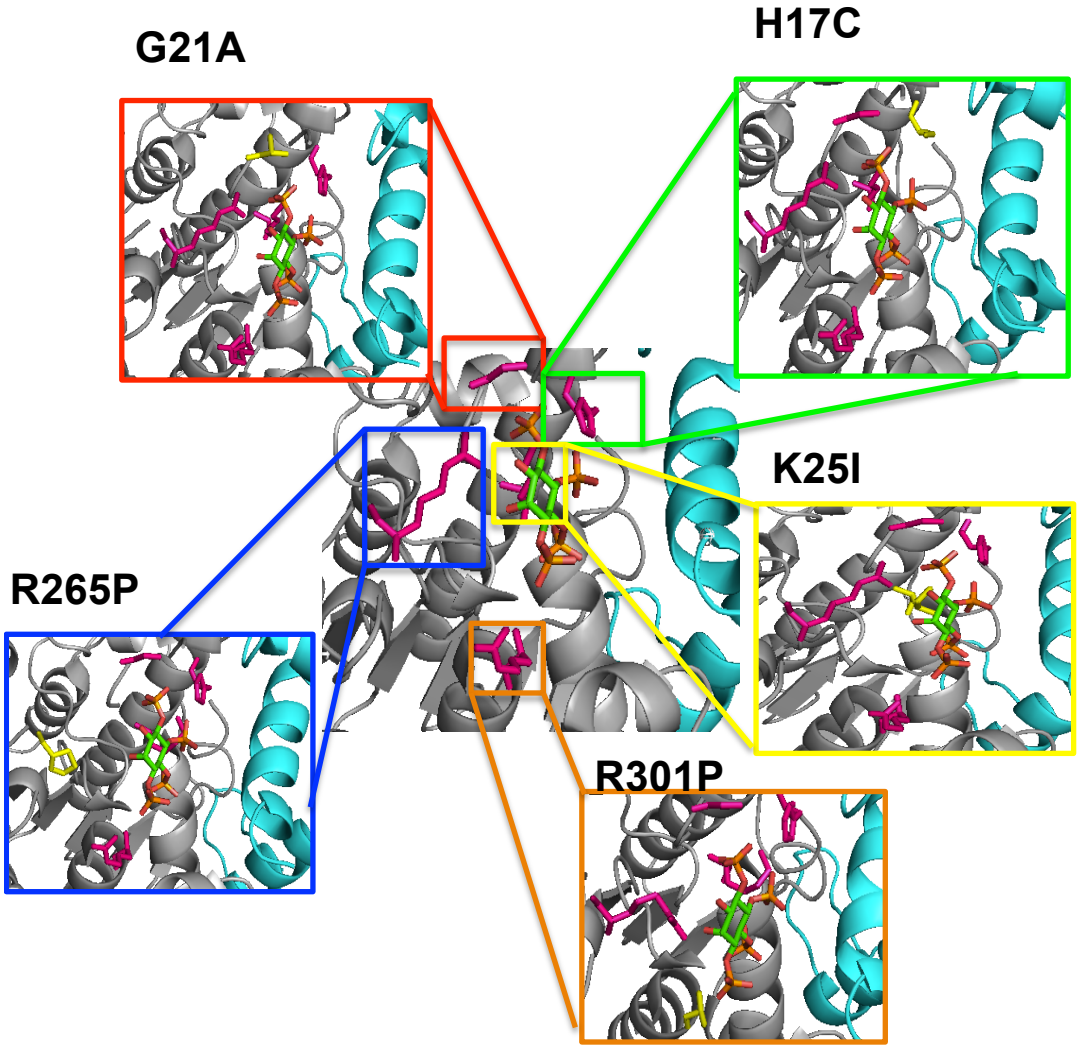

Figure 5.4 Structural representation of HDAC3 mutants. IP_4-collating residues (pink) in HDAC3 are highlighted and the associated mutated residue (yellow) are depicted. Residues are mutated to the equivalent residue in HDAC8. PDB code: 4A69.

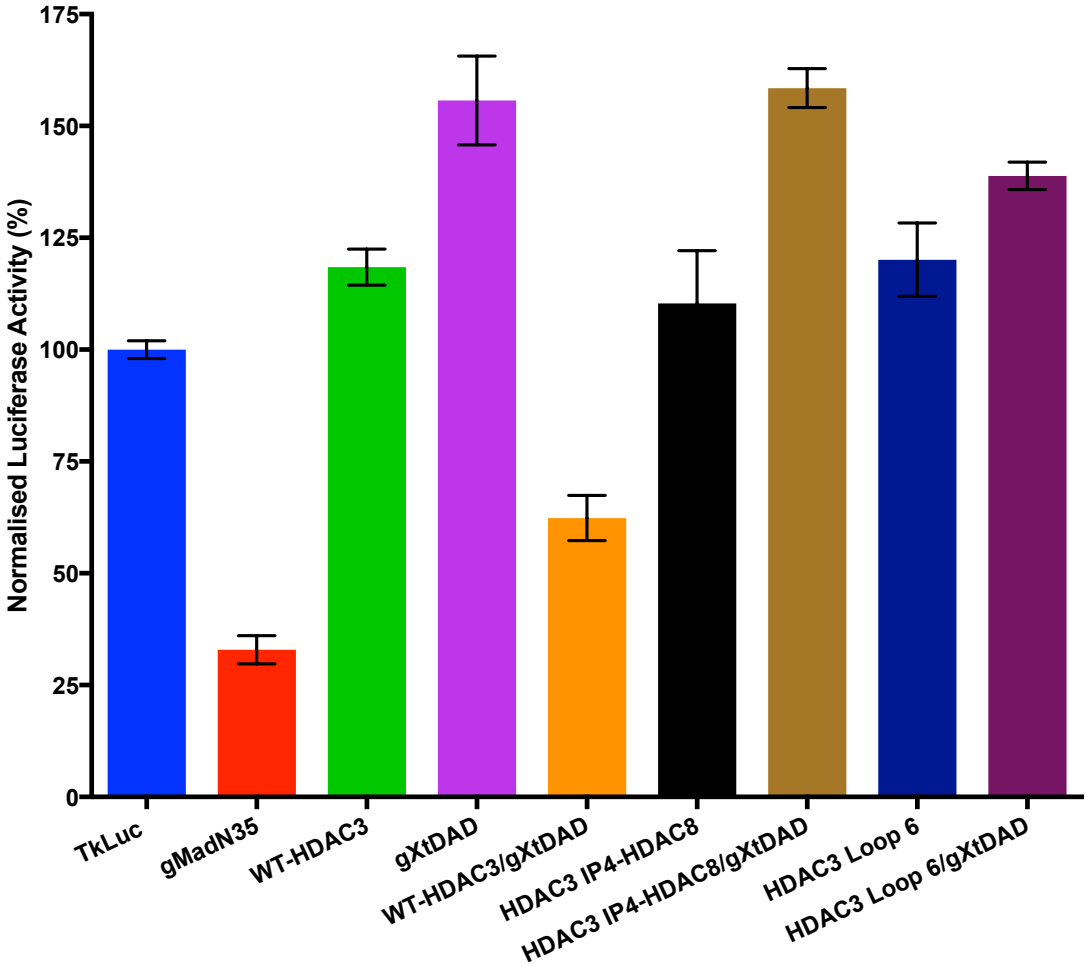

Figure 5.5 HDAC3 IP_4 mutants relieve transcriptional repression. Co-transfection of untagged HDAC3 mutants (IP4-HDAC8: lane 7 and Loop 6: lane 9) with Gal4-XtDAD fusion protein relieves transcriptional repression of the luciferase reporter construct compared to wild type (lane 5). The mean luciferase activity (n=3) ±SEM is shown.

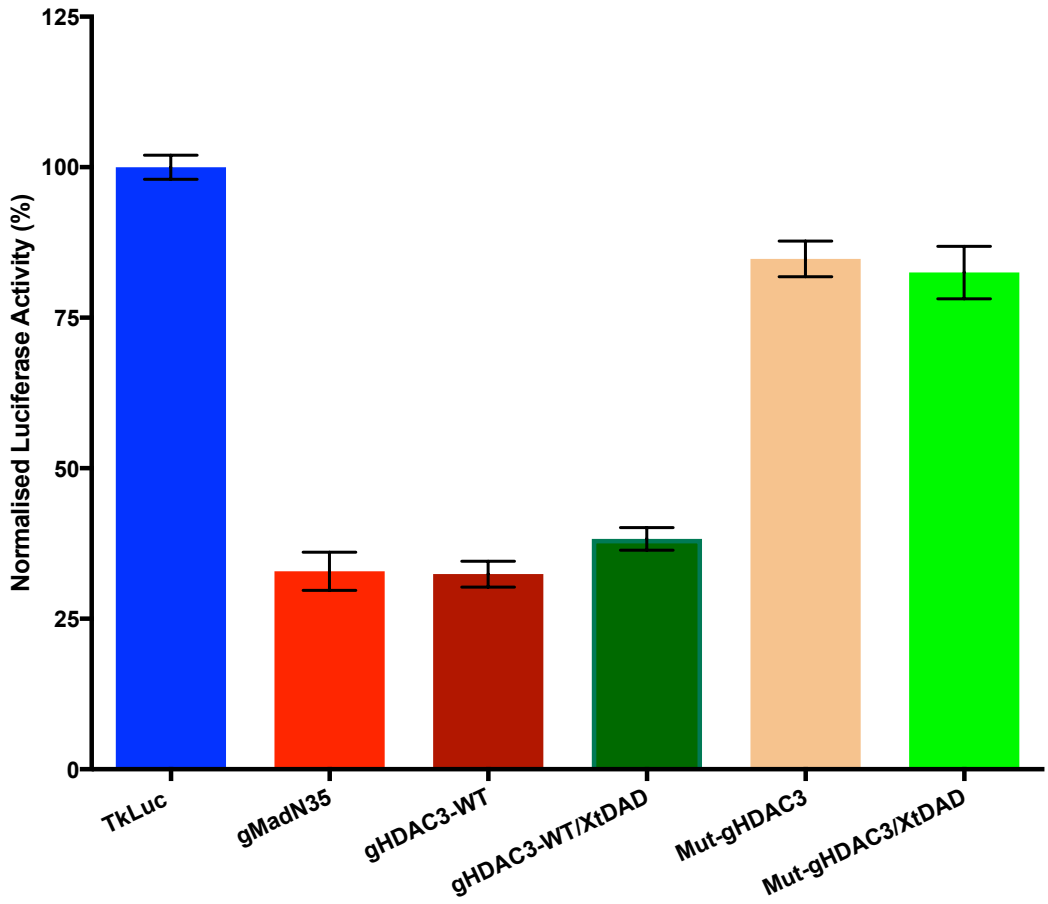

Figure 5.6 Confirmation of transcriptional repression by HDAC3. Wild-type Gal4-HDAC3 (lane 3) acts as a robust repressor whereas mutant Gal4-HDAC3 (H17C G21A K25I R265P L266M R301A; lane 5) is unable to repress the reporter gene. The mean luciferase activity (n=3) ±SEM is shown.

Reciprocal experiments in which mutant HDAC3 was expressed as Gal4-DBD fusion protein showed comparable results. As shown in FIGURE 5.6, in isolation, Gal4-HDAC3-WT (lane 3) is a robust repressor of luciferase gene expression with a 70% reduction in activity, comparable to the level of repression achieved by Gal-MadN35. Co-transfection with the untagged XtDAD construct (lane 4) was unable to increase the repressive activity of HDAC3 suggesting that Gal4-HDAC3-WT is driving repression of the promoter through the recruitment of endogenous co-repressor protein components. Importantly, repression of the luciferase reporter is impaired when a Gal4-HDAC3 mutant (lane 5) is transfected into cells; here, all IP_4

interacting residues and Loop 6 have been mutated such that IP_4 is no longer able to bind. When compared with wild type repression of Gal4-HDAC3-WT of approximately 70% (lane 3), there is 100% luciferase activity (no repression of the reporter construct by the mutant HDAC3 protein) indicating that once interaction with inositol phosphate is affected, HDAC activity is impaired and transcriptional repression is perturbed.

Next, mutations were made to SMRT in the deacetylase activation domain (DAD) which contains multiple residues which co-ordinate IP_4, namely Ty470, Tyr471, Lys474 and Lys475. Upon mutation to alanine, wild-type luciferase expression is significantly relieved indicating that disruption of IP binding through SMRT directly impacts on the ability of the HDAC3:SMRT complex to bring about transcriptional repression.

Compared to wild-type repression shown by the Gal4-DBD-XtDAD fusion protein co-transfected with HDAC3, double XtDAD mutant K474A/K475A (Figure 5.7, lane 6) alone showed increased luciferase expression 4-fold. Co-transfection of the mutant with wild-type HDAC3 was insufficient to modulate luciferase activity further (lane 7) indicating that disrupting the IP_4 interaction via the SMRT protein is sufficient to perturb the repressive ability of the HDAC3:SMRT complex. Such results were also paralleled in the second gXtDAD double mutant, Y470A Y471A. The mutant was able to relieve repression of the luciferase reporter 3-fold compared to wild-type (Figure 5.8 lane 6) with addition of wild-type HDAC3 unable to significantly modulate luciferase activity further (lane 7).

Interestingly, co-transfection of HDAC3 mutants alongside the SMRT mutants only showed a modest increase in luciferase expression, exhibiting comparable luciferase activity to wild-type HDAC3 co-transfection (Figures 5.7 and 5.8, lanes 8 and 9). This is unexpected since the interaction with IP_4 has been impeded by both protein partners which we would expect to have a significant effect on protein binding, interaction and activity. As such, luciferase gene expression would be predicted to be much higher. Since this is not the case, it suggests that the two proteins

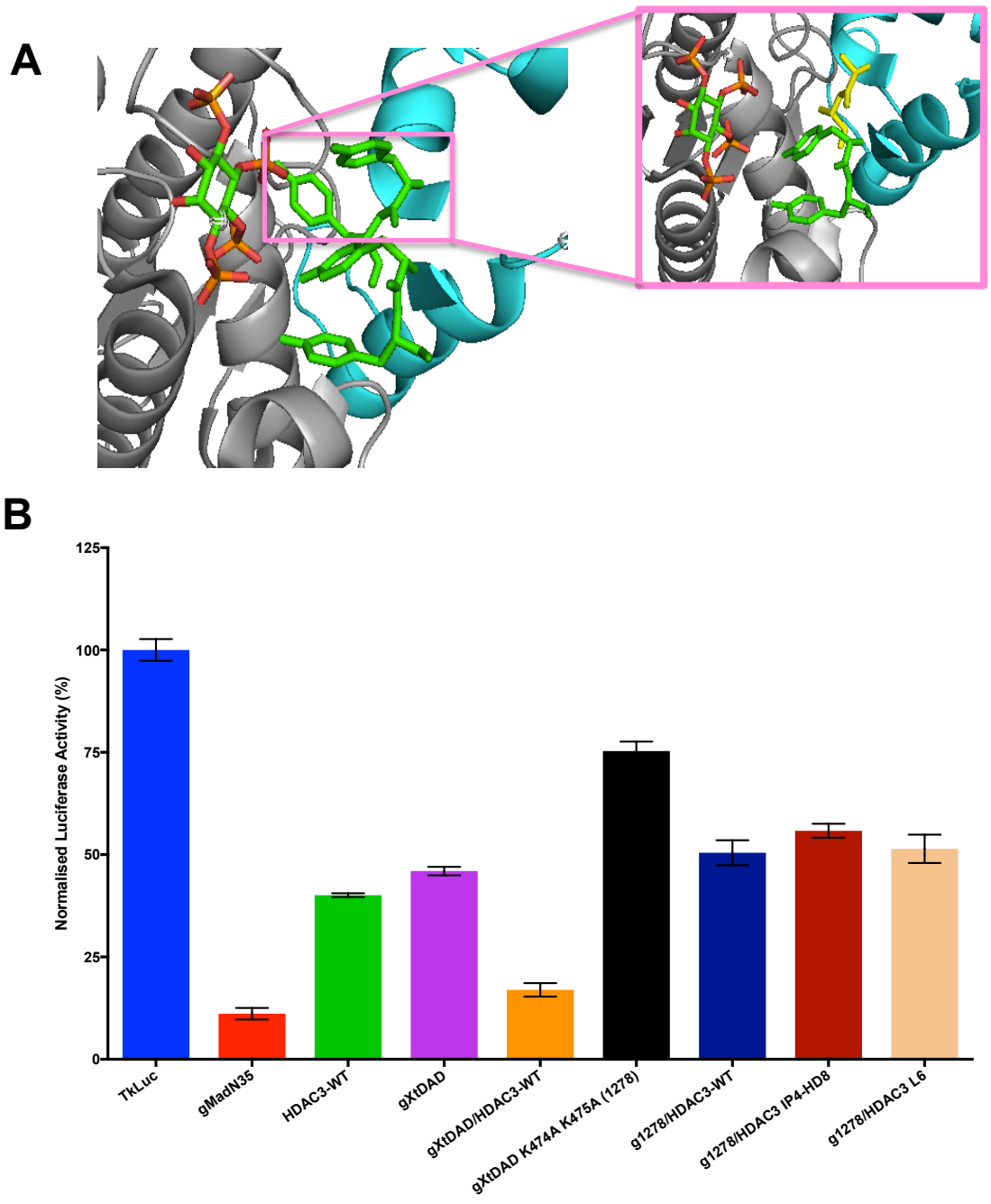

Figure 5.7 SMRT Y474A Y475A mutant relieves transcriptional repression. (A) Structural representation of SMRT mutant. PDB code: 4A69. (B) Compared to wild type repression by SMRT and HDAC3 proteins (lane 5, orange), transcriptional repression is relieved through co-transfection of Gal4-XtDAD SMRT mutants and untagged wild type (lane 7) and mutant HDAC3 (lanes 8 and 9). The mean luciferase activity (n=3) ±SEM is shown.

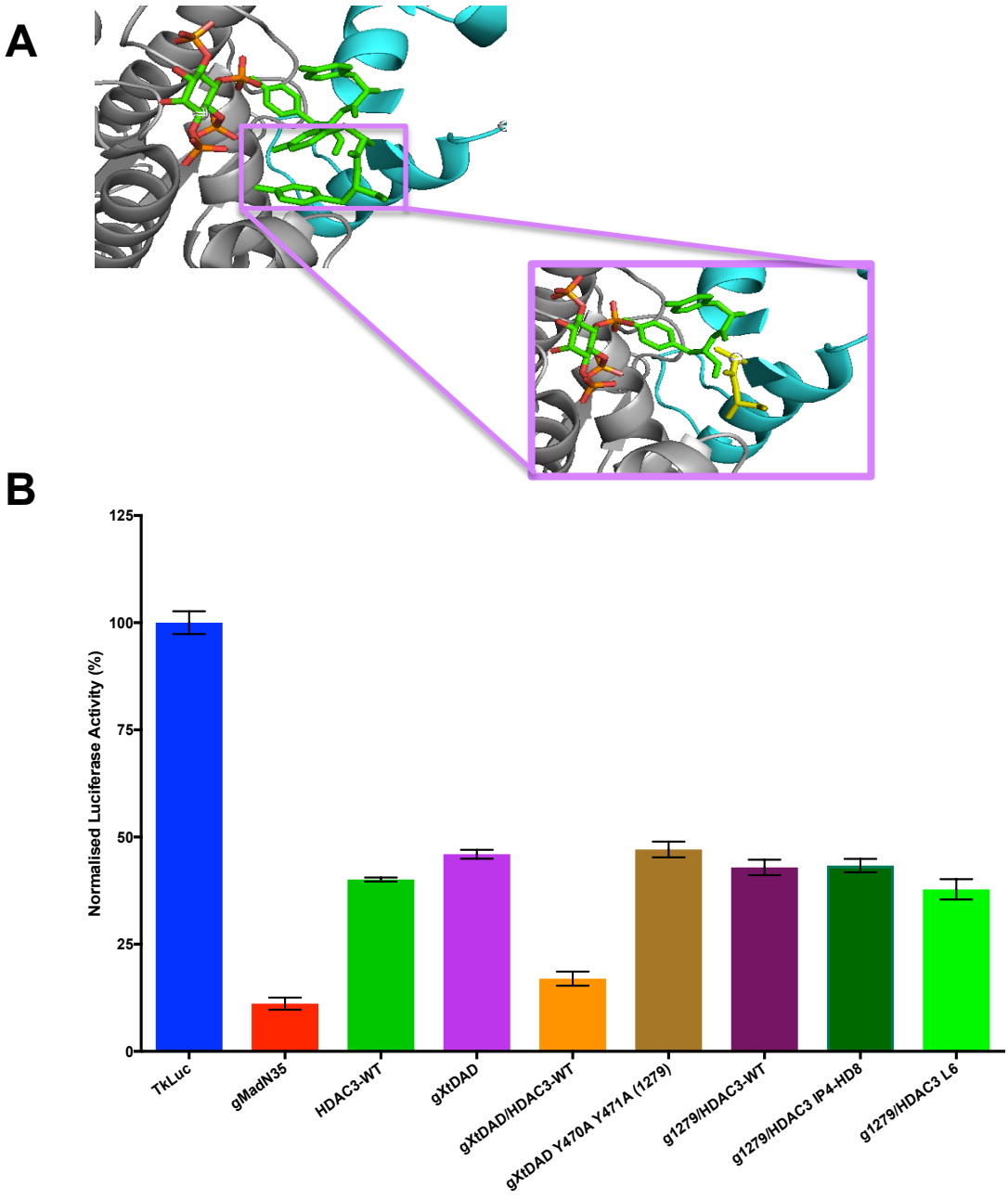

Figure 5.8 SMRT Y470A Y471A mutant relieves transcriptional repression. (A) Structural representation of SMRT mutant. PDB code: 4A69. (B) Compared to wild type repression by SMRT and HDAC3 proteins (lane 5, orange), transcriptional repression is relieved through co-transfection of Gal4-XtDAD SMRT mutants and untagged wild type (lane 7) and mutant HDAC3 (lanes 8 and 9). The mean luciferase activity (n=3) ±SEM is shown.

are still able to interact, although to a lesser extent that wild type SMRT and HDAC3. Nevertheless, mutant SMRT and HDAC3 proteins still exhibit increased luciferase expression, ranging from a 1.8-fold to a 2.6-fold increase, compared to wild-type proteins which suggests that disruption of IP_4 binding in the HDAC3:SMRT complex directly impacts HDAC3-mediated repression.

5.4 Insights into the mechanism of activation of HDAC3 by inositol phosphates

One of the key interactions between HDAC3 and IP_4 is that of Arginine 265 which forms a salt bridge with the 4-phosphate of IP_4. Mutation of this single residue (R265P) is sufficient to perturb enzymatic activity suggesting that this residue is critical for HDAC3 activity (Watson *et al.*, 2012)This mutation has been also shown to induce a conformational change of the enzyme, stabilising the protein in its ternary complex conformation thereby confirming it as an essential residue for enzymatic stability as well as activation (Arrar *et al.*, 2013)

Thermodynamic studies suggests that the loss of enzymatic activity in the R265 mutant is not due to a loss of binding of IP_4 since there in only a modest increase in the dissociation constant when bound to 2-FAM-IP_5 suggesting that this mutant complex is able to bind inositol phosphate but not become activated by it (Watson *et al.*, 2016). Accordingly, the mutant complex can only be weakly activated by exogenous addition of inositol phosphate. In addition to this, FIGURE 5.9 shows that R265P significantly impairs the ability of the complex to repress transcription of the luciferase reporter gene, confirming the significance of the interaction between R265 of HDAC3 with the phosphate in this position on the inositol ring for full enzymatic activation.

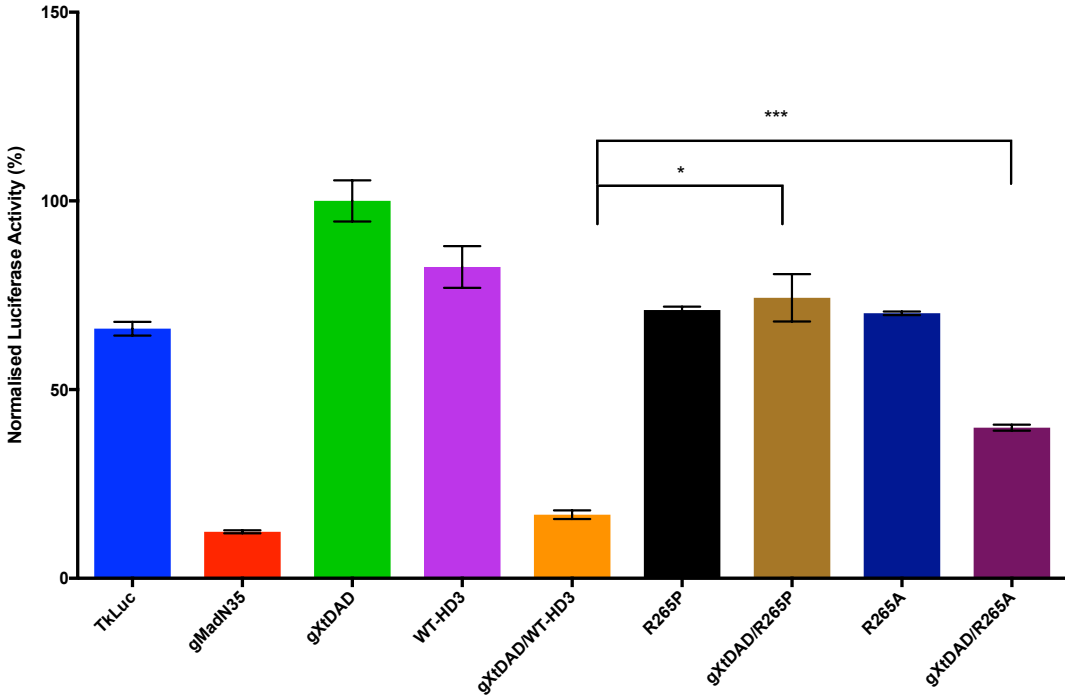

Figure 5.9 The interaction of Arginine 265 of HDAC3 and IP_4 is essential for HDAC3 activation. Both R265P and R265A mutants show a relief in repression 2 fold when co-transfected alongside a Gal4-XtDAD construct indicating that the interaction of this residue with IP_4 is essential for HDAC3:SMRT mediated repression. Mean luciferase values (n=3) ± SEM is shown.

5.5 Modulation of intracellular inositol phosphate concentration

Since impairing the binding of IP_4 to the HDAC3:SMRT complex appeared to impact HDAC3:SMRT mediated transcriptional repression, this prompted us to ask whether modulating the intracellular concentration of inositol phosphates within cells would also affect repression in an analogous fashion. This was attempted in two ways: (i) the addition of chemical inhibitors of IPMK; and (ii) short hairpin-RNA (shRNA) mediated knockdown of two enzymes critical for inositol phosphate metabolism, IPMK and IPPK. IPMK mediates the sequential phosphorylation of IP_3 to IP_4 and IP_5 whereas IPPK mediates the subsequent phosphorylation of IP_5 to IP_6, the precursor of inositol pyrophosphates (Verbsky *et al.*, 2005; Frederick *et al.*, 2005).

5.5.1 Chemical inhibition of IPMK through chlorogenic and aurintricarboxylic acid (CHA and ATA)

Based upon the sequential phosphorylation of IP_3 to IP_4 and IP_5 mediated by IPMK, it would be expected that treatment of cells with an IPMK inhibitor would reduce the intracellular levels of IP_4 thereby negatively impacting HDAC3:SMRT mediated repression. The effects of two IPMK inhibitors which have been shown to inhibit IPMK *in vitro* (Mayr *et al.*, 2005) were assessed. Firstly, HEK293T cells were cultured in the presence of varying concentrations of chlorogenic acid (CHA; 1, 10 and 100 µg/ml) for 24 hours post-transfection. Initial analysis indicated that, regardless of concentration used, treatment with CHA has no effect on luciferase expression and showed comparable luciferase activity to untreated Gal4-HDAC3 cells (FIGURE 5.10A). Additionally, at the highest concentration, CHA appeared to affect cell viability since cell numbers were significantly reduced and morphology was altered following treatment (data not shown). Cells were then cultured in the presence of CHA for an additional 24 hours to assess whether additional incubation time with inhibitor would allow for a greater inhibitory effect of IPMK and a possible greater effect on transcriptional repression. However, a 48-hour incubation with CHA showed similar results to treatment for 24 hours, indicating that the presence of the IPMK inhibitor CHA appears to have little effect on Gal4-HDAC3 mediated repression (FIGURE 5.10B).

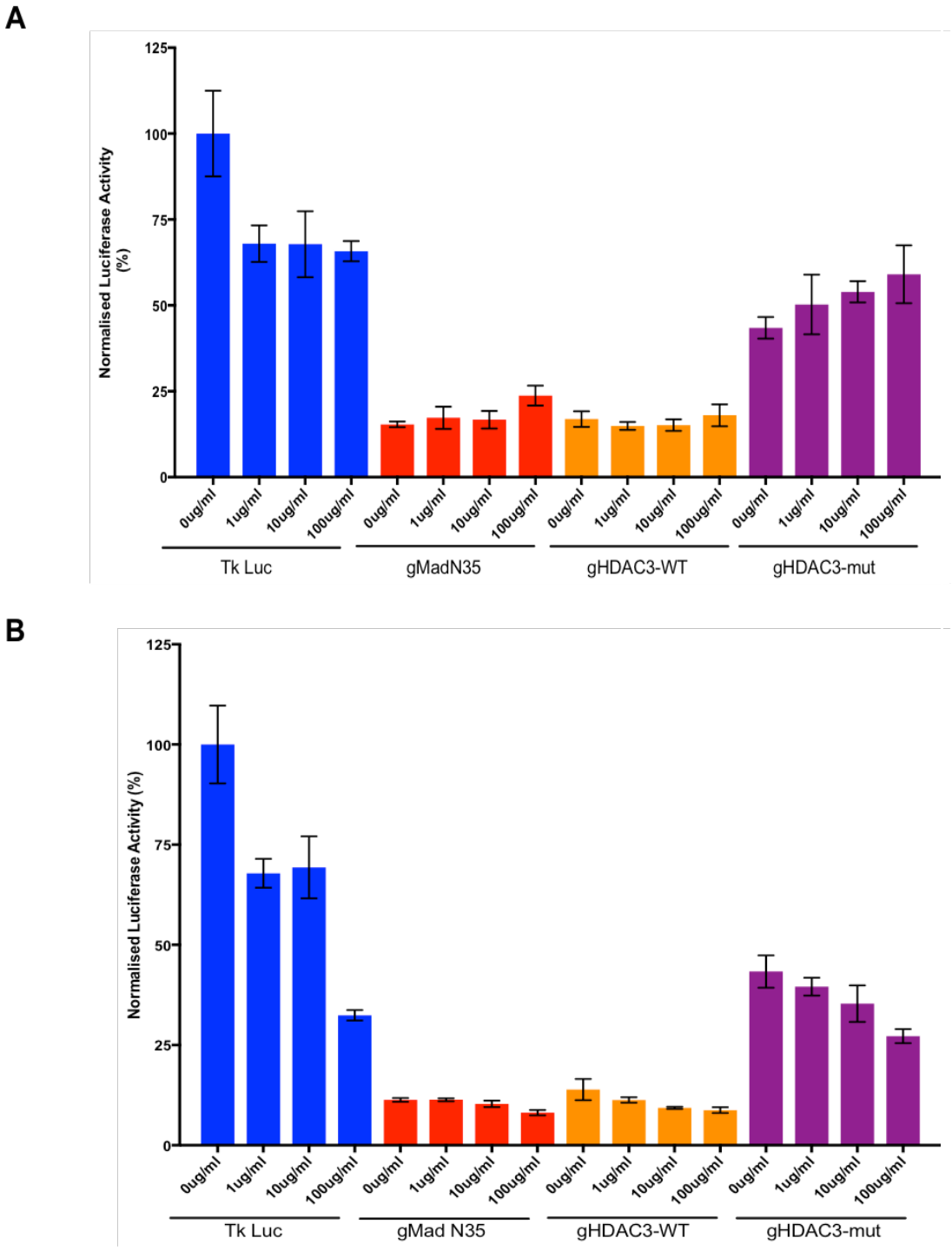

Figure 5.10 Inhibition of IPMK by chlorogenic acid (CHA) does not impact the repressive ability of the HDAC3:SMRT complex. Cell culture media was supplemented with CHA at the concentrations indicated for (A) 24 hours or (B) 48 hours following transfection with Gal4-HDAC3 constructs (wild-type (orange) and mutant (H17C G21A K25I R265P L266M R301A; purple). There was no relief in repression of the luciferase reporter construct. The mean luciferase activity (n=3) ±SEM is shown.

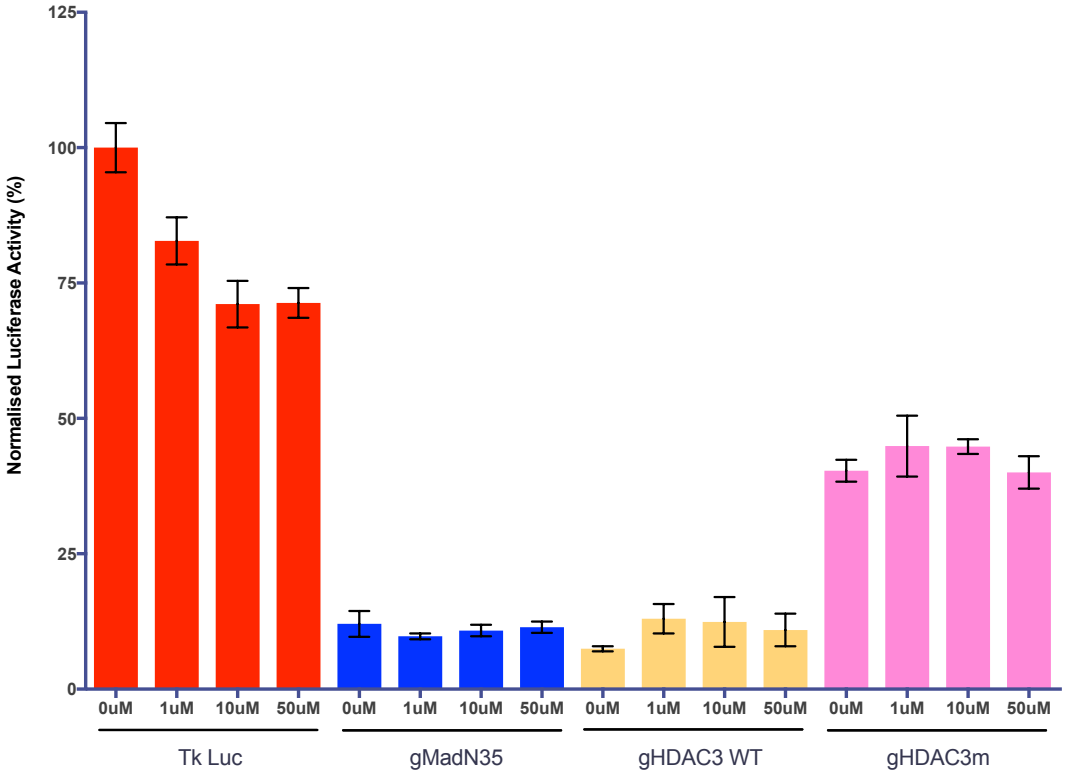

Figure 5.11 Inhibition of IPMK by aurintricarboxylic acid (ATA) shows negligible effect on luciferase reporter gene repression. Media was supplemented with ATA at the concentrations indicated for 24 hours following transfection of Gal4-HDAC3 wild-type and mutant (H17C G21A K25I R265P L266M R301A) constructs. There was a 2-fold relief in repression of Gal4-HDAC3 WT at 1μM ATA although at higher concentration, no further de-repression of luciferase was achieved. The mean luciferase activity (n=3) ±SEM is shown.

However, CHA has been shown to only inhibit IPMK *in vitro* to a maximum of 60% (Mayr *et al.*, 2005). Additionally, the bioavailability of the inhibitor in HEK293T cells is unknown. Accordingly, residual activity of IPMK may be sufficient enough to not significantly impact on the levels of IP_4 and as such, the effect on HDAC3:SMRT mediated repression would be unidentifiable. Aurintricarboxylic acid (ATA) has been shown to inhibit IPMK maximally (to 100%) *in vitro* thus cells were cultured in the presence of ATA at varying concentrations (1, 10 and 50 μM) for 24 hours post-transfection. Whilst there was no statistical significance in the increase in repression by Gal4-HDAC3-WT between untreated and treated (1 μM)

cells, there was nevertheless a 2-fold de-repression by Gal4-HDAC3-WT in the presence of 1 μM ATA, a concentration similar to that known to inhibit IPMK (FIGURE 5.11). Cells were then cultured at lower concentrations of ATA closer to the known inhibitory concentration of IPMK (0.5, 1 and 3 μM) for 48 hours prior to assaying for reporter expression. No observable increase in luciferase activity could be identified in Gal4-HDAC3-WT treated cells after 72 hours at any concentration of ATA (data not shown) suggesting, in this assay at least, chemical inhibition of IPMK and assessing the repressive ability of the HDAC3:SMRT complex in the absence of IP_4 remains inconclusive. Quantification of inositol phosphates following inhibitor treatment and further understanding on the bioavailability of the inhibitors *in vivo* will be necessary to facilitate understanding on their impact on HDAC3:SMRT mediated transcriptional repression.

5.5.2 IPMK shRNAs

As an alternative method to manipulate intracellular levels of IPs, transient transfection of short hairpin-RNA (shRNA) constructs was used to knockdown IPMK or IPPK. Through activation of the endogenous RNAi pathway, shRNA constructs deplete levels of IPMK and IPPK protein, either through mRNA cleavage or repression of protein translation in the case of constructs targeting the coding sequence, or the 3'UTR of mRNA respectively (Gu *et al.*, 2009). Consequently, it would be expected that knockdown of both IPMK and IPPK would affect the ratio of intracellular inositol phosphates by inhibiting the ability of IP_3 to be phosphorylated into higher order inositol phosphates in the case of IPMK knockdown or a build up of IP_4 and IP_5 in the case of IPPK knockdown (Verbsky *et al.*, 2005; Frederick *et al.*, 2005). This would directly impact the ability of Gal4-HDAC3 to bring about repression when tethered to the luciferase reporter gene by altering IP_4 availability for activation of the HDAC3.

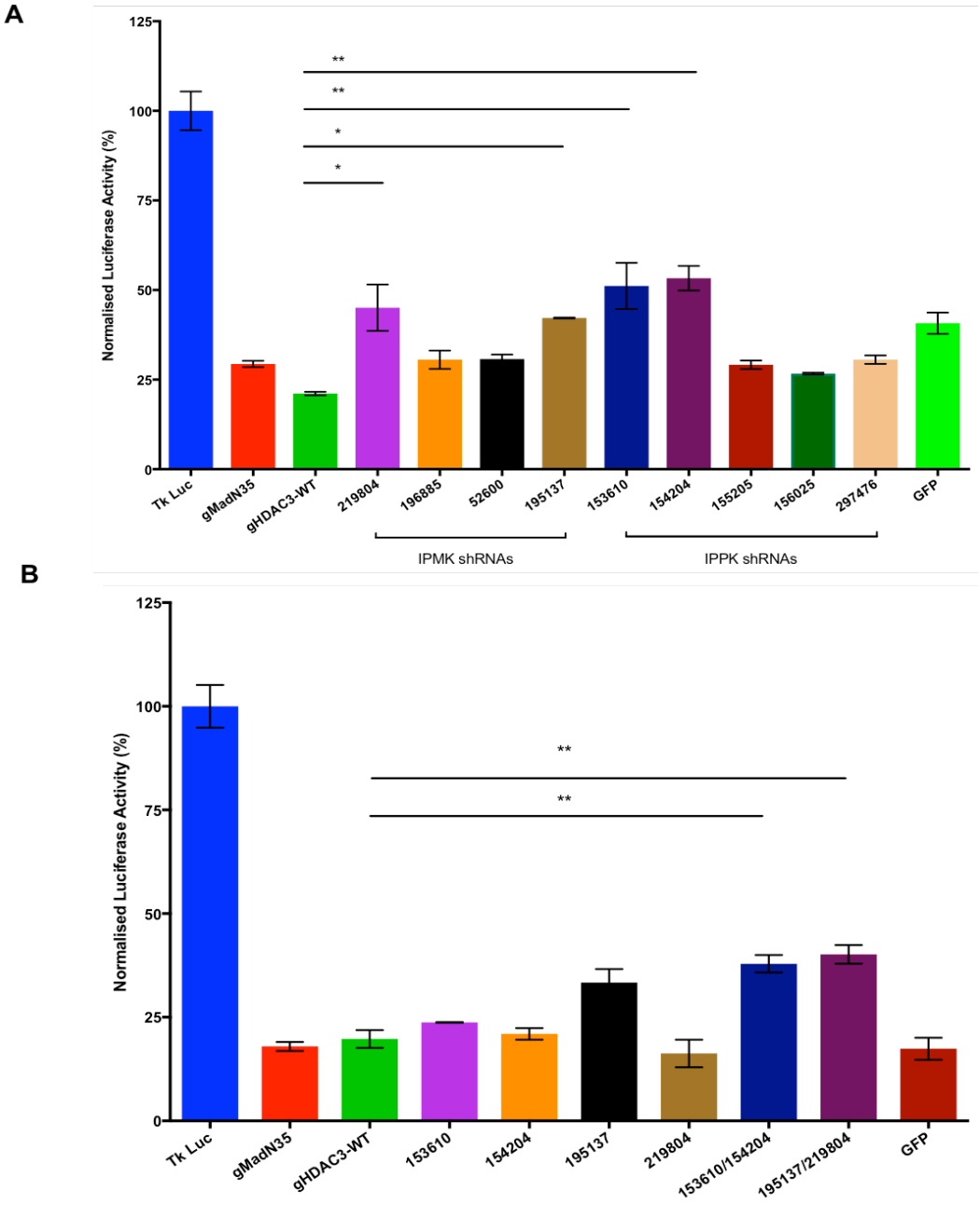

Figure 5.12 IPMK and IPPK knockdown relieves HDAC3:SMRT mediated repression. Upon co-transfection of shRNA constructs to knockdown IPMK and IPPK, repression mediated by Gal4-HDAC3 is relieved 2 fold by constructs transfected individually (A) or in parallel (B). IPMK shRNAs 153610 and 154204 and IPKK shRNAs 195137 and 219804 are denoted in (B) by 610, 204, 137 and 804 respectively. Significance (p value) was calculated using a two-tailed t test (* <0.01, **<0.01). Mean luciferase activity (n=3) ±SEM is shown.

A panel of four different shRNAs against IPMK and five against IPPK (detailed in Appendix Three; original reference numbers retained) targeting different parts of the protein transcripts were purchased from Sigma Aldrich. Protein knockdown was validated by the company although this could not be confirmed since commercially available antibodies were unable to recognize endogenous levels of the protein due to low expression in HEK293T cells. shRNA constructs were transiently transfected alongside the reporter assay plasmids and gHDAC3-WT for 48 hours prior to assaying for reporter gene expression. Two shRNA constructs for both IPMK and IPPK appeared to impair the repressive ability of the HDAC3:SMRT complex (FIGURE 5.12A). Compared to Gal4-HDAC3 alone, co-transfection with IPMK shRNAs 219804 and 195137 showed two-fold greater luciferase activity (lanes 4 and 7). This is to be expected since knockdown of IPMK would be predicted to cause a decrease in IP_4 levels and thus decrease HDAC3 activity through an inability to form a functional HDAC3:SMRT complex. However, constructs 153610 and 154204 targeted to knockdown IPPK also showed ~2.5-fold increase in luciferase activity i.e. a relief in repression (lanes 8 and 9). This is counterintuitive to what would be expected for IPPK knockdown since we would expect knockdown to cause an increase in IP_4 and IP_5 levels within cells therefore increasing HDAC3:SMRT mediated repression. This suggests that there may be flux within the inositol phosphate metabolic pathway upon protein knockdown such that there is an effect on the ratio of other inositol phosphates sufficiently to alter the repressive capability of HDAC3:SMRT.

It is possible that to achieve a higher level of protein knockdown, combinations of different shRNAs that target different regions of mRNA, for example the 3'UTR and the coding sequence or two different regions of the coding sequence simultaneously, can be co-transfected together. The two most effective shRNAs identified in the assay were co-transfected in parallel into 293T cells; when compared to wild type Gal4-HDAC3, co-transfection of the two shRNA constructs showed an increased reporter gene activity by ~2-fold which is comparable to shRNA constructs alone

(FIGURE 5.12B; lanes 8 and 9). This indicates that combination of shRNAs for an individual protein does not achieve greater knockdown efficiencies and individual shRNAs are sufficient to modulate protein levels in cells and thereby alter HDAC3:SMRT mediated repression in isolation.

5.6 Conclusion

In the present study, we demonstrate that mutation of key IP_4 binding residues in both the deacetylase activation domain (DAD) of SMRT and HDAC3 directly impacts the repressive ability of the co-repressor complex. Activation of HDAC3 is facilitated through the presence of IP_4 at the interface of the HDAC enzyme and its cognate co-repressor protein (Watson *et al.*, 2012). HDAC3:SMRT has been shown to bring about repression of the luciferase reporter gene (FIGURE 5.1) and acts as a direct comparison between protein constructs in which residues that mediate the interaction with IP_4 have been mutated (FIGURES 5.4 and 5.5). In all instances, mutating residues in both SMRT and HDAC3 negatively impacts on the ability of the HDAC3:SMRT complex to repress transcription. Presumably, this results from an impaired ability of IP_4 binding, a failure to fully activate HDAC3 and a de-repression (increase) in luciferase gene activity.

Manipulation of intracellular inositol phosphate levels either through chemical inhibition of enzymes involved in inositol phosphate metabolism (FIGURES 5.6 and 5.7) or through RNAi-mediated protein knockdown (FIGURE 5.8) remains somewhat inconclusive due to the inability to quantify whether inositol phosphate levels have been altered in cells following treatment. However, a relief in repression is identified upon RNAi-mediated knockdown of IPMK suggesting that IP levels have been sufficiently altered to affect HDAC3:SMRT mediated repression.

Whilst the data in this chapter does not conclusively show that HDAC3:SMRT mediated repression *in vivo* is inositol phosphate dependent, it does suggest that suggest that directly impacting the ability

of HDAC3:SMRT to bind and become activated by inositol phosphate has a detrimental effect on HDAC3:SMRT mediated repression. Further studies are required in which inositol phosphate levels can be quantified to definitively correlate altered inositol phosphate levels and HDAC3:SMRT mediated transcriptional repression.

Chapter Six: Discussion

6.1 HDAC3 loss affects co-repressor complex integrity.

To assess the embryonic requirement of HDAC3, we generated a mouse embryonic stem cell line in which HDAC3 can be conditionally deleted (Figure 3.1). Loss of HDAC3 resulted in a decrease in protein levels of both TBL1X and NCoR1 (Figure 3.6) suggesting that HDAC3 may contribute to the structural integrity of the HDAC3:SMRT/NCoR complex. Recent work identified a deacetylase-independent function of HDAC3 since mutations that abolish enzymatic activity still result in changes in target gene expression but have no effect on promoter acetylation levels (Sun *et al.*, 2013) . Subsequent mutations to the enzyme that abolish the interaction with its cognate co-repressor protein NCoR rendered the enzyme non-functional *in vivo* suggesting that HDAC3 acts as a scaffolding protein to preserve the integrity of the complex. Upon binding of HDAC3 to it's cognate co-repressor SMRT/NCoR, the deacetylase activation domain (DAD) of the co-repressor protein undergoes gross conformational changes such that it lies along the surface of the enzyme making extensive intermolecular interactions (Watson *et al.*, 2012). Loss of HDAC3 is likely to render this region solvent exposed and therefore lead to increased protein turnover.

Surprisingly, loss of HDAC3 resulted in only a minimal effect on global deacetylase activity (Figure 3.7) and only modest increase in the acetylation levels of histone H3 (Figure 3.8). In contrast to HDAC1/2 double knockout cells which showed a 50% reduction in total deacetylase activity, HDAC3 knockout cells showed only a 15% decrease in deacetylase activity. HDAC3 is found exclusively in the SMRT/NCoR complex whereas HDAC1 and HDAC2 are recruited into multiple transcriptional co-repressor complexes: Sin3A, NuRD, CoREST and MIDAC (Laherty *et al.*, 1997; Xue *et al.*, 1998; You *et al.*, 2001; Bantscheff *et al.*, 2011) . The significant decrease in total deacetylase activity in the absence of HDAC1 and HDAC2 can be accounted for through the total

absence of both deacetylases and loss in activity of all HDAC1/2 containing complexes whereas only a small proportion of total deacetylase activity appears to be accounted for by the loss of the HDAC3:SMRT/NCoR complex. Accordingly, HDAC1 and HDAC2 appear to the most dominant deacetylases in ES cells with HDAC3 only playing a minor role in regulating the ES acetylome.

There are minimal changes in H3 acetylation marks in the absence of HDAC3. ES cells maintain a plastic chromatin structure such that genes can be rapidly activated upon receiving appropriate inductive differentiation signals; as such, the high basal levels of acetylation of cells would account for the minimal changes in acetylation observed when HDAC3 is lost. However, consistent with other studies in which HDAC3 levels have been depleted, loss of HDAC3 was associated with an increase in deposition of both H3K18 and H3K27 acetylation marks (Zhang *et al.*, 2004; Urvalek & Gudas, 2014) . Both marks are associated with enhancer sequences with H3K27 marking active enhancers as compared with poised enhancers in ES cells in the absence of H3K4 trimethylation (Creyghton *et al.*, 2010) . Recruitment of HDACs to actively transcribed genes is believed to cause the “resetting” of chromatin following the actions of HATs and RNA polymerase II during transcription (Dovey *et al.*, 2010) .

Although there are minimal changes to total deacetylase activity, when coupled to an increase in histone acetylation marks associated with enhancers, this suggests that HDAC3 may be functioning at the level of individual genes. Microarray analysis (discussed later) suggests that there are many changes in gene expression in the absence of HDAC3 thus HDAC3 is clearly able to exert its function despite only a small change in total deacetylase activity, suggesting a role for HDAC3 in gene-specific regulation.

Recently, active enhancers have been demonstrated to be sites of active transcription, generating unstable transcripts known as enhancer RNA.

eRNA-producing enhancers have been shown to be highly enriched for the active H3K27ac histone mark and expression of eRNA transcripts correlates with the transcriptional of neighbouring genes (De Santa *et al.*, 2010; Danko *et al.*, 2015).

It would be informative to perform H3K27ac chromatin immunoprecipitation (ChIP)-seq experiments in HDAC3 control and knockout EBs to deduce whether there was an increase in H3K27ac deposition, particularly at the endodermal genes that have been shown to be upregulated in knockouts such as *Foxa2, Gata4* and *Gata6*. This would answer whether HDAC3 is acting in a gene-specific fashion to regulate expression of both the gene and associated eRNA transcripts. In the former case, an increase in H3K27ac at gene promoters in the absence of HDAC3 would potentiate gene expression from these sites whilst in the latter scenario, the negative regulation of eRNA production would be relieved in the absence of HDAC3, leading to increased eRNA production and an associated increase in endodermal gene expression.

6.2 Loss of HDAC3 inhibits cell proliferation.

HDACs have been implicated in cell cycle progression through the regulation of key cell cycle modulators. HDAC3 in particular has been shown to regulate the expression of the CDK inhibitor p21 (Wilson *et al.*, 2006) as well as a role in the repression of E2F-dependent gene transcription (Panteleeva *et al.*, 2004) . ES cells showed both a reduced proliferative capacity in the absence of HDAC3 and a delay in population doubling time (Figure 3.9) confirming a role of HDAC3 in cell cycle progression. Consistent with HDAC3 knockout studies in alternative cell systems (Bhaskara *et al.*, 2008; Summers *et al.*, 2013) , HDAC3 loss was associated with reduced numbers of EdU-positive cells and a delay in cells reaching S-phase indicating a cycling defect in null cells (Figure 3.10). Analysis in other studies confirms this as a result of increased DNA double strand breaks and inefficient DNA repair in the absence of HDAC3. Consequently, the accumulation of DNA damage results in the triggering

of the S-phase checkpoint and subsequent S-phase arrest (Bhaskara *et al.*, 2008) . It is likely that a similar phenotype occurs in *Hdac3*$^{-/-}$ ES cells which would also account for the reduced clonogenicity shown by knockout cells (Figure 3.11A).

6.3 Initial differentiation of HDAC3 knockout EBs is unaffected.

Following the implantation of an embryo, gastrulation is a key event in early embryonic development, occurring around embryonic day e6.5 (Tam & Behringer, 1997) . Pluripotent epiblast cells are allocated to the three primary germ layers, mesoderm, definitive endoderm and ectoderm which are the progenitors of all tissue lineages; patterning occurs along the anterior-posterior axis and lineage specification is induced in response to signalling molecules (Loebel *et al.*, 2003) .

EB differentiation of ES cells in an *in vitro* model of differentiation that mimic the early post-implantation embryo; in the absence of LIF, cells form aggregates (Figure 4.1) comprised of an outer surface layer of primitive endoderm and other lineages being derived from the core of the aggregate (Keller, 1995; Leahy *et al.*, 1999) . HDAC3 knockout cells were able to form EB aggregates within 2 days and phenocopied control cells at this stage, suggesting that exit from pluripotency and initial differentiation had occurred. Accordingly, pluripotent markers *Oct4, Nanog, Sox2* and *Klf4* are repressed throughout the duration of the EB time course (Figure 4.4), confirming cells had successfully exited the pluripotent stem cell factor. These pluripotent factors are repressed in the absence of a repressive factor (HDAC3) suggesting that they are the targets of other transcriptional repressors, not HDAC3.

Similarly, expression of *brachyury*, one of the earliest genes expressed during mesendoderm formation, and *fgf5,* a prominent marker of primitive ectoderm formation, were consistent with controls (Figure 4.5). *Brachyury* is expressed in the epiblast and primitive streak (from which mesendoderm is derived) from embryonic day e6.5 at the onset of

gastrulation before expression is restricted from e7.5 (Wilkinson *et al.*, 1990) . Similarly, *fgf5* is initially widely expressed throughout the ectoderm from embryonic day e5.25 before being repressed by e8.0 (Hebert *et al.*, 1991) . In HDAC3 knockout EBs, expression of both genes is detected by day 3 of EB differentiation where *fgf5* expression peaks (occurring later for *brachyury* at day 5 of EB differentiation), prior to repression of both factors by day 7 of differentiation (Figure 4.5). This expression data of marker genes correlates with the temporal expression of factors during embryogenesis suggesting that initial differentiation of HDAC3 knockout EBs is unaffected.

6.4 Deletion of HDAC3 predisposes hepatic differentiation in ES cells.

Immunohistochemistry data demonstrates that HDAC3 is widely distributed in pre-implantation embryos, predominantly enriched on heterochromatin surrounding the nucleolus (Ma & Schultz, 2008) suggesting that the protein plays a key role in the regulation of gene expression during early embryogenesis. HDAC3 null embryos are embryonic lethal by embryonic day e.9.5 (Montgomery *et al.*, 2008; Bhaskara *et al.*, 2008) suggesting that initial gastrulation steps will have occurred. Since *brachyury* and *fgf5* expression is normal in knockout EBs, this implies that it is later downstream lineage specification during gastrulation that impacts viability. Beyond 4 days of culture, HDAC3 knockout EBs are morphologically abnormal showing a significant reduction in size and are irregularly shaped (Figure 4.1) suggesting aberrant differentiation or increased cell death.

Microarray analysis suggested that EBs lacking HDAC3 were predisposed to differentiate towards endodermal lineages, particularly the hepatic lineage. Hepatic specification is initiated from FGF signalling from the cardiac mesoderm to induce hepatic cell fate in the foregut endoderm and is characterised through the expression of key transcription factors including *Gata4, Foxa2, HNF1β* and *HNF4α,* which potentiate the

differentiation of bipotent progenitor cells. The expression levels of mesendodermal markers (*Foxa2, Gata4, Gata6)* as well as hepatic specific markers (*HNF1β* and *HNF4α*) were increased in knockout EBs suggesting that HDAC3 may play a role in liver development (Figure 6.6).

HDAC3 has been implicated to play a wide variety of roles within the liver including lipogenesis and metabolic processes (Sun *et al.*, 2012; Knutson *et al.*, 2008; Sun *et al.*, 2013) although a role of HDAC3 mediating liver development has yet to be elucidated. *NCoR*$^{-/-}$ knockout mice exhibit embryonic lethality with one of the observed phenotypes included a reduction in liver size suggesting that the HDAC3:SMRT/NCoR complex may play a role during liver development (Jepsen *et al.*, 2000) Interestingly, culture of stem cells in media containing HDAC inhibitors valproic acid (VPA) or sodium butyrate (NaBut) has been shown to induce differentiation to hepatic progenitor cells and hepatocytes (Zhou *et al.*, 2007; Dong *et al.*, 2009; Hay *et al.*, 2008) suggesting that epigenetic regulation mediated by histone acetylation is important for early hepatic development although how HDACs, and specifically HDAC3, play a role in this is unknown.

Foxa2, Gata4, Gata6, HNF1β, HNF4α and *HNF6* all function as a complex transcriptional network to control expression of each other in a hierarchical fashion as well as activate downstream liver-specific genes (Kyrmizi *et al.*, 2006) . Key to this network are *HNF1β, HNF4α* and *HNF6;* Odom *et al.* demonstrated that the nuclear receptor *HNF4α* is the most significant of the hepatic factors assessed in the network with approximately 50% of active genes tested in the liver being bound by *HNF4α* and RNA polymerase II suggesting this transcription factor is key to controlling liver gene expression (Li *et al.*, 2000; Odom *et al.*, 2004) . Similarly, loss-of-function studies show that there is a failure to express many liver-specific genes in the absence of *HNF4α* highlighting its essential role in hepatic differentiation (Li *et al.*, 2000)

HDAC3 and HNF4α have been shown to directly interact with each other (Torres-Padilla *et al.*, 2002) thus it is possible that aberrant liver differentiation in HDAC3 knockout EBs may be due to direct repression of HNF4α by HDAC3; accordingly, this would cause hypoacetylation at the promoters of HNF4α-target genes and blocked hepatic gene expression. Confirmation of the interaction of HDAC3 with HNF4α isoforms found during embryonic development through chromatin immunoprecipitation (ChIP) experiments would be required to confirm this hypothesis.

However, this is only likely to be a partial explanation for the increased hepatic differentiation in HDAC3 knockout EBs. *Gata4, Gata6* and *Foxa2* expression occurs earlier than *HNF4α (*from embryonic day e4.75) in the definitive endoderm and precedes hepatic specification by hepatic nuclear factor members (Nemer & Nemer, 2003; Cai *et al.*, 2008; Rojas *et al.*, 2010) ; all show aberrant expression in HDAC3 knockout EBs. Interestingly, FoxA and Gata4 occupy hepatic albumin (*Alb1)* enhancer elements in foregut endoderm prior to albumin transcription and are believed to open chromatin and potentiate hepatic gene expression(Jang *et al.*, 2015; Ozawa *et al.*, 2001) It would be interesting to speculate whether HDAC3 interacts with Foxa2 or Gata4 in mouse embryonic stem cells and regulate endodermal fate: interaction of HDAC3 with these factors would induce histone hypoacetylation at the promoters of Foxa2/Gata4-target genes thereby blocking endodermal gene expression and lineage specification.

6.5 IP_4 regulates HDAC3:SMRT mediated repression

Recent work has shown that the deacetylase activity of HDAC1 and HDAC3 is modulated through the binding of Ins-(1,4,5,6)-P_4 (inositol phosphate; IP_4) in a highly basic pocket at the interface between the HDAC enzyme and its cognate co-repressor protein (Watson *et al.*, 2012; Millard *et al.*, 2013) . Exogenous application of IP to the Class I HDAC-containing complexes SMRT, NuRD and MiDAC results in robust complex activation suggesting that IP may act as a regulator of HDAC activity *in*

vivo (Itoh *et al.*, 2015; Watson *et al.*, 2016) . To understand the significance of IP binding and to identify whether IP affects the ability of HDAC3 to bring about repression *in vivo,* mutations were made to key IP interacting residues in both SMRT and HDAC3 and their effects on HDAC3:SMRT-mediated transcriptional repression of a reporter gene were assessed. Both HDAC3 (Figure 5.4) and SMRT mutants (Figure 5.5) were unable to bring about repression of the reporter gene construct compared to wildtype proteins indicating that disrupting the interaction between the IP molecule and the co-repressor complex is sufficient to perturb HDAC3:SMRT-mediated transcriptional repression and that HDAC3:SMRT activity is dependent on the presence of an IP molecule.

Mutation of key IP_4 collating residues (Y478A in NCoR and Y470A in SMRT) have been shown to abolish deacetylase activity in mice and interestingly, knock-in mice bearing these mutation are able to survive into adulthood despite any detectable HDAC activity in the embryo (Sun *et al.*, 2013). Similarly, deacetylase-dead HDAC3 mutants can rescue hepatosteatosis and repress lipogenic genes expression in HDAC3-depleted mouse liver (You *et al.*, 2013). Whilst the activity of HDAC3 does appear to be IP dependent, this suggests that the role of HDAC3 extends beyond its deacetylase function thus it would be interesting to generate a stable ES cell line in which an catalytically inactive mutant is expressed to investigate the role of deacetylation by HDAC3.

Manipulation of inositol phosphate levels in cells would also be expected to affect HDAC3:SMRT transcriptional repression in an analogous fashion. IP metabolism is co-ordinated through the actions of two enzymes: IPMK which catalyses the sequential phosphorylation of IP_3 to IP_4 and IP_5 whereas IPPK catalyses the subsequent phosphorylation to generate IP_6. Both enzymes play an essential role during embryogenesis since null embryos are embryonic lethal (embryonic day e9.5 and between e8.5 and e9.5 for IPMK and IPPK respectively (Verbsky *et al.*, 2005; Frederick *et al.*, 2005) around the same time as lethality occurs in HDAC3 knockout animals. Both enzymes were depleted using shRNA and caused a relief in

repression of the reporter gene construct (Figure 5.8). This is expected in the case of IPMK knockdown since this would cause a decrease in IP_4 levels in cells. As such, the inability of HDAC3:SMRT to bring about reporter gene repression is presumably due to the reduced levels of IP being able to be incorporated into the HDAC3:SMRT complex resulting in a non-functional enzyme complex. Conversely, knockdown of IPPK, which catalyses the phosphorylation IP_5 to $InsP_6$ also resulted in a relief in repression of the reporter gene construct. This is somewhat counterintuitive to what would be expected since knockdown of the enzyme would be expected to cause an increase in in IP_4 and IP_5 levels within cells, both of which have been shown to activate HDAC3 *in vitro* (Watson *et al.*, 2016) . Intracellular IP levels are dynamic thus it is possible that causing a bottleneck in the pathway by preventing IP_5 from being phosphorylated to generate IP_6 affects the ratio of other inositol phosphates sufficiently to alter the repressive capability of HDAC3:SMRT. Similarly, it is possible that the IP levels in cells may be limiting for full HDAC3 activation thus a relief in repression may be shown as the HDAC3:SMRT complex may not be fully activated in the presence of altered IP levels.

Further manipulation of intracellular inositol phosphate levels through treatment with the IPMK inhibitors chlorogenic acid (Figure 5.10) and aurintricarboxylic acid (Figure 5.11) were inconclusive; initial incubation for 24 hours as well as extended incubation for up to 72 hours showed comparable luciferase expression to untreated controls. However, at this institution, we currently lack the ability to quantify IP levels in cells so it is possible that IP levels have not been sufficiently modulated to affect HDAC3:SMRT mediated repression. Measurement of IP levels by high-performance liquid chromatography (HPLC) in the presence of both protein knockdown and chemical inhibition of IP enzymes would allow us to definitively correlate altered IP levels and HDAC3:SMRT mediated repression.

Both mutational analysis of IP binding and shRNA experiments indicate that impaired ability of IP binding or altered levels of IP in cells directly impacts HDAC3:SMRT mediated repression. Presumably this is due to the inability to form a functional co-repressor complex and a failure to induce enzyme activation suggesting that HDAC activity is regulated by IP. As such, it is conceivable that there is an IP:HDAC3 feedback mechanism to regulate the activity of HDAC3. ChIP data from human embryonic stem cells (Wang *et al.*, 2009) shows that HDAC3 is not found bound in the vicinity of either IPMK or IPPK but instead is found at the promoter of PTEN, a phosphoinositide 3-phosphatase, which has been shown to dephosphorylate IP_5 to IP_4 (Caffrey *et al.*, 2001). An increase in HDAC3 activity through the formation of the HDAC3:IP:SMRT co-repressor complex could lead to reduced levels of IP_4 through transcriptional repression of PTEN. Consequently, there would be a reduction in HDAC3 activity due to an inability to form a functional activated HDAC3 complex in the face of reduced IP_4 levels thereby leading to de-repression of PTEN and subsequent increase in IP_4 levels. HPLC experiments in wildtype, heterozygous ($^{+/-}$) and knockout HDAC3 cells would allow us to further understand the regulation of HDAC3:SMRT since this would allow us to assess whether the balance of IPs in cells is altered upon HDAC3 loss and identify if any one isoform is more prevalent than another.

The conservation of IP binding residues in other Class I HDAC enzymes and co-repressors (e.g. HDAC1/MTA1) suggests that IP regulation might be a generalized mechanism of HDAC activity. HDAC1 mutants in which the positively charged inositol phosphate collating residues have been replaced with glutamine reduced the deacetylase activity of HDAC1 and were unable to rescue the viability of HDAC1/2 double knockout cells (Jamaladdin *et al.*, 2014) suggesting that IP binding is essential for HDAC1 activity *in vivo.* To confirm this is the case with HDAC3, rescue experiments using wildtype and HDAC3 IP mutants in HDAC3 knockout cells would allow us to assess their ability to rescue the phenotype of HDAC3 loss; if HDAC3 is regulated by IP *in vivo,* IP mutants would mimic knockout cells in relation to the cell cycle defects exhibited and would

exhibit the same morphological defects during EB differentiation as well as show aberrant expression of endodermal markers (*Gata4, Gata6, HNF4α, HNF1β, Foxa2* etc*)* identified in Chapter Four.

6.6 Summary

In this thesis, we have shown that HDAC3 is required for the integrity of the HDAC3:SMRT co-repressor complex. Loss of HDAC3 does not cause a significant reduction in total deacetylase activity and only minor increases in the acetylation levels of histones are shown. However, these increases are associated with gene enhancers suggesting HDAC3 may function in a gene-specific manner. Knockout ES cells are able to differentiate although are morphologically abnormal and significantly reduced in size, with microarray analysis indicating that endodermal markers are over-expressed whereas mesodermal markers are under-expressed suggesting HDAC3 plays an important role in regulating gene expression during development. We also demonstrate that impairing inositol phosphate (IP_4) binding through mutation of the IP binding site in both HDAC3 and SMRT significantly impairs the ability of the HDAC3:SMRT complex indicating that IP is a regulator of HDACs *in vivo.*

Appendices

Appendix One: PCR primers and restriction enzymes

Table A1.1 Cloning and recombineering primer sequences.

Primer	Primer sequence
T3_primer	GAATTAACCCTCACTAAAGGG
pgk_seq1	GGAAGTAGCACGTCTCACTAG

Table A1.2 Southern blot primer sequences

Primer	Primer sequence
HD3-Int-5	GCCGTGGTATTGGGAATGTC
HD3-Int-3	CCCTCACCATCGTATCCCTC
HD3-5probe-5	GGGAAGCCTTCTGAGACTGT
HD3-5probe-3	GGATGTTGAGACCTGGGGAA
HD3-3probe-5	CTCGGACTTGCTATGTAGAC
HD3-3probe-3	TGTTACAAGCAGCTGGACCG

Table A1.2 UPL Dual hydrolysis Probe Library: Q-RT PCR primer sequences, probe ID and amplicon sizes. Probes supplied by Roche Diagnostics. Universal Probe Library reference gene, GAPDH control probe and primers were used as a reference gene in all multiplex reactions (product of Roche Applied Science, cat number: 05046211001).

Primer	Direction	Universal Probe Library Sequence	UPL probe	Amplicon size
HDAC1	F	tggtctctaccgaaaaatggag	73	78
	R	tcatcactgtggtacttggtca		
HDAC2	F	ctccacgggtggttcagt	45	71
	R	cccaattgacagccatatca		
NCoR1	F	tttcagcgagttggtcagag	83	71
	R	tcagaaatctcatgctcactcc		
NCoR2	F	tgctcctgagtctttgaggaa	79	80
	R	gggggtggtgttggtactc		
HDAC3	F	caccaagagccttgatgcctt	-	230
	R	gcagctccaggataccaattact		

Table A1.4 Restriction enzymes.

Enzyme	Company	Buffer
***Psha* I**	NEB	CutSmart
***Hind* III**	NEB	NEB 2.1
***Dpn* I**	NEB	CutSmart

Appendix Two: Plasmids

Figure A2.1 HDAC3-cKO-Neo targeting vector

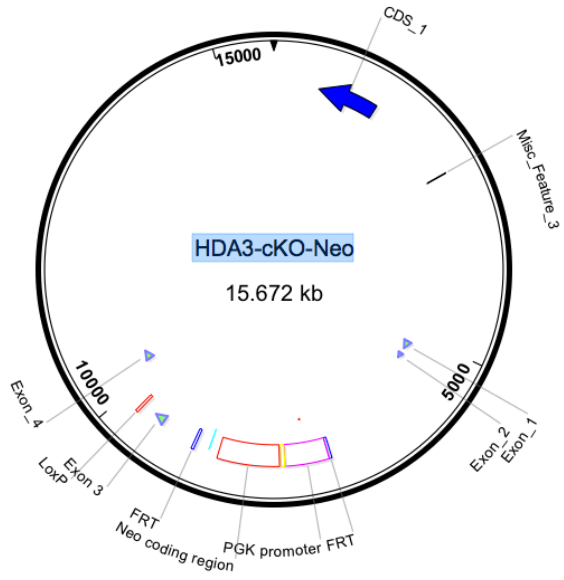

Figure A2.2 HDAC3-cKO-Hyg targeting vector

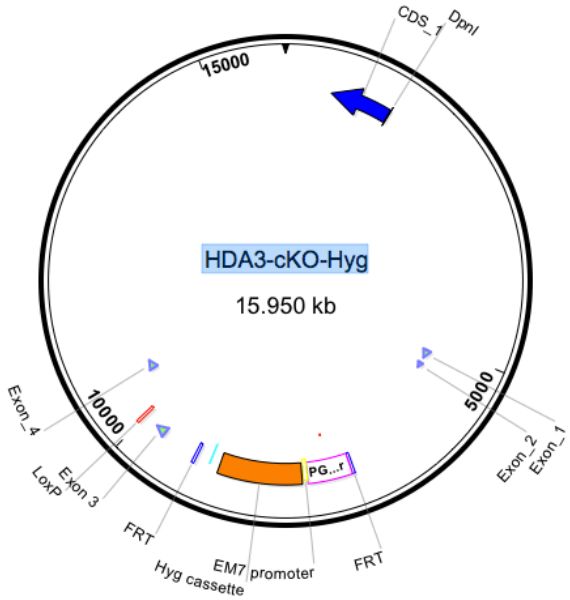

Figure A2.3 HDAC3-cKO-Hyg, Hyg_SC5_seq2 predicted and sequence trace consensus

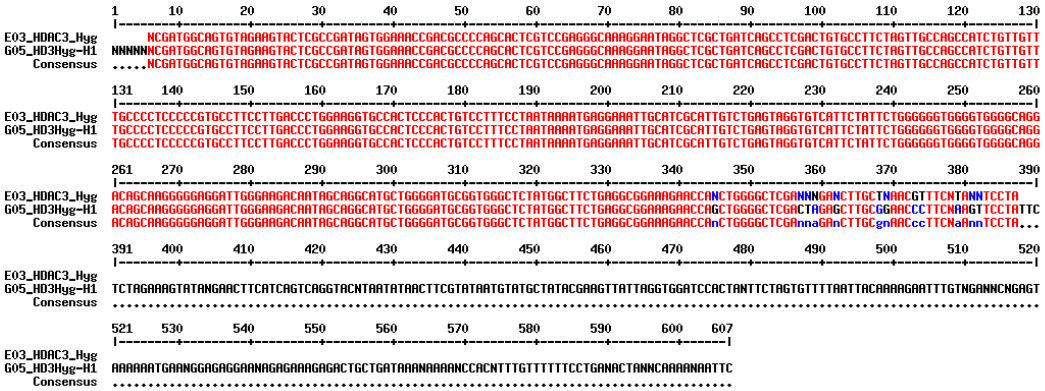

Table A2.1 Luciferase reporter assay plasmids

Expression of plasmids constructs confirmed in Watson *et al., 2013.*

Plasmid	Protein	Domain	Mutation	Tag
Tk Luciferase	Luciferase	Full length	-	Gal4 UAS
Beta-gal	Beta-galactosidase	Full length	-	None
MadN35	Mad	1-33	-	Gal4-DBD
gXtDAD (PJW1216)	SMRT	Xt-DAD 350-480	-	Gal4-DBD
gXtDAD (PJW1278)	SMRT	350-480	K474A K475A	Gal4-DBD
gXtDAD (PJW1279)	SMRT	350-480	Y470A Y471A	Gal4-DBD
HDAC3 (PJW371)	HDAC3	Full length	-	-
HDAC3 IP4-HD8 (PJW801)	HDAC3	Full length	H17C G21A K25I R265P R301A	-

HDAC3 Loop 6 (PJW790)	HDAC3	Full length	R265P L266M	-
HDAC3 R265P (PJW788)	HDAC3	Full length	R265P	-
HDAC3 Y298F(PJW1119)	HDAC3	Full length	Y298F	-
gHDAC3-mut (PJW801)	HDAC3	Full length	H17C G21A K25I R265P L266M R301A	Gal4-DBD

Appendix Three: Antibodies

Table 3.1 Western blotting antibodies

Antibody	Clonality	Source	Dilution	Company	Catalogue Number
HDAC1	Monoclonal	Rabbit	1:2000	Abcam	ab109411
HDAC2	Monoclonal	Mouse	1:2000	Millipore	05-814
HDAC3	Monoclonal	Rabbit	1:2000	Abcam	ab32369
TBL1R	Monoclonal	Mouse	1:1000	Santa Cruz	sc100908
NCOR1	Polyclonal	Rabbit	1:1000	Abcam	ab24552
A-TUBULIN	Monoclonal	Mouse	1:10,000	Sigma	T5168
OCT4	Monoclonal	Mouse	1:2000	Santa Cruz	sc5729
NANOG	Polyclonal	Rabbit	1:2500	Bethyl Laboratories	A300-397A

Table 3.2 Histone modification antibodies

Antibody	Clonality	Source	Dilution	Company	Catalogue Number
H3	Monoclonal	Mouse	1:2000	Upstate	05-499
H3K27ac	Polyclonal	Rabbit	1:1000	Active Motif	39135
H3K9ac	Polyclonal	Rabbit	1:1000	Active Motif	39917
H3K18ac	Polyclonal	Rabbit	1:1000	Active Motif	39755
H3K14ac	Polyclonal	Rabbit	1:1000	Active Motif	39599
H3K56ac	Polyclonal	Rabbit	1:1000	Active Motif	39281

Table 3.3 Secondary antibodies

Antibody	Dilution	Company	Catalogue Number
Alexa Fluor goat α mouse IRDye 800CW	1:10,000	LiCOR	926-32210
Alexa Fluor donkey α rabbit IRDye 680LT	1:10,000	LiCOR	926-68023

Appendix Four: shRNA constructs

	Product Number	Region	Target sequence	Hairpin sequence
IPMK	TRCN0000219804	CDS	GGTCAGCAAGTACCCATTAAT	CCGGGGTCAGCAAGTACCCATTAATCTCGAGATTAATGGGTACTTGCTGACCTTTTTG
IPMK	TRCN0000196885	3' UTR	GCACCTTTAATGCTATGTAAA	CCGGGCACCTTTAATGCTATGTAAACTCGAGTTTACATAGCATTAAAGGTGCTTTTTG
IPMK	TRCN0000052600	CDS	GCAAGTTCATTACTCTTTGTT	CCGGGCAAGTTCATTACTCTTTGTTCTCGAGAACAAAGAGTAATGAACTTGCTTTTTG
IPMK	TRCN0000195137	CDS	CAGAAGTACTAGAGTACAATA	CCGGCAGAAGTACTAGAGTACAATACTCGAGTATTGTACTCTAGTACTTCTGTTTTTTG
IPPK	TRCN0000153610	CDS	CGGCAAGATCGTCAACTATTA	CCGGCGGCAAGATCGTCAACTATTACTCGAGTAATAGTTGACGATCTTGCCGTTTTTTG
IPPK	TRCN0000154204	CDS	CCTTGATCTCTACTCAGGAAA	CCGGCCTAATTTAACCAGACTCCAACTCGAGTTGGAGTCTGGTTAAATTAGGTTTTTTG
IPPK	TRCN0000155205	CDS	GCCGATTCTGTGTGTAGAGAT	CCGGGCCGATTCTGTGTGTAGAGATCTCGAGATCTCTACACACAGAATCGGCTTTTTTG
IPPK	TRCN0000156052	CDS	CTTGACCTTTCCACTGAGGAT	CCGGCTTGACCTTTCCACTGAGGATCTCGAGATCCTCAGTGGAAAGGTCAAGTTTTTTG
IPPK	TRCN0000297476	CDS	GCCGATTCTGTGTGTAGAGAT	CCGGGCCGATTCTGTGTGTAGAGATCTCGAGATCTCTACACACAGAATCGGCTTTTTG

Bibliography

Allfrey, V.G., Faulkner, R., Mirsky, A.E., 1964. Acetylation and Methylation of Histones and their Possible Role in the Regulation of RNA Synthesis. *Proceedings of the National Academy of Sciences of the United States of America.* **51,** 786-794.

Andres, M.E., Burger, C., Peral-Rubio, M.J., Battaglioli, E., Anderson, M.E., Grimes, J., Dallman, J., Ballas, N., Mandel, G., 1999. CoREST: a functional corepressor required for regulation of neural-specific gene expression. *Proceedings of the National Academy of Sciences of the United States of America.* **96,** 9873-9878.

Ang, S.L., Wierda, A., Wong, D., Stevens, K.A., Cascio, S., Rossant, J., Zaret, K.S., 1993. The formation and maintenance of the definitive endoderm lineage in the mouse: involvement of HNF3/forkhead proteins. *Development (Cambridge, England).* **119,** 1301-1315.

Arrar, M., de Oliveira, C.A., McCammon, J.A., 2013. Inactivating mutation in histone deacetylase 3 stabilizes its active conformation. *Protein Science : A Publication of the Protein Society.* **22,** 1306-1312.

Avilion, A.A., Nicolis, S.K., Pevny, L.H., Perez, L., Vivian, N., Lovell-Badge, R., 2003. Multipotent cell lineages in early mouse development depend on SOX2 function. *Genes & Development.* **17,** 126-140.

Ayer, D.E., Lawrence, Q.A., Eisenman, R.N., 1995. Mad-Max transcriptional repression is mediated by ternary complex formation with mammalian homologs of yeast repressor Sin3. *Cell.* **80,** 767-776.

Bantscheff, M., Hopf, C., Savitski, M.M., Dittmann, A., Grandi, P., Michon, A.M., Schlegl, J., Abraham, Y., Becher, I., Bergamini, G., Boesche, M., Delling, M., Dumpelfeld, B., Eberhard, D., Huthmacher, C., Mathieson, T., Poeckel, D., Reader, V., Strunk, K., Sweetman, G., Kruse, U., Neubauer, G., Ramsden, N.G., Drewes, G., 2011. Chemoproteomics profiling of

HDAC inhibitors reveals selective targeting of HDAC complexes. *Nature Biotechnology.* **29,** 255-265.

Bernstein, B.E., Tong, J.K., Schreiber, S.L., 2000. Genomewide studies of histone deacetylase function in yeast. *Proceedings of the National Academy of Sciences of the United States of America.* **97,** 13708-13713.

Bhaskara, S., Chyla, B.J., Amann, J.M., Knutson, S.K., Cortez, D., Sun, Z.W., Hiebert, S.W., 2008. Deletion of histone deacetylase 3 reveals critical roles in S phase progression and DNA damage control. *Molecular Cell.* **30,** 61-72.

Bhaskara, S., Knutson, S.K., Jiang, G., Chandrasekharan, M.B., Wilson, A.J., Zheng, S., Yenamandra, A., Locke, K., Yuan, J.L., Bonine-Summers, A.R., Wells, C.E., Kaiser, J.F., Washington, M.K., Zhao, Z., Wagner, F.F., Sun, Z.W., Xia, F., Holson, E.B., Khabele, D., Hiebert, S.W., 2010. Hdac3 is essential for the maintenance of chromatin structure and genome stability. *Cancer Cell.* **18,** 436-447.

Bowen, N.J., Fujita, N., Kajita, M., Wade, P.A., 2004. Mi-2/NuRD: multiple complexes for many purposes.. *Biochim.Biophys.Acta.* **1677,** 52-57.

Boyer, L.A., Lee, T.I., Cole, M.F., Johnstone, S.E., Levine, S.S., Zucker, J.P., Guenther, M.G., Kumar, R.M., Murray, H.L., Jenner, R.G., Gifford, D.K., Melton, D.A., Jaenisch, R., Young, R.A., 2005. Core transcriptional regulatory circuitry in human embryonic stem cells. *Cell.* **122,** 947-956.

Brunmeir, R., Lagger, S., Seiser, C., 2009. Histone deacetylase 1 and 2-controlled embryonic development
. *The International Journal of Developmental Biology.* **53,** 275-276-289.

Buchholz, F., Angrand, P.O., Stewart, A.F., 1998. Improved properties of FLP recombinase evolved by cycling mutagenesis. *Nature Biotechnology.* **16,** 657-662.

Caffrey, J.J., Darden, T., Wenk, M.R., Shears, S.B., 2001. Expanding coincident signaling by PTEN through its inositol 1,3,4,5,6-pentakisphosphate 3-phosphatase activity. *FEBS Letters.* **499,** 6-10.

Cai, K.Q., Capo-Chichi, C.D., Rula, M.E., Yang, D.H., Xu, X.X., 2008. Dynamic GATA6 expression in primitive endoderm formation and maturation in early mouse embryogenesis. *Developmental Dynamics : An Official Publication of the American Association of Anatomists.* **237,** 2820-2829.

Calo, E. & Wysocka, J., 2013. Modification of enhancer chromatin: what, how, and why? *Molecular Cell.* **49,** 825-837.

Chambers, I., Colby, D., Robertson, M., Nichols, J., Lee, S., Tweedie, S., Smith, A., 2003. Functional expression cloning of Nanog, a pluripotency sustaining factor in embryonic stem cells. *Cell.* **113,** 643-655.

Chang, S., Young, B.D., Li, S., Qi, X., Richardson, J.A., Olson, E.N., 2006. Histone deacetylase 7 maintains vascular integrity by repressing matrix metalloproteinase 10. *Cell.* **126,** 321-334.

Codina, A., Love, J.D., Li, Y., Lazar, M.A., Neuhaus, D., Schwabe, J.W., 2005. Structural insights into the interaction and activation of histone deacetylase 3 by nuclear receptor corepressors. *Proceedings of the National Academy of Sciences of the United States of America.* **102,** 6009-6014.

Codina, A., Love, J.D., Li, Y., Lazar, M.A., Neuhaus, D., Schwabe, J.W.R., 2005. Structural insights into the interaction and activation of histone deacetylase 3 by nuclear receptor corepressors. *Proceedings of the National Academy of Sciences of the United States of America.* **102,** 6009-6014.

Creyghton, M.P., Cheng, A.W., Welstead, G.G., Kooistra, T., Carey, B.W., Steine, E.J., Hanna, J., Lodato, M.A., Frampton, G.M., Sharp, P.A., Boyer, L.A., Young, R.A., Jaenisch, R., 2010. Histone H3K27ac separates active

from poised enhancers and predicts developmental state. *Proceedings of the National Academy of Sciences of the United States of America.* **107,** 21931-21936.

Dangond, F., Hafler, D.A., Tong, J.K., Randall, J., Kojima, R., Utku, N., Gullans, S.R., 1998. Differential display cloning of a novel human histone deacetylase (HDAC3) cDNA from PHA-activated immune cells. *Biochemical and Biophysical Research Communications.* **242,** 648-652.

Danko, C.G., Hyland, S.L., Core, L.J., Martins, A.L., Waters, C.T., Lee, H.W., Cheung, V.G., Kraus, W.L., Lis, J.T., Siepel, A., 2015. Identification of active transcriptional regulatory elements from GRO-seq data. *Nature Methods.* **12,** 433-438.

De Santa, F., Barozzi, I., Mietton, F., Ghisletti, S., Polletti, S., Tusi, B.K., Muller, H., Ragoussis, J., Wei, C.L., Natoli, G., 2010. A large fraction of extragenic RNA pol II transcription sites overlap enhancers. *PLoS Biology.* **8,** e1000384.

Deng, C.X., Wynshaw-Boris, A., Shen, M.M., Daugherty, C., Ornitz, D.M., Leder, P., 1994. Murine FGFR-1 is required for early postimplantation growth and axial organization. *Genes & Development.* **8,** 3045-3057.

Dillon, S.C., Zhang, X., Trievel, R.C., Cheng, X., 2005. The SET-domain protein superfamily: protein lysine methyltransferases. *Genome Biology.* **6,** 227.

Dong, X.J., Zhang, G.R., Zhou, Q.J., Pan, R.L., Chen, Y., Xiang, L.X., Shao, J.Z., 2009. Direct hepatic differentiation of mouse embryonic stem cells induced by valproic acid and cytokines. *World Journal of Gastroenterology.* **15,** 5165-5175.

Dovey, O.M., Foster, C.T., Cowley, S.M., 2010. Histone deacetylase 1 (HDAC1), but not HDAC2, controls embryonic stem cell differentiation. *Proc.Natl.Acad.Sci.U.S.A.* **107,** 8242-8243-8247.

Eisen, J.A., Sweder, K.S., Hanawalt, P.C., 1995. Evolution of the SNF2 family of proteins: subfamilies with distinct sequences and functions. *Nucleic Acids Research.* **23,** 2715-2723.

El Alami, M., Messenguy, F., Scherens, B., Dubois, E., 2003. Arg82p is a bifunctional protein whose inositol polyphosphate kinase activity is essential for nitrogen and PHO gene expression but not for Mcm1p chaperoning in yeast. *Molecular Microbiology.* **49,** 457-468.

Evans, M.J. & Kaufman, M.H., 1981. Establishment in culture of pluripotential cells from mouse embryos. *Nature.* **292,** 154-156.

Feil, R., Brocard, J., Mascrez, B., LeMeur, M., Metzger, D., Chambon, P., 1996. Ligand-activated site-specific recombination in mice. *Proceedings of the National Academy of Sciences of the United States of America.* **93,** 10887-10890.

Feil, S., Valtcheva, N., Feil, R., 2009. Inducible Cre mice. *Methods in Molecular Biology (Clifton, N.J.).* **530,** 343-363.

Feng, D., Liu, T., Sun, Z., Bugge, A., Mullican, S.E., Alenghat, T., Liu, X.S., Lazar, M.A., 2011. A circadian rhythm orchestrated by histone deacetylase 3 controls hepatic lipid metabolism. *Science (New York, N.Y.).* **331,** 1315-1319.

Finnin, M.S., Donigan, J.R., Cohen, A., Richon, V.M., Rifkind, R.A., Marks, P.A., Breslow, R., Pavletich, N.P., 1999. Structures of a histone deacetylase homologue bound to the TSA and SAHA inhibitors. *Nature.* **401,** 188-189-193.

Foster, C.T., Dovey, O.M., Lezina, L., Luo, J.L., Gant, T.W., Barlev, N., Bradley, A., Cowley, S.M., 2010. Lysine-specific demethylase 1 regulates the embryonic transcriptome and CoREST stability. *Molecular and Cellular Biology.* **30,** 4851-4863.

Frederick, J.P., Mattiske, D., Wofford, J.A., Megosh, L.C., Drake, L.Y., Chiou, S.T., Hogan, B.L., York, J.D., 2005. An essential role for an inositol polyphosphate multikinase, Ipk2, in mouse embryogenesis and second messenger production. *Proceedings of the National Academy of Sciences of the United States of America.* **102,** 8454-8459.

Gao, L., Cueto, M.A., Asselbergs, F., Atadja, P., 2002. Cloning and Functional Characterization of HDAC11, a Novel Member of the Human Histone Deacetylase Family. *Journal of Biological Chemistry.* **277,** 25748-25749-25755.

Garcea, R.L. & Alberts, B.M., 1980. Comparative studies of histone acetylation in nucleosomes, nuclei, and intact cells. Evidence for special factors which modify acetylase action. *The Journal of Biological Chemistry.* **255,** 11454-11463.

Gordillo, M., Evans, T., Gouon-Evans, V., 2015. Orchestrating liver development. *Development (Cambridge, England).* **142,** 2094-2108.

Grozinger, C.M. & Schreiber, S.L., 2000. Regulation of histone deacetylase 4 and 5 and transcriptional activity by 14-3-3-dependent cellular localization. *Proceedings of the National Academy of Sciences of the United States of America.* **97,** 7835-7840.

Grzenda, A., Lomberk, G., Zhang, J., Urruti, R., 2009. Sin3: Master scaffold and transcriptional corepressor. *Biochimica Et Biophysica Acta.* **1789,** 443-444-450.

Gu, S., Jin, L., Zhang, F., Sarnow, P., Kay, M.A., 2009. Biological basis for restriction of microRNA targets to the 3' untranslated region in mammalian mRNAs. *Nature Structural & Molecular Biology.* **16,** 144-150.

Guardiola, A.R. & Yao, T.P., 2002. Molecular cloning and characterization of a novel histone deacetylase HDAC10. *The Journal of Biological Chemistry.* **277,** 3350-3356.

Guenther, M.G., Barak, O., Lazar, M.A., 2001. The SMRT and N-CoR corepressors are activating co-factors for histone deacetylase-3. *Mol. Cell. Biol.* **21,** 6091-6092-6101.

Guenther, M.G., Barak, O., Lazar, M.A., 2001. The SMRT and N-CoR corepressors are activating cofactors for histone deacetylase 3. *Molecular and Cellular Biology.* **21,** 6091-6101.

Guenther, M.G., Lane, W.S., Fischle, W., Verdin, E., Lazar, M.A., Shiekhattar, R., 2000. A core SMRT corepressor complex containing HDAC3 and TBL1, a WD40-repeat protein linked to deafness. *Genes & Development.* **14,** 1048-1057.

Haberland, M., Mokalled, M.H., Montgomery, R.L., Olson, E.N., 2009. Epigenetic control of skull morphogenesis by histone deacetylase 8. *Genes & Development.* **23,** 1625-1630.

Hay, D.C., Zhao, D., Fletcher, J., Hewitt, Z.A., McLean, D., Urruticoechea-Uriguen, A., Black, J.R., Elcombe, C., Ross, J.A., Wolf, R., Cui, W., 2008. Efficient differentiation of hepatocytes from human embryonic stem cells exhibiting markers recapitulating liver development in vivo. *Stem Cells (Dayton, Ohio).* **26,** 894-902.

Hebert, J.M., Boyle, M., Martin, G.R., 1991. mRNA localization studies suggest that murine FGF-5 plays a role in gastrulation. *Development (Cambridge, England).* **112,** 407-415.

Hendrich, B., Guy, J., Ramsahoye, B., Wilson, V.A., Bird, A., 2001. Closely related proteins MBD2 and MBD3 play distinctive but interacting roles in mouse development. *Genes & Development.* **15,** 710-723.

Hook, S.S., Orian, A., Cowley, S.M., Eisenman, R.N., 2002. Histone deacetylase 6 binds polyubiquitin through its zinc finger (PAZ domain) and copurifies with deubiquitinating enzymes. *Proceedings of the National Academy of Sciences of the United States of America.* **99,** 13425-13430.

Hu, E., Chen, Z., Fredrickson, T., Zhu, Y., Kirkpatrick, R., Zhang, G.F., Johanson, K., Sung, C.M., Liu, R., Winkler, J., 2000. Cloning and characterization of a novel human class I histone deacetylase that functions as a transcription repressor. *The Journal of Biological Chemistry.* **275,** 15254-15264.

Hu, X. & Lazar, M.A., 1999. The CoRNR motif controls the recruitment of corepressors by nuclear hormone receptors. *Nature.* **402,** 93-96.

Itoh, T., Fairall, L., Muskett, F.W., Milano, C.P., Watson, P.J., Arnaudo, N., Saleh, A., Millard, C.J., El-Mezgueldi, M., Martino, F., Schwabe, J.W., 2015. Structural and functional characterization of a cell cycle associated HDAC1/2 complex reveals the structural basis for complex assembly and nucleosome targeting. *Nucleic Acids Research.* **43,** 2033-2044.

Jacobsen, C.M., Narita, N., Bielinska, M., Syder, A.J., Gordon, J.I., Wilson, D.B., 2002. Genetic mosaic analysis reveals that GATA-4 is required for proper differentiation of mouse gastric epithelium. *Developmental Biology.* **241,** 34-46.

Jamaladdin, S., Kelly, R.D., O'Regan, L., Dovey, O.M., Hodson, G.E., Millard, C.J., Portolano, N., Fry, A.M., Schwabe, J.W., Cowley, S.M., 2014. Histone deacetylase (HDAC) 1 and 2 are essential for accurate cell division and the pluripotency of embryonic stem cells. *Proceedings of the National Academy of Sciences of the United States of America.* **111,** 9840-9845.

Jang, S.M., An, J.H., Kim, C.H., Kim, J.W., Choi, K.H., 2015. Transcription factor FOXA2-centered transcriptional regulation network in non-small cell lung cancer. *Biochemical and Biophysical Research Communications.* **463,** 961-967.

Jepsen, K., Hermanson, O., Onami, T.M., Gleiberman, A.S., Lunyak, V., McEvilly, R.J., Kurokawa, R., Kumar, V., Liu, F., Seto, E., Hedrick, S.M., Mandel, G., Glass, C.K., Rose, D.W., Rosenfeld, M.G., 2000.

Combinatorial roles of the nuclear receptor corepressor in transcription and development. *Cell.* **102,** 753-763.

Jepsen, K., Solum, D., Zhou, T., McEvilly, R.J., Kim, H.J., Glass, C.K., Hermanson, O., Rosenfeld, M.G., 2007. SMRT-mediated repression of an H3K27 demethylase in progression from neural stem cell to neuron. *Nature.* **450,** 415-419.

Jepsen, K., Solum, D., Zhou, T., McEvilly, R.J., Kim, H.J., Glass, C.K., Hermanson, O., Rosenfeld, M.G., 2007. SMRT-mediated repression of an H3K27 demethylase in progression from neural stem cell to neuron. *Nature.* **450,** 415-419.

Kanai-Azuma, M., Kanai, Y., Gad, J.M., Tajima, Y., Taya, C., Kurohmaru, M., Sanai, Y., Yonekawa, H., Yazaki, K., Tam, P.P., Hayashi, Y., 2002. Depletion of definitive gut endoderm in Sox17-null mutant mice. *Development (Cambridge, England).* **129,** 2367-2379.

Keller, G.M., 1995. In vitro differentiation of embryonic stem cells. *Current Opinion in Cell Biology.* **7,** 862-869.

Kim, E., Tyagi, R., Lee, J.Y., Park, J., Kim, Y.R., Beon, J., Chen, P.Y., Cha, J.Y., Snyder, S.H., Kim, S., 2013. Inositol polyphosphate multikinase is a coactivator for serum response factor-dependent induction of immediate early genes. *Proceedings of the National Academy of Sciences of the United States of America.* **110,** 19938-19943.

Knutson, S.K., Chyla, B.J., Amann, J.M., Bhaskara, S., Huppert, S.S., Hiebert, S.W., 2008. Liver-specific deletion of histone deacetylase 3 disrupts metabolic transcriptional networks. *The EMBO Journal.* **27,** 1017-1028.

Kornberg, R.D. & Lorch, Y., 1999. Twenty-five years of the nucleosome, fundmamental particle of the eukaryotic chromosome. *Cell.* **98,** 285-286-294.

Kouzarides, T., 2007. Chromatin modifications and their function. *Cell.* **128,** 693-705.

Kunath, T., Saba-El-Leil, M.K., Almousailleakh, M., Wray, J., Meloche, S., Smith, A., 2007. FGF stimulation of the Erk1/2 signalling cascade triggers transition of pluripotent embryonic stem cells from self-renewal to lineage commitment. *Development (Cambridge, England).* **134,** 2895-2902.

Kurdistani, S.K., Robyr, D., Tavazoie, S., Grunstein, M., 2002. Genome-wide binding map of the histone deacetylase Rpd3 in yeast. *Nature Genetics.* **31,** 248-254.

Kyrmizi, I., Hatzis, P., Katrakili, N., Tronche, F., Gonzalez, F.J., Talianidis, I., 2006. Plasticity and expanding complexity of the hepatic transcription factor network during liver development. *Genes & Development.* **20,** 2293-2305.

Lagger, G., O'Carroll, D., Rembold, M., Khier, H., Tischler, J., Weitzer, G., Schuettengruber, B., Hauser, C., Brunmeir, R., Jenuwein, T., Seiser, C., 2002. Essential function of histone deacetylase 1 in proliferation control and CDK inhibitor repression. *The EMBO Journal.* **21,** 2672-2681.

Laherty, C.D., Yang, W.M., Sun, J.M., Davie, J.R., Seto, E., Eisenman, R.N., 1997. Histone deacetylases associated with the mSin3 corepressor mediate mad transcriptional repression. *Cell.* **89,** 349-350-356.

Laherty, C.D., Yang, W.M., Sun, J.M., Davie, J.R., Seto, E., Eisenman, R.N., 1997. Histone deacetylases associated with the mSin3 corepressor mediate mad transcriptional repression. *Cell.* **89,** 349-356.

Lakso, M., Pichel, J.G., Gorman, J.R., Sauer, B., Okamoto, Y., Lee, E., Alt, F.W., Westphal, H., 1996. Efficient in vivo manipulation of mouse genomic sequences at the zygote stage. *Proceedings of the National Academy of Sciences of the United States of America.* **93,** 5860-5865.

Lawson, K.A., Meneses, J.J., Pedersen, R.A., 1991. Clonal analysis of epiblast fate during germ layer formation in the mouse embryo. *Development (Cambridge, England).* **113,** 891-911.

Leahy, A., Xiong, J.W., Kuhnert, F., Stuhlmann, H., 1999. Use of developmental marker genes to define temporal and spatial patterns of differentiation during embryoid body formation. *The Journal of Experimental Zoology.* **284,** 67-81.

Leitch, H.G., Blair, K., Mansfield, W., Ayetey, H., Humphreys, P., Nichols, J., Surani, M.A., Smith, A., 2010. Embryonic germ cells from mice and rats exhibit properties consistent with a generic pluripotent ground state. *Development (Cambridge, England).* **137,** 2279-2287.

Leyman, A., Pouillon, V., Bostan, A., Schurmans, S., Erneux, C., Pesesse, X., 2007. The absence of expression of the three isoenzymes of the inositol 1,4,5-trisphosphate 3-kinase does not prevent the formation of inositol pentakisphosphate and hexakisphosphate in mouse embryonic fibroblasts. *Cellular Signalling.* **19,** 1497-1504.

Li, J., Ning, G., Duncan, S.A., 2000. Mammalian hepatocyte differentiation requires the transcription factor HNF-4alpha. *Genes & Development.* **14,** 464-474.

Li, J., Wang, J., Wang, J., Nawaz, Z., Liu, J.M., Qin, J., Wong, J., 2000. Both corepressor proteins SMRT and N-CoR exist in large protein complexes containing HDAC3. *The EMBO Journal.* **19,** 4342-4350.

Liang, J., Wan, M., Zhang, Y., Gu, P., Xin, H., Jung, S.Y., Qin, J., Wong, J., Cooney, A.J., Liu, D., Songyang, Z., 2008. Nanog and Oct4 associate with unique transcriptional repression complexes in embryonic stem cells. *Nature Cell Biology.* **10,** 731-739.

Liu, P., Jenkins, N.A., Copeland, N.G., 2003. A highly efficient recombineering-based method for generating conditional knockout mutations. *Genome Research.* **13,** 476-484.

Lo, W.S., Trievel, R.C., Rojas, J.R., Duggan, L., Hsu, J.Y., Allis, C.D., Marmorstein, R., Berger, S.L., 2000. Phosphorylation of serine 10 in histone H3 is functionally linked in vitro and in vivo to Gcn5-mediated acetylation at lysine 14. *Molecular Cell.* **5,** 917-926.

Loebel, D.A., Watson, C.M., De Young, R.A., Tam, P.P., 2003. Lineage choice and differentiation in mouse embryos and embryonic stem cells. *Developmental Biology.* **264,** 1-14.

Loh, Y.H., Wu, Q., Chew, J.L., Vega, V.B., Zhang, W., Chen, X., Bourque, G., George, J., Leong, B., Liu, J., Wong, K.Y., Sung, K.W., Lee, C.W., Zhao, X.D., Chiu, K.P., Lipovich, L., Kuznetsov, V.A., Robson, P., Stanton, L.W., Wei, C.L., Ruan, Y., Lim, B., Ng, H.H., 2006. The Oct4 and Nanog transcription network regulates pluripotency in mouse embryonic stem cells. *Nature Genetics.* **38,** 431-440.

Lolas, M., Valenzuela, P.D., Tjian, R., Liu, Z., 2014. Charting Brachyury-mediated developmental pathways during early mouse embryogenesis. *Proceedings of the National Academy of Sciences of the United States of America.* **111,** 4478-4483.

Lu, C.C., Brennan, J., Robertson, E.J., 2001. From fertilization to gastrulation: axis formation in the mouse embryo. *Current Opinion in Genetics & Development.* **11,** 384-392.

Luger, K. & Richmond, T.J., 1998. The histone tails of the nucleosome. *Current Opinion in Genetics and Development.* **8,** 140-141-146.

Luger, K., Mader, A.W., Richmond, R.K., Sargent, D.F., Richmond, T.J., 1997. Crystal structure of the nucleosome core particle at 2.8 A resolution. *Nature.* **389,** 251-260.

Ma, P. & Schultz, R.M., 2008. Histone deacetylase 1 (HDAC1) regulates histone acetylation, development, and gene expression in preimplantation mouse embryos. *Developmental Biology.* **319,** 110-120.

Martello, G., Sugimoto, T., Diamanti, E., Joshi, A., Hannah, R., Ohtsuka, S., Gottgens, B., Niwa, H., Smith, A., 2012. Esrrb is a pivotal target of the Gsk3/Tcf3 axis regulating embryonic stem cell self-renewal. *Cell Stem Cell.* **11,** 491-504.

Mayr, G.W., Windhorst, S., Hillemeier, K., 2005. Antiproliferative plant and synthetic polyphenolics are specific inhibitors of vertebrate inositol-1,4,5-trisphosphate 3-kinases and inositol polyphosphate multikinase. *The Journal of Biological Chemistry.* **280,** 13229-13240.

Mejat, A., Ramond, F., Bassel-Duby, R., Khochbin, S., Olson, E.N., Schaeffer, L., 2005. Histone deacetylase 9 couples neuronal activity to muscle chromatin acetylation and gene expression. *Nature Neuroscience.* **8,** 313-321.

Millard, C.J., Watson, P.J., Celardo, I., Gordiyenko, Y., Cowley, S.M., Robinson, C.V., Fairall, L., Schwabe, J.W., 2013. Class I HDACs share a common mechanism of regulation by inositol phosphates. *Molecular Cell.* **51,** 57-67.

Montgomery, R.L., Davis, C.A., Potthoff, M.J., Haberland, M., Fielitz, J., Qi, X., Hill, J.A., Richardson, J.A., Olson, E.N., 2007. Histone deacetylases 1 and 2 redundantly regulate cardiac morphogenesis, growth, and contractility. *Genes & Development.* **21,** 1790-1802.

Montgomery, R.L., Potthoff, M.J., Haberland, M., Qi, X., Matsuzaki, S., Humphries, K.M., Richardson, J.A., Bassel-Duby, R., Olson, E.N., 2008. Maintenance of cardiac energy metabolism by histone deacetylase 3 in mice. *The Journal of Clinical Investigation.* **118,** 3588-3597.

Mullican, S.E., Gaddis, C.A., Alenghat, T., Nair, M.G., Giacomin, P.R., Everett, L.J., Feng, D., Steger, D.J., Schug, J., Artis, D., Lazar, M.A., 2011. Histone deacetylase 3 is an epigenomic brake in macrophage alternative activation. *Genes & Development.* **25,** 2480-2488.

Nagy, L., Kao, H.Y., Love, J.D., Li, C., Banayo, E., Gooch, J.T., Krishna, V., Chatterjee, K., Evans, R.M., Schwabe, J.W., 1999. Mechanism of corepressor binding and release from nuclear hormone receptors. *Genes & Development.* **13,** 3209-3216.

Nakano, T., Kodama, H., Honjo, T., 1994. Generation of lymphohematopoietic cells from embryonic stem cells in culture. *Science (New York, N.Y.).* **265,** 1098-1101.

Nemer, G. & Nemer, M., 2003. Transcriptional activation of BMP-4 and regulation of mammalian organogenesis by GATA-4 and -6. *Developmental Biology.* **254,** 131-148.

Nichols, J., Zevnik, B., Anastassiadis, K., Niwa, H., Klewe-Nebenius, D., Chambers, I., Scholer, H., Smith, A., 1998. Formation of pluripotent stem cells in the mammalian embryo depends on the POU transcription factor Oct4. *Cell.* **95,** 379-391.

Nishikawa, S.I., Nishikawa, S., Hirashima, M., Matsuyoshi, N., Kodama, H., 1998. Progressive lineage analysis by cell sorting and culture identifies FLK1+VE-cadherin+ cells at a diverging point of endothelial and hemopoietic lineages. *Development (Cambridge, England).* **125,** 1747-1757.

Niwa, H., Burdon, T., Chambers, I., Smith, A., 1998. Self-renewal of pluripotent embryonic stem cells is mediated via activation of STAT3. *Genes & Development.* **12,** 2048-2060.

Oberoi, J., Fairall, L., Watson, P.J., Yang, J.C., Czimmerer, Z., Kampmann, T., Goult, B.T., Greenwood, J.A., Gooch, J.T., Kallenberger, B.C., Nagy, L., Neuhaus, D., Schwabe, J.W., 2011. Structural basis for the assembly of the SMRT/NCoR core transcriptional repression machinery. *Nature Structural & Molecular Biology.* **18,** 177-184.

Odom, A.R., Stahlberg, A., Wente, S.R., York, J.D., 2000. A role for nuclear inositol 1,4,5-trisphosphate kinase in transcriptional control. *Science (New York, N.Y.).* **287,** 2026-2029.

Odom, D.T., Zizlsperger, N., Gordon, D.B., Bell, G.W., Rinaldi, N.J., Murray, H.L., Volkert, T.L., Schreiber, J., Rolfe, P.A., Gifford, D.K., Fraenkel, E., Bell, G.I., Young, R.A., 2004. Control of pancreas and liver gene expression by HNF transcription factors. *Science (New York, N.Y.).* **303,** 1378-1381.

Ordentlich, P., Downes, M., Xie, W., Genin, A., Spinner, N.B., Evans, R.M., 1999. Unique forms of human and mouse nuclear receptor corepressor SMRT. *Proceedings of the National Academy of Sciences of the United States of America.* **96,** 2639-2644.

Ozawa, Y., Towatari, M., Tsuzuki, S., Hayakawa, F., Maeda, T., Miyata, Y., Tanimoto, M., Saito, H., 2001. Histone deacetylase 3 associates with and represses the transcription factor GATA-2. *Blood.* **98,** 2116-2123.

Panteleeva, I., Rouaux, C., Larmet, Y., Boutillier, S., Loeffler, J.P., Boutillier, A.L., 2004. HDAC-3 participates in the repression of e2f-dependent gene transcription in primary differentiated neurons. *Annals of the New York Academy of Sciences.* **1030,** 656-660.

Park, E.J., Schroen, D.J., Yang, M., Li, H., Li, L., Chen, J.D., 1999. SMRTe, a silencing mediator for retinoid and thyroid hormone receptors-extended isoform that is more related to the nuclear receptor corepressor. *Proceedings of the National Academy of Sciences of the United States of America.* **96,** 3519-3524.

Peart, M.J., Smyth, G.K., van Laar, R.K., Bowtell, D.D., Richon, V.M., Marks, P.A., Holloway, A.J., Johnstone, R.W., 2005. Identification and functional significance of genes regulated by structurally different histone deacetylase inhibitors. *Proceedings of the National Academy of Sciences of the United States of America.* **102,** 3697-3702.

Privalsky, M.L., 2004. The role of corepressors in transcriptional regulation by nuclear hormone receptors. *Annual Review of Physiology.* **66,** 315-360.

Resnick, A.C., Snowman, A.M., Kang, B.N., Hurt, K.J., Snyder, S.H., Saiardi, A., 2005. Inositol polyphosphate multikinase is a nuclear PI3-kinase with transcriptional regulatory activity. *Proceedings of the National Academy of Sciences of the United States of America.* **102,** 12783-12788.

Ringner, M., 2008. What is principal component analysis? *Nature Biotechnology.* **26,** 303-304.

Rodda, D.J., Chew, J.L., Lim, L.H., Loh, Y.H., Wang, B., Ng, H.H., Robson, P., 2005. Transcriptional regulation of nanog by OCT4 and SOX2. *The Journal of Biological Chemistry.* **280,** 24731-24737.

Rohwedel, J., Maltsev, V., Bober, E., Arnold, H.H., Hescheler, J., Wobus, A.M., 1994. Muscle cell differentiation of embryonic stem cells reflects myogenesis in vivo: developmentally regulated expression of myogenic determination genes and functional expression of ionic currents. *Developmental Biology.* **164,** 87-101.

Rojas, A., Schachterle, W., Xu, S.M., Martin, F., Black, B.L., 2010. Direct transcriptional regulation of Gata4 during early endoderm specification is controlled by FoxA2 binding to an intronic enhancer. *Developmental Biology.* **346,** 346-355.

Rossetto, D., Avvakumov, N., Cote, J., 2012. Histone phosphorylation: a chromatin modification involved in diverse nuclear events. *Epigenetics.* **7,** 1098-1108.

Ruiz-Carrillo, A., Wangh, L.J., Allfrey, V.G., 1975. Processing of newly synthesized histone molecules. *Science (New York, N.Y.).* **190,** 117-128.

Shi, Y., Lan, F., Matson, C., Mulligan, P., Whetstine, J.R., Cole, P.A., Casero, R.A., Shi, Y., 2004. Histone demethylation mediated by the nuclear amine oxidase homolog LSD1. *Cell.* **119,** 941-953.

Smith, A.G., 2001. Embryo-derived stem cells: of mice and men. *Annual Review of Cell and Developmental Biology.* **17,** 435-462.

Smith, A.G., Heath, J.K., Donaldson, D.D., Wong, G.G., Moreau, J., Stahl, M., Rogers, D., 1988. Inhibition of pluripotential embryonic stem cell differentiation by purified polypeptides. *Nature.* **336,** 688-690.

Sterner, D.E. & Berger, S.L., 2000. Acetylation of histones and transcription-related factors. *Microbiology and Molecular Biology Reviews : MMBR.* **64,** 435-459.

Strahl, B.D. & Allis, C.D., 2000. The language of covalent histone modifications. *Nature.* **403,** 41-42-45.

Summers, A.R., Fischer, M.A., Stengel, K.R., Zhao, Y., Kaiser, J.F., Wells, C.E., Hunt, A., Bhaskara, S., Luzwick, J.W., Sampathi, S., Chen, X., Thompson, M.A., Cortez, D., Hiebert, S.W., 2013. HDAC3 is essential for DNA replication in hematopoietic progenitor cells. *The Journal of Clinical Investigation.* **123,** 3112-3123.

Sun, Z., Feng, D., Fang, B., Mullican, S.E., You, S.H., Lim, H.W., Everett, L.J., Nabel, C.S., Li, Y., Selvakumaran, V., Won, K.J., Lazar, M.A., 2013. Deacetylase-independent function of HDAC3 in transcription and metabolism requires nuclear receptor corepressor. *Molecular Cell.* **52,** 769-782.

Sun, Z., Feng, D., Fang, B., Mullican, S.E., You, S.H., Lim, H.W., Everett, L.J., Nabel, C.S., Li, Y., Selvakumaran, V., Won, K.J., Lazar, M.A., 2013. Deacetylase-Independent Function of HDAC3 in Transcription and Metabolism Requires Nuclear Receptor Corepressor. *Molecular Cell.* **52,** 769-782.

Sun, Z., Miller, R.A., Patel, R.T., Chen, J., Dhir, R., Wang, H., Zhang, D., Graham, M.J., Unterman, T.G., Shulman, G.I., Sztalryd, C., Bennett, M.J., Ahima, R.S., Birnbaum, M.J., Lazar, M.A., 2012. Hepatic Hdac3 promotes

gluconeogenesis by repressing lipid synthesis and sequestration. *Nature Medicine.* **18,** 934-942.

Tada, S., Era, T., Furusawa, C., Sakurai, H., Nishikawa, S., Kinoshita, M., Nakao, K., Chiba, T., Nishikawa, S., 2005. Characterization of mesendoderm: a diverging point of the definitive endoderm and mesoderm in embryonic stem cell differentiation culture. *Development (Cambridge, England).* **132,** 4363-4374.

Tam, P.P. & Behringer, R.R., 1997. Mouse gastrulation: the formation of a mammalian body plan. *Mechanisms of Development.* **68,** 3-25.

Taunton, J., Hassig, C.A., Schreiber, S.L., 1996. A Mammalian Histone Deacetylase Related to the Yeast Transcriptional Regulator Rpd3p. *Science.* **272,** 408-409-411.

Thiagalingam, S., Cheng, K., Lee, H.J., Mineva, N., Thiagalingam, A., Ponte, J.F., 2000. Histone Deacetylases: Unique Players in Shaping the Epigenetic Histone Code. *Annals.* **983,** 84-85-100.

Thoma, F., Koller, T., Klug, A., 1979. Involvement of histone H1 in the organization of the nucleosome and of the salt-dependent superstructures of chromatin. *The Journal of Cell Biology.* **83,** 403-427.

Tong, J.J., Liu, J., Bertos, N.R., Yang, X.J., 2002. Identification of HDAC10, a novel class II human histone deacetylase containing a leucine-rich domain. *Nucleic Acids Research.* **30,** 1114-1123.

Torres-Padilla, M.E., Sladek, F.M., Weiss, M.C., 2002. Developmentally regulated N-terminal variants of the nuclear receptor hepatocyte nuclear factor 4alpha mediate multiple interactions through coactivator and corepressor-histone deacetylase complexes. *The Journal of Biological Chemistry.* **277,** 44677-44687.

Trivedi, C.M., Luo, Y., Yin, Z., Zhang, M., Zhu, W., Wang, T., Floss, T., Goettlicher, M., Noppinger, P.R., Wurst, W., Ferrari, V.A., Abrams, C.S.,

Gruber, P.J., Epstein, J.A., 2007. Hdac2 regulates the cardiac hypertrophic response by modulating Gsk3 beta activity. *Nature Medicine.* **13,** 324-331.

Tsukada, Y., Fang, J., Erdjument-Bromage, H., Warren, M.E., Borchers, C.H., Tempst, P., Zhang, Y., 2006. Histone demethylation by a family of JmjC domain-containing proteins. *Nature.* **439,** 811-816.

Urvalek, A.M. & Gudas, L.J., 2014. Retinoic acid and histone deacetylases regulate epigenetic changes in embryonic stem cells. *The Journal of Biological Chemistry.* **289,** 19519-19530.

Vega, R.B., Matsuda, K., Oh, J., Barbosa, A.C., Yang, X., Meadows, E., McAnally, J., Pomajzl, C., Shelton, J.M., Richardson, J.A., Karsenty, G., Olson, E.N., 2004. Histone deacetylase 4 controls chondrocyte hypertrophy during skeletogenesis. *Cell.* **119,** 555-566.

Verbsky, J., Lavine, K., Majerus, P.W., 2005. Disruption of the mouse inositol 1,3,4,5,6-pentakisphosphate 2-kinase gene, associated lethality, and tissue distribution of 2-kinase expression. *Proceedings of the National Academy of Sciences of the United States of America.* **102,** 8448-8453.

Villagra, A., Cheng, F., Wang, H.W., Suarez, I., Glozak, M., Maurin, M., Nguyen, D., Wright, K.L., Atadja, P.W., Bhalla, K., Pinilla-Ibarz, J., Seto, E., Sotomayor, E.M., 2009. The histone deacetylase HDAC11 regulates the expression of interleukin 10 and immune tolerance. *Nature Immunology.* **10,** 92-100.

Vooijs, M., Jonkers, J., Berns, A., 2001. A highly efficient ligand-regulated Cre recombinase mouse line shows that LoxP recombination is position dependent. *EMBO Reports.* **2,** 292-297.

Wang, H., Wang, L., Erdjument-Bromage, H., Vidal, M., Tempst, P., Jones, R.S., Zhang, Y., 2004. Role of histone H2A ubiquitination in Polycomb silencing. *Nature.* **431,** 873-878.

Wang, H., Zhai, L., Xu, J., Joo, H.Y., Jackson, S., Erdjument-Bromage, H., Tempst, P., Xiong, Y., Zhang, Y., 2006. Histone H3 and H4 ubiquitylation by the CUL4-DDB-ROC1 ubiquitin ligase facilitates cellular response to DNA damage. *Molecular Cell.* **22,** 383-394.

Wang, L. & Chen, Y.G., 2016. Signaling Control of Differentiation of Embryonic Stem Cells toward Mesendoderm. *Journal of Molecular Biology.* **428,** 1409-1422.

Wang, Z., Zang, C., Cui, K., Schones, D.E., Barski, A., Peng, W., Zhao, K., 2009. Genome-wide mapping of HATs and HDACs reveals distinct functions in active and inactive genes. *Cell.* **138,** 1019-1031.

Wang, Z., Zang, C., Cui, K., Schones, D.E., Barski, A., Peng, W., Zhao, K., 2009. Genome-wide mapping of HATs and HDACs reveals distinct functions in active and inactive genes. *Cell.* **138,** 1019-1031.

Watson, P.J., Fairall, L., Santos, G.M., Schwabe, J.W.R., 2012. Structure of HDAC3 bound to co-repressor and inositol tetraphosphate. *Nature.* **481,** 335-336-341.

Watson, P.J., Fairall, L., Santos, G.M., Schwabe, J.W., 2012. Structure of HDAC3 bound to co-repressor and inositol tetraphosphate. *Nature.* **481,** 335-340.

Watson, P.J., Millard, C.J., Riley, A.M., Robertson, N.S., Wright, L.C., Godage, H.Y., Cowley, S.M., Jamieson, A.G., Potter, B.V., Schwabe, J.W., 2016. Insights into the activation mechanism of class I HDAC complexes by inositol phosphates. *Nature Communications.* **7,** 11262.

Wei, Y., Yu, L., Bowen, J., Gorovsky, M.A., Allis, C.D., 1999. Phosphorylation of histone H3 is required for proper chromosome condensation and segregation. *Cell.* **97,** 99-109.

Wells, J. & Farnham, P.J., 2002. Characterizing transcription factor binding sites using formaldehyde crosslinking and immunoprecipitation. *Methods (San Diego, Calif.).* **26,** 48-56.

Wen, Y.D., Perissi, V., Staszewski, L.M., Yang, W.M., Krones, A., Glass, C.K., Rosenfeld, M.G., Seto, E., 2000. The histone deacetylase-3 complex contains nuclear receptor corepressors. *Proceedings of the National Academy of Sciences of the United States of America.* **97,** 7202-7207.

Wilkinson, D.G., Bhatt, S., Herrmann, B.G., 1990. Expression pattern of the mouse T gene and its role in mesoderm formation. *Nature.* **343,** 657-659.

Williams, R.L., Hilton, D.J., Pease, S., Willson, T.A., Stewart, C.L., Gearing, D.P., Wagner, E.F., Metcalf, D., Nicola, N.A., Gough, N.M., 1988. Myeloid leukaemia inhibitory factor maintains the developmental potential of embryonic stem cells. *Nature.* **336,** 684-687.

Wilson, A.J., Byun, D.S., Popova, N., Murray, L.B., L'Italien, K., Sowa, Y., Arango, D., Velcich, A., Augenlicht, L.H., Mariadason, J.M., 2006. Histone deacetylase 3 (HDAC3) and other class I HDACs regulate colon cell maturation and p21 expression and are deregulated in human colon cancer. *The Journal of Biological Chemistry.* **281,** 13548-13558.

Xu, R. & Snyder, S.H., 2013. Gene transcription by p53 requires inositol polyphosphate multikinase as a co-activator. *Cell Cycle (Georgetown, Tex.).* **12,** 1819-1820.

Xue, Y., Wong, J., Moreno, G.T., Young, M.K., Cote, J., Wang, W., 1998. NURD, a novel complex with both ATP-dependent chromatin-remodeling and histone deactetylase activities. *Molecular Cell.* **2,** 851-852-861.

Xue, Y., Wong, J., Moreno, G.T., Young, M.K., Cote, J., Wang, W., 1998. NURD, a novel complex with both ATP-dependent chromatin-remodeling and histone deacetylase activities. *Molecular Cell.* **2,** 851-861.

Yang, W.M., Yao, Y.L., Sun, J.M., Davie, J.R., Seto, E., 1997. Isolation and characterization of cDNAs corresponding to an additional member of the human histone deacetylase gene family. *The Journal of Biological Chemistry.* **272,** 28001-28007.

Ying, Q.L., Nichols, J., Chambers, I., Smith, A., 2003. BMP induction of Id proteins suppresses differentiation and sustains embryonic stem cell self-renewal in collaboration with STAT3. *Cell.* **115,** 281-292.

Ying, Q.L., Wray, J., Nichols, J., Batlle-Morera, L., Doble, B., Woodgett, J., Cohen, P., Smith, A., 2008. The ground state of embryonic stem cell self-renewal. *Nature.* **453,** 519-523.

Yoon, H.G., Chan, D.W., Huang, Z.Q., Li, J., Fondell, J.D., Qin, J., Wong, J., 2003. Purification and functional characterization of the human N-CoR complex: the roles of HDAC3, TBL1 and TBLR1. *The EMBO Journal.* **22,** 1336-1346.

You, A., Tong, J.K., Grozinger, C.M., Schreiber, S.L., 2001. CoREST is an integral component of the CoREST- human histone deacetylase complex. *Proceedings of the National Academy of Sciences of the United States of America.* **98,** 1454-1458.

You, S.H., Lim, H.W., Sun, Z., Broache, M., Won, K.J., Lazar, M.A., 2013. Nuclear receptor co-repressors are required for the histone-deacetylase activity of HDAC3 in vivo. *Nature Structural & Molecular Biology.* **20,** 182-187.

Zhang, C.L., McKinsey, T.A., Chang, S., Antos, C.L., Hill, J.A., Olson, E.N., 2002. Class II histone deacetylases act as signal-responsive repressors of cardiac hypertrophy. *Cell.* **110,** 479-488.

Zhang, J., Kalkum, M., Chait, B.T., Roeder, R.G., 2002. The N-CoR-HDAC3 nuclear receptor corepressor complex inhibits the JNK pathway through the integral subunit GPS2. *Molecular Cell.* **9,** 611-623.

Zhang, X., Ozawa, Y., Lee, H., Wen, Y.D., Tan, T.H., Wadzinski, B.E., Seto, E., 2005. Histone deacetylase 3 (HDAC3) activity is regulated by interaction with protein serine/threonine phosphatase 4. *Genes & Development.* **19,** 827-839.

Zhang, X., Wharton, W., Yuan, Z., Tsai, S.C., Olashaw, N., Seto, E., 2004. Activation of the growth-differentiation factor 11 gene by the histone deacetylase (HDAC) inhibitor trichostatin A and repression by HDAC3. *Molecular and Cellular Biology.* **24,** 5106-5118.

Zhang, Y., Ng, H.H., Erdjument-Bromage, H., Tempst, P., Bird, A., Reinberg, D., 1999. Analysis of the NuRD subunits reveals a histone deacetylase core complex and a connection with DNA methylation. *Genes & Development.* **13,** 1924-1935.

Zhong, S., Goto, H., Inagaki, M., Dong, Z., 2003. Phosphorylation at serine 28 and acetylation at lysine 9 of histone H3 induced by trichostatin A. *Oncogene.* **22,** 5291-5297.

Zhou, Q.J., Xiang, L.X., Shao, J.Z., Hu, R.Z., Lu, Y.L., Yao, H., Dai, L.C., 2007. In vitro differentiation of hepatic progenitor cells from mouse embryonic stem cells induced by sodium butyrate. *Journal of Cellular Biochemistry.* **100,** 29-42.

Zhou, Y.B., Gerchman, S.E., Ramakrishnan, V., Travers, A., Muyldermans, S., 1998. Position and orientation of the globular domain of linker histone H5 on the nucleosome. *Nature.* **395,** 402-405.

Zhu, B., Zheng, Y., Pham, A.D., Mandal, S.S., Erdjument-Bromage, H., Tempst, P., Reinberg, D., 2005. Monoubiquitination of human histone H2B: the factors involved and their roles in HOX gene regulation. *Molecular Cell.* **20,** 601-611.

Zimmermann, S., Kiefer, F., Prudenziati, M., Spiller, C., Hansen, J., Floss, T., Wurst, W., Minucci, S., Gottlicher, M., 2007. Reduced body size and

decreased intestinal tumor rates in HDAC2-mutant mice. *Cancer Research.* **67,** 9047-9054.